SYNTHESIS AND CHARACTERISATION OF NOVEL

EPOXY-CLAY NANOCOMPOSITES

A dissertation

Submitted in partial fulfillment

of the requirement for the award of the degree

of

MASTER OF ENGINEERING

in

Polymer Technology

by

HITESH SONI
(Roll No.: 03/ Poly/ 03)
2003-2005

DELHI COLLEGE OF ENGINEERING
SHAHBAD-DAULATPUR
BAWANA ROAD
DELHI- 110042

CERTIFICATE

This is to certify that Mr. HITESH SONI has carried out his major research project entitled **"SYNTHESIS AND CHARACTERISATION OF NOVEL EPOXY-CLAY NANOCOMPOSITES"** under our joint supervision and guidance during the session 2004-2005 for the partial fulfillment of Master of Engineering degree in Polymer Technology of Delhi University. To the best of our knowledge and belief, this work has not been submitted to any other university or institution for the award of any degree or diploma.

PROFESSOR (Dr.) G. L. VERMA
Head, Department of Applied Chemistry
Delhi College of Engineering
Delhi.

Dr. D. K. SETUA
Scientist 'F'
Head, E&SM Division
DMSRDE, Kanpur.

Dr. VINEETA NIGAM
Scientist 'C'
E&SM Division

.

ACKNOWLEDGEMENT

I wish to express my deep sense of gratitude and indebtedness to my supervisors Prof. G. L. Verma, Head, Deptt. Of Applied Chemistry, Delhi College of Engineering, Delhi and Dr. D. K. Setua, Head, E&SM Division, DMSRDE, Kanpur for their invaluable guidance, constant encouragement and generous co-operation, at every stage of this work, without which this work would not have been possible.

I am thankful to Dr. Madumita Saroop, Visiting Faculty in Applied Chemistry Deptt. Delhi College of Engineering and Dr. Vineeta Nigam Scientist 'C', E&SM division DMSRDE for their invaluable guidance and co-operation.

I am thankful to Dr. K. Bhasker Rao, Director, DMSRDE for providing me all necessary facilities to carry out my research work.

I am thankful to Dr. S. K. Shukla and Dr. N. C. Mehra from USIC, University of Delhi for their invaluable help.

I am thankful to Mr. C. M. Gandhi, Director, Sperry Plast Limited for providing all necessary facilities at their lab.

I am thankful to Mr. Ajeet Shrivastava, Mr. A. K. Pandey, Mr. Amitabh Chakarvorty, Mr. C.V. Vishawakarma, Mr. Y.N. Gupta, Mr. G.D. Pandey, Mr. Kumar Gaurav, Mr. Satish Toppo, Mr. Dhiraj Chadha, Mr. Rajender, Miss. Rachana Singh, Miss. Nidhi Aggarwal, Pushpa Bhargawa Mam and Miss. Kavita Aggarwal for providing me all necessary support to complete this work.

I wish to offer my thanks to my friends Mr. Maneesh Sharma, Mr. Amit Kumar Thakur, Mr. Nimesh Mishra, Mr. Sandeep Sginotra, Mr. Vineet Kumar, Mr. Santosh Kumar, Mr. Reetesh Kumar Singh, Mr. Amit Saxena and Mr. Rajeev Ranjan for their support.

I am thankful to my family for their moral support and co-operation during this project.

I am thankful to all my professors, laboratory staff, administrative Staff and library staff for their co-operation.

Hitesh Soni

CONTENTS

Chapter 1	Introduction		1
	1.1	Polymer Clay Nanocomposites	3
	1.2	Epoxy-Resin	28
	1.3	Clays	30
	1.4	Epoxy-Clay Nanocomposites	33
Chapter 2	Experimental		46
	2.1	Materials	46
	2.2	Nanocomposite Preparation	47
	2.3	Characterization Techniques	48
Chapter 3	Results and Discussion		55
	3.1	Wide Angle X-Ray Diffraction	55
	3.2	Fourier-Transform Infra-Red Spectroscopy (FTIR)	59
	3.3	Tensile Strength and Modulus	62
	3.4	Flexural Strength and Modulus	65
	3.5	Impact Strength	67
	3.6	Differential Scanning Calorimetry (DSC)	69
	3.7	Thermogravimetric Analysis (TGA)	72
	3.8	Dynamic Mechanical Analysis (DMA)	75
	3.9	Scanning Electron Microscopy (SEM)	80
Chapter 4	Summary and Conclusion		88
Chapter 5	Scope of Future Work		89
References			90

CHAPTER 1

Introduction

Composite materials consist of two or more materials and generally a reinforcing structure surrounded by a continuous matrix. The role of matrix is to hold the structure together. Usually, the matrix is of lower strength than the reinforcement. The different types of matrix used include carbon glass, polymer, ceramic and metal. The composite may be classified depending on their reinforcement. These are fibrous composites (fibers), laminar composites, particulate composites (particles, beads). The mechanical and thermal properties of composite materials are far better than the pure matrix.

Nanocomposites are a new class of composites that are particle-filled polymers for which at least one dimension of the dispersed particles is in the nanometer range. One can distinguish three types of nanocomposites, depending on how many dimensions of the dispersed particles are in the nanometer range. When the three dimensions are in the order of nanometers, we are dealing with isodimensional nanoparticles, such as spherical silica nanoparticles obtained by in situ sol–gel methods [1 and 2] or by polymerization promoted directly from their surface [3], but also can include semiconductor nanoclusters [4] and others [2]. When two dimensions are in the nanometer scale and the third is larger, forming an elongated structure, we speak about nanotubes or whiskers as, for example, carbon nanotubes [5] or cellulose whiskers [6 and 7] which are extensively studied as reinforcing nanofillers yielding materials with exceptional properties. The third type of nanocomposites is characterized by only one dimension in the nanometer range. In this case the filler is present in the form of sheets of one to a few nanometer thick to hundreds to thousands nanometers long. This family of composites can be gathered under the name of polymer-layered crystal nanocomposites. These materials are almost exclusively obtained by the intercalation of the polymer (or a monomer

subsequently polymerized) inside the galleries of layered host crystals. There are a wide variety of both synthetic and natural crystalline fillers that are able, under specific conditions, to intercalate a polymer.

In recent years polymer/layered silicate (PLS) nanocomposites have attracted great interest, both in industry and in academia, because they often exhibit remarkable improvement in materials properties when compared with virgin polymer or conventional micro- and macro-composites. These improvements can include high moduli, increased strength and heat resistance, decreased gas permeability and flammability and increased biodegradability of biodegradable polymers .Two major findings have stimulated the revival of interest in these materials: first, the report from the Toyota research group of a Nylon-6 (N6)/montmorillonite (MMT) nanocomposite [8], for which very small amounts of layered silicate loadings resulted in pronounced improvements of thermal and mechanical properties; and second, the observation by Vaia et al. [9] that it is possible to melt-mix polymers with layered silicates, without the use of organic solvents.

The clay based polymer nanocomposites may be immiscible or exfoliated or intercalated depending on the orientations of clay layers in polymer matrix. This orientation of clay layers largely governs by the factors such as nature of clay, polymer and organic surfactants and polymerization process and clay-polymer interaction. Various polymer/clay nanocomposites have been reported such as polystyrene-clay, epoxy-clay, polyurethane-clay, polyethylene-clay, poly (ethylene oxide)-clay nanocomposites etc. The characteristics of these composites are discussed in the preceding sections.

1.1 Polymer-Clay Nanocomposites

Structure and properties of layered silicates

Common clays are naturally occurring mineral and thus subject to natural variability in the construction. The purity of clays can affect the final nanocomposite properties. The crystal structure of clay minerals consists of silicate layers that contain sheets of SiO_4 tetrahedral and sheets of [Me (O, OH] octahedral, where Me = Metal arranged in such a way that a central octahedral sheet of alumina or magnesia is sandwiched between two external silica tetrahedrals at an edge so that the oxygen ions of the octahedral sheet do also belong to the tetrahedral sheets. The layer thickness is around 1 nm and the lateral dimensions of these layers may vary from 300 Å to several microns and even larger depending on the particular silicate. These platelets have high aspect ratio typically 100-1500 with a degree of flexibility and very high surface area, up to hundreds of m^2 per gm [10]. These layers are stacked with a regular Vander Walls gap in between them called the interlayer or the gallery. Isomorphic substitution within the layers (for example, Al^{3+} replaced by Mg^{2+} or by Fe^{2+}, or Mg^{2+} replaced by Li^{+}) generates negative charges that are counterbalanced by alkali or alkaline earth cations situated in the interlayer. As the forces that hold the stacks together are relatively weak, the intercalation of small molecules between the layers is easy.

Montmorillonite, hectorite and saponite are the most commonly used layered silicates. Their structure is given in Figures. 1. 1 [10] and 1.2[12] while their chemical formula are shown in Table 1.1[12]

Table 1.1 Structure and chemistry of mica-type silicates [2]

Silicate Type	Location of Isomorphous Substitution	Formula
Montmorillonite	Octahedral	Mx $[Al_{4-x}Mgx]$ $(Si_8)O_{20}(OH)_4$

Hectorite	Octahedral	Mx $[Mg_6$-xLix] $(Si_8)O_{20}(OH)_4$
Saponite	Tetrahedral	Mx $[Mg_6](Si_{8-6}Alx)$ $O_{20}(OH)_4$

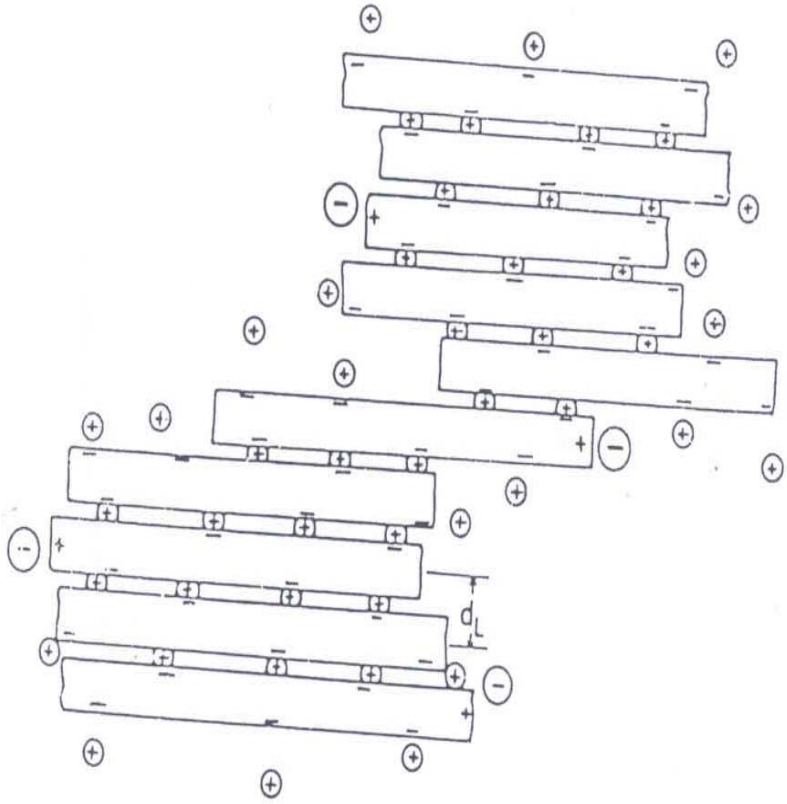

Fig 1.1 Structure of layer silicate d_L = basal spacing [10]

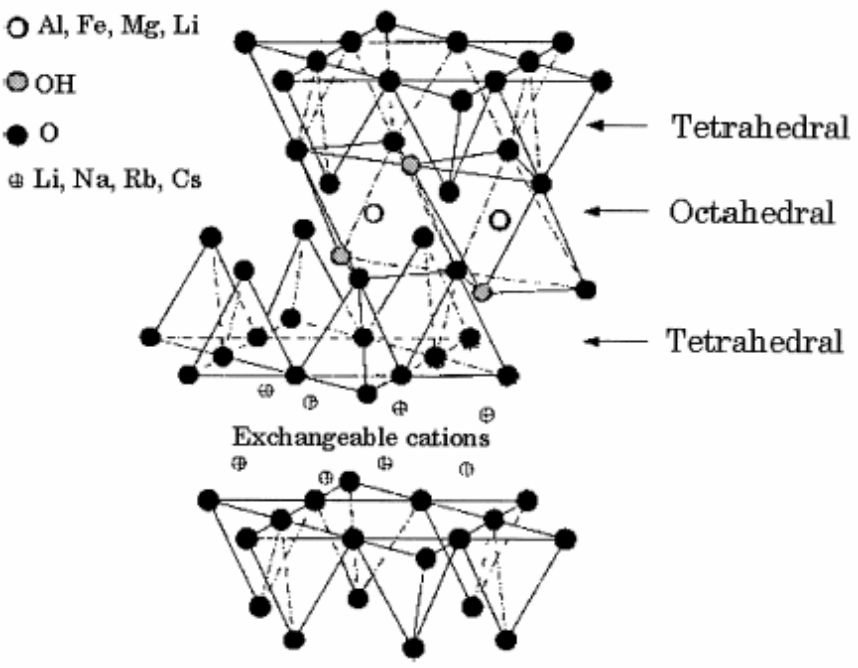

Figure 1.2 The structure of layered silicates [12]

This type of clay is characterized by a moderate negative surface charge (known as the cation exchange capacity, (CEC) and expressed in meq/100 g. The charge of the layer is not locally constant as it varies from layer to layer and must rather be considered as an average value over the whole crystal. Proportionally, even if a small part of the charge balancing cations is located on the external crystallite surface, the majority of these exchangeable cations are located inside the galleries. When the hydrated cations are ion-exchanged with organic cations such as more bulky alkylammoniums, it usually results in a larger interlayer spacing.

Layered silicates have two types of structure: tetrahedral-substituted and octahedral substituted. In the case of tetrahedrally substituted layered silicates the negative charge is located on the surface of silicate layers, and hence, the polymer matrices interact more readily with these than with octahedrally substituted material.

Two particular characteristics of layered silicates that are generally considered for PLS nanocomposites. The first is the ability of the silicate

particles to disperse into individual layers. The second characteristic is the ability to fine-tune their surface chemistry through ion exchange reactions with organic and inorganic cations. These two characteristics are, of course, interrelated since the degree of dispersion of layered silicate in a particular polymer matrix depends on the interlayer cation.

Modification of Clay

One important consequence of the charged nature of the clay is that they are generally highly hydrophilic in nature (because of the presence of hydrated Na+ or K+) and therefore they are compatible only with hydrophilic polymers like Polyethelene oxide (PEO), or Polyvinyl alcohol (PVA). So with most of polymers the physical mixture of a polymer and layered silicate may not form a nanocomposite. This situation is analogous to polymer blends, and in most cases separation into discrete phases takes place. In immiscible systems, which typically correspond to the more conventionally filled polymers, the poor physical interaction between the organic and the inorganic components leads to poor mechanical and thermal properties. Thus it is necessary to alternate the polarity of clay to make it organophilic, which is a prerequisite for formation of clay-polymer nanocomposites so that strong interactions between the polymer and the layered silicate in PLS nanocomposites lead to the organic and inorganic phases being dispersed at the nanometer level. As a result, nanocomposites exhibit unique properties not shared by their micro counterparts or conventionally filled polymers .In order to make clays organophilic, the hydrated cations of the interlayer of normally hydrophilic clay can be exchanged with the cationic surfactants such as primary, secondary, tertiary, and quaternary alkylammonium or alkylphosphonium cations [12]. For example, in montmorillonite, the sodium ions in the clay can be exchanged for an amino acid such as 12-dodecanoic acid (ADA).

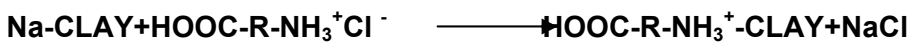

Alkylammonium or alkylphosphonium cations in the organosilicates lower the surface energy of the inorganic host and improve the wetting characteristics

of the polymer matrix, and result in a larger interlayer spacing. Additionally, the alkylammonium or alkylphosphonium cations can provide functional groups that can react with the polymer matrix, or in some cases initiate the polymerization of monomers to improve the strength of the interface between the inorganic and the polymer matrix [13,14].

The structure of the interlayer of the organo-clay can be described as saying that the cationic head group of the alkyl ammonium molecule preferentially resides at the layer surface, leaving the organic tail radiating away from the surface. In a given temperature range, two parameters then define the equilibrium layer spacing: the cation exchange capacity of the layered silicate, driving the packing of the chains, and the chain length of organic tail(s). According to X-ray diffraction (XRD) data, the organic chains have been long thought to lie either parallel to the silicate layer, forming mono or bilayers or, depending on the packing density and the chain length, to radiate away from the surface, forming mono or even bimolecular tilted 'paraffinic' arrangement [10] as shown in Figure 1. 3.

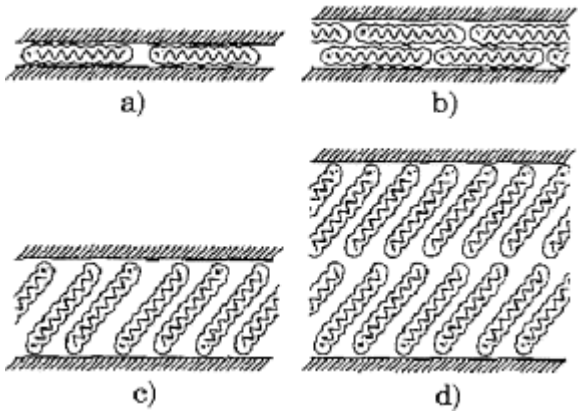

Figure 1.3 Alkyl chain aggregation in layered silicates: (a) lateral monolayer; (b) lateral bilayer; (c) paraffin-type monolayer and (d) paraffin-type bilayer.

A more appropriate explanation was proposed by Vaia et.al on the basis of FTIR experiments. They showed that alkyl chains can vary from liquid-like to solid-like, with the liquid-like structure dominating as the interlayer density or chain length decreases (see Figure1.4), or as the temperature increases. This

occurs because of the relatively small energy differences between the *trans* and *gauche* conformers; the idealized models described earlier assume all *trans* conformations. In addition, for longer chain length surfactants, the surfactants in the layered silicate can show thermal transition akin to melting or liquid-crystalline to liquid-like transitions upon heating.

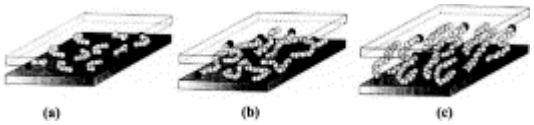

Figure 1.4 Alkyl chain aggregation models: (a) short chain lengths, the molecules are effectively isolated from each other, (b) medium lengths, quasi-discrete layers form with various degree of in plane disorder and interdigitation between the layers and (c) long lengths, interlayer order increases leading to a liquid-crystalline polymer environment. Open circles represent the CH_2 segments while cationic head groups are represented by filled circle [15].

Smectite and vermiculites easily exchange their interlayer charge, which are commonly Ca^{+2},Mg^{+2} and Na^{+}. The potassium ions are so tightly fixed between mica layers that the hydration shells are displaced and the cation exchange requires special condition [10]. Smectites bind a large variety of organic cations. The cations retain a high degree of flexibility in the interlayer spacing and the number of interlayer cations varies randomly (within certain limit) between interlayer space.

An alternative method for the modification of clay is based on use of block or graft polymers where one component of the polymer is compatible with the clay and the other with polymer matrix. A typical block copolymer would consist of a clay compatible hydrophilic block and a polymer compatible hydrophobic block.

Nanocomposite Preparation

Various methods of preparation have been proposed to synthesize clay based polymer nanocomposites. They include the following processes [12].

- **Exfoliation–adsorption:** The layered silicate is exfoliated into single layers using a solvent in which the polymer (or a prepolymer in case of insoluble polymers such as polyimide) is soluble. It is well known that such layered silicates, owing to the weak forces that stack the layers together can be easily dispersed in an adequate solvent. The polymer then adsorbs onto the delaminated sheets and when the solvent is evaporated (or the mixture precipitated), the sheets reassemble, sandwiching the polymer to form, in the best case, an ordered multilayer structure. Under this process are also gathered the nanocomposites obtained through emulsion polymerization where the layered silicate is dispersed in the aqueous phase.

- **In situ intercalative polymerization:** In this technique, the layered silicate is swollen within the liquid monomer (or a monomer solution) so as the polymer formation can occur in between the intercalated sheets. Polymerization can be initiated either by heat or radiation, by the diffusion of a suitable initiator or by an organic initiator or catalyst fixed through cationic exchange inside the interlayer before the swelling step by the monomer.

- **Melt intercalation:** The layered silicate is mixed with the polymer matrix in the molten state. Under these conditions and if the layer surfaces are sufficiently compatible with the chosen polymer, the polymer can crawl into the interlayer space and form either an intercalated or an exfoliated nanocomposite. In this technique, no solvent is required. . This method has great advantages over either in situ intercalative polymerization or polymer solution intercalation. First, this method is environmentally benign due to the absence of organic solvents. Second, it is compatible with current industrial process, such as extrusion and injection molding. The melt intercalation method allows the use of polymers which were previously not suitable for in situ polymerization or solution intercalation but is mainly useful for thermoplastic polymers.

  Recently, the melt intercalation technique has become the standard for the preparation of PLS nanocomposites. During polymer intercalation from

solution, a relatively large number of solvent molecules have to be desorbed from the host to accommodate the incoming polymer chains. The desorbed solvent molecules gain one translational degree of freedom, and the resulting entropic gain compensates for the decrease in conformational entropy of the confined polymer chains. Therefore, there are many advantages to direct melt intercalation over solution intercalation. For example, direct melt intercalation is highly specific for the polymer, leading to new hybrids that were previously inaccessible. In addition, the absence of a solvent makes direct melt intercalation an environmentally sound and an economically favorable method for industries from a waste perspective.

- **Template synthesis:** This technique, where the silicates are formed in situ in an aqueous solution containing the polymer and the silicate building blocks has been widely used for the synthesis of double-layer hydroxide-based nanocomposites [16,17] but is far less developed for layered silicates. In this technique, based on self-assembly forces, the polymer aids the nucleation and growth of the inorganic host crystals and gets trapped within the layers as they grow.

➢ **Exfoliation–adsorption**

This technique has been widely used with water-soluble polymers e.g. poly (vinyl alcohol) (PVOH), poly (ethylene oxide) (PEO), poly (vinylpyrrolidone) (PVPyr) or poly (acrylic acid) (PAA) as well as with polymers solubles in other solvents e.g. nanocomposites of PCL/clay and PLA/clay in chloroform as a co-solvent, and high-density polyethylene (HDPE) with xylene and benzonitrile.

The thermodynamics involved in this method are described in the following. For the overall process, in which polymer is exchanged with the previously intercalated solvent in the gallery, a negative variation in the Gibbs free energy is required. The driving force for the polymer intercalation into layered silicate from solution is the entropy gained by desorption of solvent molecules, which compensates for the decreased entropy of the confined, intercalated chains [18]. Using this method, intercalation only occurs for certain

polymer/solvent pairs. This method is good for the intercalation of polymers with little or no polarity into layered structures, and facilitates production of thin films with polymer-oriented clay intercalated layers. However, from commercial point of view, this method involves the copious use of organic solvents, which is usually environmentally unfriendly and economically prohibitive.

Poly (styrene-co-methyl methyacrylate) / Na-montmorillonite nanocompo -sites can be synthesized by emulsion polymerization with a reactive surfactant AMPS (2-acryiamido-2-methyl-1-propane sulfonic) [19].

Wu et al. [20] reported the intercalation of PEO in Na^+-MMT and Na^+-hectorite using this method in acetonitrile, allowing the stoichiometric incorporation of one or two polymer chains in between the silicate layers and increasing the inter sheet spacing from 0.98 to 1.36 and 1.71 nm, respectively. Study of the chain conformation using 2D double-quantum NMR on ^{13}C enriched PEO intercalated in Na^+-hectorite reveals that the conformation of the '–OC–CO–' bonds of PEO is (90±5)% *gauche*, inducing constraints on the chain conformation in the interlayer [21].

Recently, Choi et al. [22] prepared PEO/MMT nanocomposites by a solvent casting method using chloroform as a co-solvent. WAXD analyses and TEM observations established the intercalated structure of these nanocomposites.

High-density polyethylene (HDPE)-based nanocomposites has been produced by dissolving the polyolefinic chains in a mixture of xylene and benzonitrile (80:20 wt%) with 20-wt% modified clay dispersed in within. The nanocomposite then recovered by precipitation from tetrahydro furan (THF) followed several washing with THF. XRD reveals a broad diffraction peak that has been shifted towards a higher interlayer spacing [23]. The large broadening of the peak may indicate that partial exfoliation has occurred which is further confirmed by TEM images.

Poly (lactide) (PLA) and poly (ε-caprolactone) (PCL) biodegradable nanocomposites were prepared by using montmorillonite modified with disteryldimethylammonium cations [12].

The Toyota Research group synthesized polyimide–montmorillonite nanocomposite [24] by mixing in dimethylacetamide a modified montmorillonite with the poly (imide) precursor, that is a poly (amic acid) obtained from the step polymerization of 4,4′-diaminodiphenyl ether with pyromellitic dianhydride. The organo-modified montmorillonite was prepared by previous intercalation with dodecylammonium hydrochloride. After elimination of the solvent, an organoclay filled poly (amic acid) film was recovered, which was thermally treated up to 300°C in order to trigger the imidization reaction and to produce the poly (imide) nanocomposite. The XRD patterns of these filled PI films do not show any diffraction peak typical of an intercalated morphology leading the authors to conclude to the formation of an exfoliated structure and explaining the excellent gas barrier properties of the resulting films.

XU et al. in [25] reported PVA-Vermiculite (PVA-VMT) nanocomposite with acid treated VMT. The samples were prepared in two steps, in the first step the VMT was first treated with hydrochloric acid as: To a 1-L polypropylene beaker containing 800 mL of 2M HCl solution, 25g of 250 mesh crude VMT was added at room temperature. The resulting slurry was magnetically stirred for 12 h. The VMT was filtered, washed with water till pH = 7 and then dried at 300^0C overnight. In the second step the delaminated VMT was then added to the PVA solution with various mixing times. The delamination process was monitored by XRD and TEM. As received VMT yielded characteristics diffraction peaks at 2 = 3.5, 7.3 and 8.7. The XRD patterns at different time intervals dictate the delamination of VMT by increase in basal spacing. The TEM photographs of the VMT indicate the presence of only about five layers (with a total thickness of 50) and most of the VMT layers were delaminated. FTIR spectra show that with the acid delamination, the hydroxyl group concentration increases in the VMT surface i.e. the peak area at approximately 3400 cm^{-1}, corresponding to –OH groups increased with extended HCL treatment. Depending upon the mixing time, both intercalated and exfoliated nanocomposite samples can be prepared.

For instance, the characteristic VMT peak at $2\theta = 7.32^0$ was shifted to $2\theta = 1.8^0$ after mixing for 12h. This suggest the formation of intercalated nanocomposites while after 24 h mixing the peak corresponding to intercalated VMT was also missing demonstrating the formation of exfoliated nanocomposites, which was confirmed by TEM micrographs which shows the VMT layers dispersed individually in PVA matrix.

- **In situ intercalative polymerization**

Many interlamellar polymerization reactions using layered silicates have long been known but it is with the work initiated by the Toyota research team on polymer-layered silicate nanocomposites that gave momentum to the field PLS nanocomposites. The 12-aminolauric acid (n=12) modified montmorillonite was chosen to develop the intercalative ring opening polymerization of ε-caprolactam [9].

Another polyamide, i.e. nylon-12, is reported to form nanocomposites using the in situ intercalative polymerization. Indeed, Reichert ET al. [26] have used 12-aminolauric acid (ALA) as both the layered silicate modifier and the monomer. XRD, TEM, Scanning TEM coupled with energy dispersive X-ray (EDX) as well as atomic force microscopy (AFM) have been used to characterize the resulting composites. They all confirm the structure as being partially exfoliated and otherwise intercalated nanocomposites.

In situ intercalative polymerization has been largely studied for producing poly (styrene)-based nanocomposites. Akelah et al. [27] modified the interlayer of Na-montmorillonite and Ca-montmorillonite by exchanging the inorganic cations with (vinyl benzyl) trimethyl ammonium chloride, increasing the interlayer spacing by 5.4 A. These modified clays were then dispersed and swollen in various solvent and co-solvent mixtures such as acetonitrile, acetonitrile/toluene and acetonitrile/THF. Styrene polymerization's were carried out in presence of N, N′-azobis (isobutyronitrile) (AIBN) and carried out at 80°C for 5 h.

A drawback of this technique remains that the macromolecule produced is not a pure PS but rather a copolymer between styrene and (vinyl benzyl) trimethyl ammonium cations.

Polyolefins represent another important family of polymers that has been investigated in order to produce nanocomposites through in situ intercalative polymerization process. Tudor et al. [28] have demonstrated the ability of soluble metallocene catalysts to intercalate inside silicate layers and to promote the coordination polymerization of propylene. A very recent report discusses also about the synthesis of poly (ethylene terephtalate) (PET) nanocomposites by using the in-situ intercalative polymerization [29].

The synthesis and characterization of polyaniline (PAn)/clay with extended chain conformation has been proposed by Wu, et al [30]. The Na-MMT was added into deionised water and stirred for 2h at 80°C, and then aniline and HCl were added. Then the mixture was washed with a large amount of deionised water several times after stirring for 6h at 80°C. Cooling to room temperature and regulating the pH value at 2 with HCl, ammonium persulfate ($(NH_4)_2S_2O_8$) was added and the polymerization process took more than 10h. The green precipitate was filtered and was washed with deionised water thoroughly and dried in vacuum. XRD pattern of PAn/MMT nanocomposite powder shows the interlayer distance as 14.82A°. The expansion is in agreement with the intercalation of single chain rather than coiled conformation.

- **Melt intercalation**

Poly (ε-caprolactone) (PCL) /clay nanocomposites were prepared by melt intercalation or melt blending [31]. Polybenzoxazine / clay hybrid nanocomposites were prepared from a polybenzoxazine precursor and organically modified montmorillonite (OMMT) as layered silicates. OMMT were prepared by the surface treatment of MMT by octyl, dodecyl or stearyl ammonium chloride [32]. Polybenzoxazine/clay hybrid nanocomposites have been prepared from organically modified montmorillonite (OMMT) and mono- or bifunctional benzoxazine [33]. OMMT was prepared by the cation exchange of

montmorillonite (MMT) with salts of amines such as phenylethylamine, aminolauric acid, tyramin and dodecyl amine.

Nylon 6-organoclay nanocomposite were prepared through melt intercalation by using a conventional twin-screw extruder [34]. Maleic anhydride grafted polyethylene /clay nanocomposites have been prepared by simple melt compounding [35]. Poly (styrene-co-acrylonitrile) (SAN)/organoclay nanocomposites have been prepared using poly (ε-caprolactone) (PCL) as a compatibilizer by Kim et el. [36]. Poly (ethylene oxide) (PEO)/Na^+-MMT and PE-PEG (polyethylene-polyethylene glycol) diblock copolymer/Na^+-MMT nanocomposites were prepared by using melt intercalation [37].

Tjong et al. [38] reported the polyethylene (PE)-layered vermiculite (VMT) nanocomposites, fabricated via direct melt compounding in a twin-screw extruder followed by injection moulding. The acid treatment of the VMT was according to process reported in [39]. The acid delaminated VMT was then treated with Maleic anhydride (MA) to get MA-delaminated VMT. The Maleic anhydride (MA) act as either the intercalation agent or as a compatibiliser for the PE and VMT phases. As received VMT shows characteristic peaks at 2 =3.88, 7.38 and 8.70o, all these peaks disappear after acid treatment. X-ray diffraction and transmission electron microscopic observations revealed the formation of exfoliated PE/VMT nanocomposites.

The same authors in [40] synthesized impact modified polypropylene (PP)/ vermiculite (VMT) nanocomposites toughened with maleated styrene-ethylene butylenes-styrene (SEBS-g-MA), compounded in a twin screw extruder and injection molded. The effect of impact modifier was studied. TEM revealed an exfoliated VMT silicate layer in ternary (PP-SEBS-g-MA)/VMT nanocomposites.

In another report Tjong et al [41] reported a novel approach to the preparation of polymer nanocomposites utilizing a low molecular weight reactive modifying reagent .The reactive reagent used is maleic anhydride which acts

both a modifier for the polymer matrix and as a swelling agent for the silicate. Vermiculite /PP nanocomposites were prepared by simple melt mixing of MAV and PP. XRD patterns show a absence of vermiculite reflections in the nanocomposites, indicating exfoliated nanocomposites, which was conformed by SEM and TEM examinations.

- **Template Synthesis**

This method is particularly adapted to water soluble polymers and some attempts have been achieved with polymers such as poly (vinyl pyrrolidone) (PVPyr), hydroxy propylmethylcellulose (HPMC), poly (acrylonitrile) (PAN), poly (dimethyldiallylammonium) (PDDA) and poly (aniline) (PANI) [42]. The method for in situ hydrothermal crystallization of a polymer/hectorite nanocomposite consists in refluxing for 2 days a 2 wt.% gel of silica sol, magnesium hydroxide sol, lithium fluoride and the desired polymer in water. XRD patterns show the formation of a polymer/hectorite-intercalated nanocomposite. Syndiotactic polystyrene (s-PS)/modified-clay nanocomposites have been prepared by solution blending by mixing pure s-PS and organophilic clay with adsorbed cetyl pyridinium chloride (CPC) in dichlorobenzene [43].

Morphology of clay/polymer nanocmposites

By using X-ray diffraction (XRD) and transmission electron spectroscopy (TEM), the structure of polymer/clay nanocomposites has been elucidated. Depending on the nature of the components used (layered silicate, organic cation and polymer matrix) and the method of preparation, three main types of composites may be obtained when a layered clay is associated with a polymer In the case where the polymer is unable to intercalate with the clay silicate layers, a phase separated composites is obtained, whose properties stay in the same range as traditional micro composites. (Fig. 5a). Except this, there are also other two types of nanocomposites. Intercalated structure (Fig. 5b) in which a single or sometimes more than one extended polymer chain is intercalated between the silicate layer resulting in a well order multilayer morphology which generally built up with alternating polymeric and inorganic layers. An exfoliated or delaminated structure is obtained if the silicate layers are completely or uniformly dispersed in a continuous polymer matrix. (Fig. 5c) [11]

For well ordered intercalate, the individual crystallite layered silicate is tightly packed.

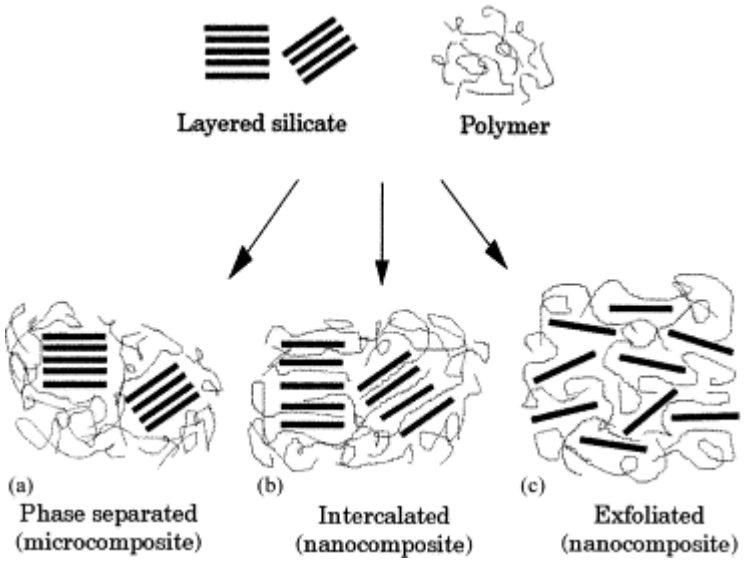

Figure 1.5 Scheme of different types of composite arising from the interaction of layered silicates and polymers: (a) phase-separated microcomposite; (b) intercalated nanocomposite and (c) exfoliated nanocomposite.

Properties of Polymer/Clay Nanocomposites

Nanocomposites consisting of a polymer and layered silicate (modified or not) frequently exhibit remarkably improved mechanical and materials properties when compared to those of pristine polymers containing a small amount (≤5 wt%) of layered silicate. Improvements include a higher modulus, increased strength and heat resistance, decreased gas permeability and flammability, and increased biodegradability of biodegradable polymers. The main reason for these improved properties in nanocomposites is the stronger interfacial interaction between the matrix and layered silicate, compared with conventional filler-reinforced systems.

- **Tensile properties**

The Young's modulus (or tensile modulus), which is the measure of stiffness of a material, has shown to be strongly improved when nanocomposites are formed. Nylon-6 nanocomposites obtained through the

intercalative ring opening polymerization of ε-caprolactam leading to the formation of exfoliated nanocomposites, show a drastic increase in the Young's modulus at rather low filler content.

Actually, the material stiffness is substantially enhanced whatever the way of preparation: polymerization within organo-modified montmorillonite (NCH), polymerization within protonated ε -caprolactam swollen montmorillonite (L-NCH) [12], and polymerization within natural montmorillonite, in the presence of ε -caprolactam and an acid catalyst (one-pot-NCH)[44]. The dependence of Young's modulus measured at 120°C for exfoliated nylon-6 nanocomposites can be directly related to the average length of the layers and hence, the aspect ratio of the dispersed nanoparticles and moreover the extent of exfoliation. The effect of clay content on the mechanical property of poly (ε-caprolactone)/ (PCL) nanocomposites has been studied and it has been found that the Young's modulus of the PCL nanocomposites is higher compared to neat PCL. This is due to the intercalated or exfoliated structure. For instance, Young's modulus is significantly increased 216 MPa to 390 MPa for the composite containing 10 wt% of modified montmorillonite (MMT) [31]. In contrast, Young' modulus of the nanocomposites formed by the non-modified montmorillonite (MMT-Na) is basically independent of the clay content within the investigated range.

The Young's modulus in polypropylene nanocomposites [45] obtained by melt intercalation was studied where the amount of maleic anhydride-modified PP (PP-MA) added to increase intercalation (and to possibly favor exfoliation) is varied. Results are compared to the corresponding microcomposite as well as to simple PP-MA/PP polymer blends. It is found that increasing the amount of PP-MA (from sample PPCH 1/1 to PPCH 1/3) not only improves intercalation or partial exfoliation, but increases also the modulus value. Comparison of PP with the simple PP-MA/PP blends rules out any possible effect of some matrix modification due to the presence of increasing amounts of PP-MA .

For PMMA [46] or PS [47] based nanocomposites, obtained by emulsion polymerization in presence of water-swollen Na-montmorillonite, the increase in

Young's modulus is relatively weak, going, e.g. from 1.21 to 1.30 GPa for pure PMMA and PMMA containing 11.3 wt.% intercalated montmorillonite, respectively.

The modulus of PS/clay was found to increase .The enhancement in modulus reasonable attributed to the high resistance exerted by MMT against the plastic deformation [47]. The strength of PS/clay nanocomposites was found to be less than PMMA/clay nanocomposites. The mechanical properties are attributed to the fixation of polymer chain into interlayer of MMT and the restricted segmental motion between the organic inorganic interfaces.

Filled polymers such as exfoliated nylon-6-based nanocomposites prepared following different methods or intercalated PMMA-based nanocomposites [46] exhibit an increase in the stress at break, that is usually explained by the presence of polar (PMMA) and even ionic interactions (nylon-6 grafted onto the layers) between the polymer and silicate layers. This increase appears to be much more pronounced in case of nylon-6 which has both an exfoliated structure and ionic bonds with the silicate layers. As far as polypropylene-based nanocomposites are concerned [45], no or only very slight tensile stress enhancement are measured . This behavior can be partially explained by the lack of interfacial adhesion between apolar PP and polar layered silicates. Addition of maleic anhydride modified polypropylene to the polypropylene matrix has, however, proved to be favorable to the intercalation of the PP chains and maintains the ultimate stress at an acceptable level. In PS-intercalated nanocomposites [47], ultimate tensile stress is even much decreased compared to PP matrix and further drops down at higher filler content. This lack of properties is attributed by the authors to the fact that only weak interactions exist at the poly (styrene)-clay interface contrary to the previous compositions in which (stronger) polar interactions may take place, strengthening the filler matrix interface.

The effect of nanocomposite formation on the elongation at break has not been widely investigated. When dispersed in thermoplastics such as for

intercalated PMMA [46] and PS [47] or intercalated–exfoliated PP, the elongation at break is reduced. In the last case, the decrease is very important, dropping from 150 and 105% for a pure PP matrix and a 6.9 wt.% non-intercalated clay microcomposite, respectively, down to 7.5% in the better case for a PP-based nanocomposite filled with 5 wt.% silicate layers.

The tensile strength of PE/VMT nanocomposites [38] increases with an increase in VMT content. For PE/2%VMT nanocomposites the tensile strength is 24.36% higher then neat PE. The enhancement results from the nanoscale dispersion of VMT with in PE and from improvement in the compatibility between VMT and PE, which is due to the grafting reaction between MA and PE. The elongation and energy at break decreases greatly with the addition of VMT. The elongation at break of the nanocomposite containing 0.5wt% is about 74.8% lower than neat PE. The reduction in tensile ductility with an increasing VMT content in the nanocomposites is a typical characteristic of short-fiber-reinforced polymer composites.

The tensile properties of PP/VMT binary blends and (PP-SEBS-g-MA)/VMT ternary blends were studied [40]. The addition of only 4wt% of VMT to PP improves tensile strength and stiffness considerably. This is due to the intrinsic high modulus of silicates that act as rigid modifier particles. Compared with that of the PP/4%VMT binary nanocomposites, the tensile strength of the (PP-SEBS-g-MA)/VMT ternary nanocomposites slightly decreases with an increase in the SEBS content. However the tensile strength of the nanocomposites containing 5 and 10% SEBS are still higher than those of maleated PP and neat PP. This is due to the nanoscale dispersion of VMT within the PP-SEBS matrix and from an improvement in the compatibility between PP, SEBS and VMT. As the SEBS content is increased to 15% and greater the tensile strength of the nanocomposite drops to that of neat PP. The elongation at break and energy at break increases greatly with the addition of SEBS.

The tensile strength of PP [41] increases by 18.3% with the addition of only 2% vermiculite and by upto 29.5% when 5% vermiculite is introduced. The introduction of vermiculite into the PP matrix increases the stiffness at the expense of the toughness of the nanocomposites. Significant reduction in the elongation at break and energy at break was observed with clay.

- **Flexural properties**

Nanocomposite researchers are generally interested in the tensile properties of final materials, but there are very few reports concerning the flexural properties of neat polymer and its nanocomposites with OMLS. Very recently, Sinha Ray et al. [48] reported the detailed measurement of flexural properties of neat PLA and various PLACNs. They conducted flexural property measurements with injection-molded samples according to the ASTM D-790 method. There was a significant increase in flexural modulus for PLACN4 when compared to that of neat PLA, followed by a much slower increase with increasing OMLS content, and a maximum at 21% for PLACN7. On the other hand, the flexural strength and distortion at break shows a remarkable increase with PLACN4, then gradually decreases with OMLS loading. According to the author, this behavior may be due to the high OMLS content, which leads to brittleness in the material.

- **Impact Properties**

Impact properties have been measured for nylon-6 based nanocomposites prepared either by in situ intercalative polymerization of Є-caprolactone using protonated amino dodecanoic acid exchanged montmorillonite [12] or by melt intercalation of nylon-6 in octadecyl ammonium exchanged montmorillonite. Both methods lead to exfoliated nanocomposites especially when the filler content does not exceed 10 wt.% because at higher filler level, melt-intercalation provides partially exfoliated partially intercalated materials. The formation of nylon-6-based nanocomposites does not reduce too much the impact properties, whatever the exfoliation process used. In the case of in situ intercalative polymerization, the Izod impact strength is reduced from 20.6 to 18.1 J/m when 4.7wt % of nanoclay is incorporated. Charpy impact

testing shows similar reduction in the impact strength from 6.21 kJ/m^2 for the filler-free matrix down to 6.06 kJ/m^2 for the 4.7 wt % nanocomposite. It is found that the decrease in the Izod impact strength of melt-intercalated nylon-6-based nanocomposites is not too much pronounced over a relatively large range of filler content. Further the notched izod impact strength of PA6, PA6CN, and PA6CN/PP-g-MAH alloys has increased significantly in the case of grafted nanocomposites.

The direct melt blending of the PP/VMT nanocomposite with SEBS-g-MA [40] appears to be an effective way of improving toughness of PP/VMT nanocomposites. The impact strength increases dramatically with the SEBS-g-MA content up to 15%. For 15% SEBS-g-MA, the impact strength is 4.5 times higher than that of nanocomposite containing no impact modifier.

- **Dynamic mechanical analysis**

Dynamic mechanical analysis (DMA) measures the response of a given material to a cyclic deformation (usually tension or three-point flexion type deformation) as a function of the temperature. DMA results are expressed by three main parameters: (i) the storage modulus (E'), corresponding to the elastic response to the deformation; (ii) the loss modulus (E''), corresponding to the plastic response to the deformation and (iii) tan δ, that is the (E'/E'') ratio, useful for determining the occurrence of molecular mobility transitions such as the glass transition temperature.

DMA analysis has been studied to track the temperature dependence of storage modulus upon the formation of an intercalated PS nanocomposites by exfoliation–adsorption during emulsion polymerization [47]. No significant difference in E' can be seen in the investigated temperature range, indicating that intercalated nanocomposites do not strongly influence the elastic properties of the matrix. On the other hand, the shift and broadening of the tan δ peak towards higher temperatures for the nanocomposite indicate an increase in the glass transition temperature together with some broadening of this transition.

This behavior has been ascribed to the restricted segmental motions at the organic–inorganic interface neighborhood of intercalated compositions.

For room temperature elastomer such as nitrile rubber [49], a three-fold increase of the storage elastic modulus is noted by the simple dispersion/exfoliation of 10 parts of organoclay per 100 parts of rubber, with a modulus as high as 8.8 MPa. This value corresponds to what can be obtained with the same matrix filled with 40 parts of carbon black per 100 parts of rubber, thus reducing by a factor of four the amount of filler.

The influence of dispersion and length of the layered particles is demonstrated in case of poly (imide)-based nanocomposites using various organoclays (hectorite, saponite, montmorillonite and synthetic mica)[24]. In this study, exfoliated structures were obtained for mica and montmorillonite clays while a partially exfoliated–partially intercalated structure was found for saponite and a mainly intercalated morphology was attributed to the hectorite-based nanocomposite. The temperature dependence of the storage modulus for these nanocomposites filled with 2 wt.% of clay and for the unfilled matrix was studied. At a given temperature, higher storage moduli results from the better nanofiller dispersion. The huge difference between exfoliated montmorillonite and exfoliated mica-based nanocomposites may be again explained by the respective aspect ratio of the dispersed silicate layers, with lengths of 0.218 and 1.23 μm, respectively, for montmorillonite and synthetic mica, as observed by TEM.

Two T_g's were observed in DMA experiments for PE/VMT Nanocomposites [38] corresponding to the Tg's of amorphous and crystalline PE phases, respectively. A very small amount of VMT results in an increase of Tg of the PE amorphous phase from -119 to -112^{o}C. However, there is no effect of VMT additions on the Tg of the PE crystalline phase. The addition of clay has little effect on the crystallization temperature (T_c) of the PE phase. Moreover the change of melting temperatures (T_m's) of the PE phase of nanocomposites with the addition of clay is comparable to that of T_c. It is also found that the

PE/4%VMT nanocomposites having the highest melting enthalpy (H) exhibits a minimum T_c value. This implies that the nanoscale dispersion of VMT with in PE leads to an increase in the crystalinity but to a decrease in T_c because of its nucleating effect. The storage Modulus of the PE/VMT nanocomposites increase significantly with an increasing VMT content i.e. the storage modulus of the nanocomposites with only 4% VMT is 1.528GPa at 250C, which is 52% higher than that of pure PE.

The DMA studies show that the storage modulus decreases with an increasing VMT content [40]. For example, the storage modulus of the nanocomposite with only 5% SEBS is 1.62 GPa which is 46% lower than that of the PP/4%VMT nanocomposite without SEBS. The introduction of an elastomer into the nanocomposites can greatly reduce their stiffness and strength.

The storage modulus increases significantly upon formation of nanocomposites [41]. The loss modulus curve for nanocomposite shows a new peak at about 67^0C when compared with neat PP. This behavior implies that a new microphase consisting of ternary molecule PP/MA/VMT is formed in the nanocomposites.

- **Thermal Properties**

Another highly interesting property exhibited by polymer-layered silicate nanocomposites concerns their increased thermal stability but also their unique ability to promote flame retardancy at quite low filling level through the formation of insulating and incombustible char.

- **Thermal Stability**

Nylon 6 nanocomposites have somewhat lower thermal stability than neat nylon 6.This is attributed to degradation of the quarternary alkylammonium

treatment on the montmorillonite, however fire retardant properties were improved. [34].

The thermal stability of a material is usually assessed by thermogravimetric analysis (TGA) where the sample mass loss due to volatilization of degraded by-products is monitored in function of a temperature ramp [12]. Blumstein first studied the indication of thermal stability improvement in nanocomposites in 1965. He studied the thermal stability of PMMA intercalated within montmorillonite and found that 10 wt.% clay intercalated PMMA degrades at temperature 40-50°C superior to the degradation of the pure unfilled PMMA matrix. The enhanced thermal property is not only due to the difference in chemical structure, but also to restricted thermal motion of the macromolecule in the silicate interlayer.

The glass transition temperature (Tg) of polyimide is higher than 250°C [50]. The effect of DMONT (dodecyl-montmorillonite) content on glass transition temperature of both rigid-rod and flexible polyimide film was studied. It is found that T_g values of the rigid-rod polyimide are higher than that of the flexible one. Moreover, T_g values of the rigid polyimide nanocomposites are lower than that of the pure one and fluctuate while there is a slight reduction of T_g values for the flexible polyimide nanocomposites except at high DMONT content (>6 wt.%). It can be explained that when temperature is raised upon curing some dodecylamine molecules in DMONT can loosen out. As a result, the imidisation extent is lowered allowing more mobility of polymeric chains so that glass transition temperatures of the nanocomposites decrease and do not seem to depend on DMONT content. These results agree with the results from FTIR and TEM. However, this side reaction is less significant to lower the glass transition temperature for the flexible polyimide (BTDA/ODA-MDA) nanocomposites. This can be explained that although the side reaction occurred while curing leads to enhance the flow or to lower glass transition temperature of these nanocomposites, the rigidity of the clay silicate layer causes a strong suppression to flow for the flexible polyimide so that both effects are cancelled

out. Increasing DMONT content to 6–9 wt.% impedes the flow significantly; even up to 400°C.

The introduction of VMT into PVA resulted in a slight increase in the Tg of the PVA-VMT nanocomposites to approximately 73oC [39], and Tg increased approximately 3.4oC only if 5 wt% VMT was introduced into the PVA. This suggests that the VMT layers were well dispersed in the PVA-VMT nanocomposites. The amorphous chains of PVA become stable and intercalated strongly with the VMT layers. In other words, the intercalated clay or VMT could restrict the motion of the PVA molecular segment. With further increase in the clay content no further increase in the Tg of the nanocomposites was observed. This could be due to the excess coagulation VMT in the PVA solutions and could not disperse individually very well. The presence of coagulated VMT might not have led to the Tg increase of PVA.

The introduction of vermiculite [41] results a slight increase in the T_g of the PP matrix to 15.8^{o}C this is due to the fact that in PP/MA/VMT nanocomposites the mobility of the PP chains is restricted by the presence of vermiculite layers. However the Tm of the nanocomposites shows a little change because the nanoscale filler do not alter the crystalline size. The 5% loss temperature ($T_{5\%}$) and the maximum weight loss temperature (T_{max}) of nanocomposite reveal that the addition of MA/VMT leads to a marked decrease in $T_{5\%}$ from 309.5 to the 280^{0}C. This could arise because the acid protonated VMT contains excess MA. Unreacted MA is easily sublimed, resulting in the decrease in the $T_{5\%.}$ On the other hand, the T_{max} of the nanocomposite tends to increase with VMT content which clearly indicate that VMT exhibits a beneficial effect on the thermal stability on PP.

- **Flame retardancy**

The flame retardant properties of nanocomposites have been very recently reviewed in detail by Gilman [51]. The main bench-scale method used to measure important parameters in the flame-retardant behavior of a material (heat release rate, peak of heat release rate, heat of combustion,) is Cone

calorimetry. In a typical experiment, the sample is exposed to a given heat flux (often taken as 35 kW/m^2) and the heat release rate (HRR) as well as the mass loss rate are recorded as a function of time. It is worth noting that reduction of the peak HRR is the most clear-cut evidence for the efficiency of a flame retardant. Moreover, gas and soot production is also measured. The HRR plot obtained for nylon-6 and a nylon-6 exfoliated nanocomposite (5 wt.% of exfoliated montmorillonite) was studied .A 63% reduction in the peak HRR is clearly observed for the nanocomposite. Cone calorimetry experiments have been carried out on other nanocomposites such as exfoliated nylon-12 (2 wt.% organoclay), exfoliated poly (methylmethacrylate-co-dodecylmethacrylate) [52], intercalated PS (3 wt.%) or intercalated PP (2 wt.%) and for each material, a significant decrease in the peak HRR is recorded while the heat of combustion, smoke and the carbon monoxide yields (other important properties in flammability concern) are usually not increased. These data tend to demonstrate that the improvement in flame retardancy does not occur by a process in the gas phase but rather by a modification of the combustion process in the condensed phase.

Experiments carried out in a radiative gasification apparatus [53] have allowed to determine that the flame retardant effect of nanocomposites mainly arises from the formation of char layers obtained through the collapse of the exfoliated and/or intercalated structures. This multilayered silicate structure may act as an excellent insulator and mass transport barrier, slowing down the escape of the volatile decomposition products as observed in nylon-6 but also in thermoset nanocomposites [54]. Whatever the nature of the matrix (thermoplastics or thermosets) and whatever the structure of the nanocomposite (exfoliated or intercalated), always the same interlayer spacing (13 Å) was found for the recovered chars as analyzed by XRD, implying the formation by combustion of a residue of the same nature.

- **Thermal Expansion Coefficient**

At low temperature operation where a material is rigid or below its glass transition temperature (Tg), the thermal expansion coefficient (CTE) is an

important parameter to indicate the thermal mismatch for protective coating application.

The effect of the polymer structures and dodecylmontmorillonite (DMONT) content on CTE behavior between nanocomposites of flexible polyimides with the rigid ones was studied It is found that the effect of organophilic clay to suppress the thermal expansion of polyimide matrix is more pronounced for the hybrids with flexible polyimide than the rigid polyimide nanocomposites. The lowering of CTE caused by the addition of DMONT is due to the fine dispersion of silicate layers in the polymer matrices, which can obstruct the expansion of polymer chains when the temperature is raised. Since the structure of the rigid rod polyimide is quite symmetry such that its thermal expansion is relatively low, the effect of DMONT (dodecylamine modified montmorillonite) content on the CTE is less significant [50]. The thermal coefficient of polyimide-based nanocomposites prepared with hexadecyl ammonium cation exchange montmorillonite can be reduced, going from 3.5×10^{-5} /K to values as low as 1.55×10^{-5}/K when 10wt%of nanofiller was dispersed.

1.2 EPOXY RESIN

Introduction

Epoxy resin is defined as a molecule containing more than one-epoxide groups. The epoxide group also termed as, oxirane or ethoxyline group, is shown.

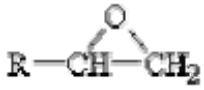

EPOXIDE

These resins are thermosetting polymers and are used as adhesives, high performance coatings and potting and encapsulating materials. These

resins have excellent electrical properties, low shrinkage, good adhesion to many metals and resistance to moisture, thermal and mechanical shock. Viscosity, epoxide equivalent weight and molecular weight are the important properties of epoxy resins.

Advantages of epoxy resin:

- Low level of creep under sustained load.
- High strength and stiffness.
- Moderately good thermal and chemical resistance.
- Low shrinkage on curing.
- Good gap feeling properties.
- Low or no VOCs present in formation.
- Great formulation capabilities due to low viscosity and many types of base resin and curing agents are available.
- Ability to curing under wide range of conditions

Disadvantages of epoxy resin:

- Rigid and brittle in nature.
- Low impact strength.
- Low peel strength.
- Requires metering and missing.
- Requires time and/or temperature of cure.
- Irritant and certain chemical can be health hazard.

Introduction of Polymer modification:

Polymer modification has became a major route to better polymer properties and wider polymer application in the 1990s.The high cost of developing a completely new polymer and the many long term performance objective a new polymer must meet have pushed firms to innovate by modification and blending rather than synthesis of a new monomer and polymer.

Unmodified epoxy resins are usually single-phase materials, while the addition of modifiers turns the toughened epoxy resin into multiphase system. When modifiers domains are correctly dispersed in discrete forms throughout the epoxy matrix, the fracture energy or toughness can be greatly improved. The reason is that cross-linked epoxy resins have limited ability to deform by shielding and crazing, especially in the triaxial stress field present inside the sample at the crack tip. However, the addition of second phase modifiers changes this situation and can significantly improve the fracture toughness.

Modifiers Used for the Epoxy Resin Toughening:

Different kinds of modifiers have been studied to improve the toughness or ductility of cured epoxy resins. The modifiers can be classified into four main groups.

- Low Molecular Weight Liquid Rubber.
- Functionally Terminated Engineering Thermoplastics.
- Reactive Ductile Diluents.
- Inorganic /Hybrid Particles.

Influence Factors on the Properties of Modified Epoxy Resins:

- Cross-link density of the epoxy-resin.
- Type of modifier or tougher.
- Microstructures resulting from the presence of a second polymeric phase.

1.3 CLAYS

The term 'clay' is used also to identify mineral particles of the size < 0.002 mm. The structure of clay silicates is similar to that of primary silicates, i.e., they are sheet silicates. These are composed of silicon tetrahedral sheets, aluminium hydroxide sheets, and / or magnesium hydroxide sheets.

Montmorillonites

These clay silicates form by crystallization from solution high in soluble silica and magnesium. Montmorillonite has a 2 : 1 layer structure. All tetrahedra

in the sheets contain Si^{4+} ions. Aluminium is the normal ion in the central sheet, but about one-eight of the octahedra contain Mg^{2+} as a substituting ion for Al^{3+}. The negative charge caused by substitution is neutralized by various hydrated cations adsorbed to the surface of the sheets. The force of bonding between cations and the sheets is not very strong and depends on the amount of water present. In dry montmorillonites the bonding force is relatively strong. When wet conditions occur, water is drawn into the interlayer space between sheets and causes the clay to swell dramatically (expanding clay). A characteristic feature of montmorillonite is the extensive surface for the adsorption of water and ions, therefore the cation exchange capacity of montmorillonite is very high. Layers of the smectite group range in thickness from 0.98 to 1.8 nm or more.

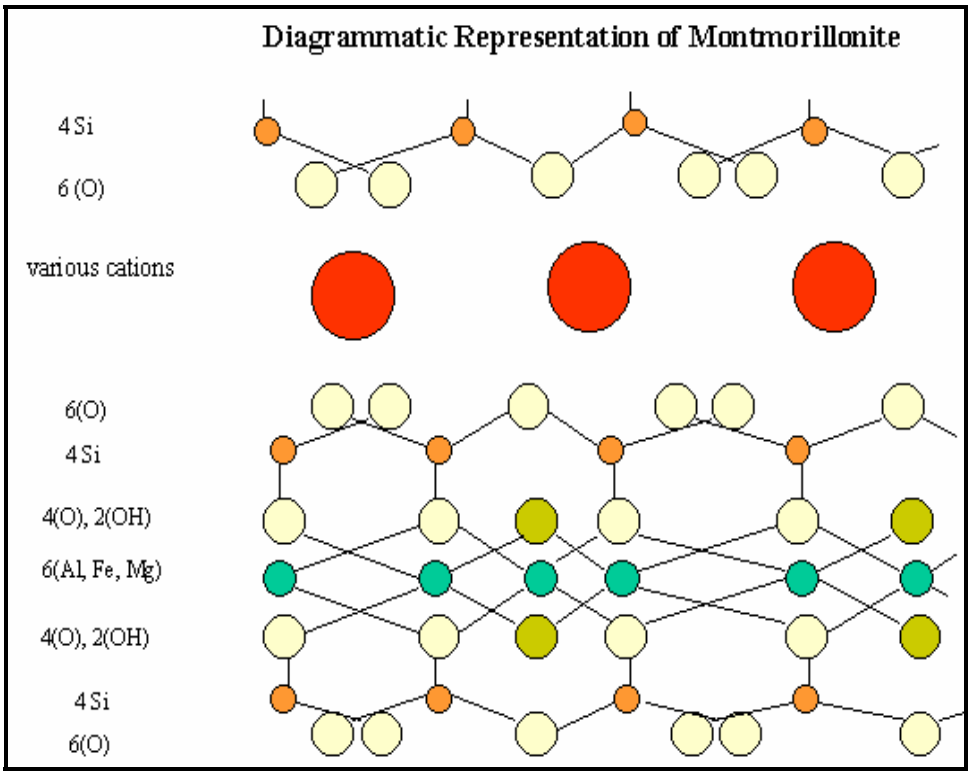

Figure 1.6 Diagrammatic representation of Montmorillonite

Vermiculites

These clays have a 2 : 1 structure of primary mica minerals. Vermiculites contain either Al^{3+} or Mg^{2+} and Fe^{2+} as normal octahedral ions, and tetrahedral sheets in which Al^{3+} occurs as a substituted ion in place of some of the Si^{4+}. Vermiculite differs from the micas in that it contains hydrated cations rather than unhydrated K^{+} in the interlayer space. The weak bonding afforded by these ions allows vermiculite to expand on wetting. Expansion is less than in montmorillonite, however. Unlike montmorillonite and kaolonite, vermiculite does not form by crystallization from solution, but instead it is formed by alteration, or the selective replacement of ions in a structure without destroying the structure (e.g. micas are altered to vermiculites). Layer spacing ranges from 1.0 to 1.5 nm or more.

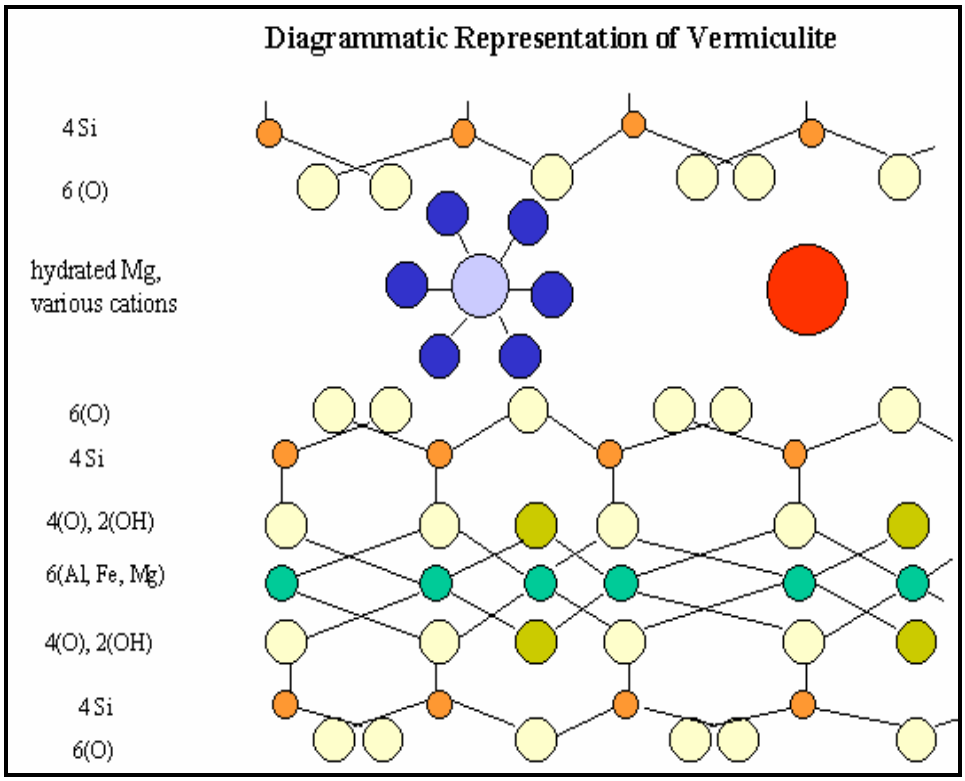

Figure 1.7 Diagrammatic representation of Vermiculite

Properties

The properties of clay minerals are summarized in Table 1.2.

Table1.2 Summary of clay mineral properties.

Clays	Type	Interlayer condition / Bonding	CEC [cmol/kg]	Swelling potential	Specific surface area [m^2/g]	Basal spacing [nm]
Montmorillonite	2 : 1 (expanding)	very weak bonding, great expansion	80 - 150	high	700 - 800	.98 -1.8 +
Vermiculite	2 : 1 (expanding)	weak bonding, great expansion	100 -150	high	500 - 700	1.0 -1.5 +

1.4 Epoxy- clay Nanocomposites

Epoxy resins find many industrial applications in adhesives, construction materials, composites, laminates, castings, and aircraft and spacecraft industries owing to their high strength, low viscosity, low volatility and low shrinkage during cure, low creep, and good adhesion to many substrates. Epoxy- clay nanocomposites have been known for long. These are prepared by in-situ polymerization method. The studies of thermoset epoxy systems considered the ring opening polymerization of epoxides to form polyether nanocomposites. Studies of both rubbery and glassy thermoset epoxy/clay nanocomposites formed using different types of amine curing agents were done, and the mechanisms leading to the monolayer exfoliation of clay layers in thermoset epoxy systems were greatly elucidated as a result. In addition, the polymer/clay interfacial properties have been shown to play a dominant role in determining the performance benefits derived from nanolayer exfoliation.

Messersmith and Giannelis [55] first reported the preparation of epoxy resin based nancomposites of OMLS based on the diglycidyl ether of bisphenol A (DGEBA), and MMT modified by bis (2-hydroxyethyl) methyl hydrogenated tallow alkylammonium cation. WAXD patterns of uncured clay-DGEBA samples also indicate that intercalation occurred, and that this intercalation improved in going from room temperature to 90 °C. In a subsequent paper, Wang and

Pinnavaia [56] reported the preparation of nanocomposites using the epoxy resin DGEBA, and the concomitant delamination of acidic forms of MMT at elevated temperatures using the self-polymerization technique.

In another study, Pinnavaia and Lan [57] reported the preparation of nanocomposites with a rubber-epoxy matrix obtained from DGEBA derivatives cured with a diamine so as to reach subambient glass transition temperatures. It has been shown that depending on the alkyl chains length of modified MMT, an intercalated and partially exfoliated or a totally exfoliated nanocomposite can be obtained. The same author's [58] also studied other parameters such as the nature of alkyl ammonium cations present in the gallery and the effect of the CEC of the MMT when DGEBA was cured with *m*-phenylene diamine.

Vineeta Nigam and D.K.Setua [59] studied the exfoliation behavior of montmorillonite in epoxy resin nanocomposites. They used an aromatic diamine [diamino diphenyl methane (DDM)] as a curing agent in combination with diglycidyl ether of bisphenol-A (DGEBA). The microstructural analysis of nanocomposites was done by WAXS and scanning electron microscopy (SEM) techniques.

Starting from another type of layered material, magadiite, which is a layered silicic acid, Pinnavaia et al. [60] developed a different kind of exfoliated structure where the layers were still organized, but spaced by approximately 80 Å of elastomeric epoxy matrix arising from the curing of DGEBA derivative by Jeffamine 2000.

Recently, Kornmann et al. [61] reported the synthesis of epoxy-based nanocomposites using two different types of MMT clays with different CECs, in order to investigate the influence of the CEC of the MMT clay on the synthesis and structure of nanocomposites.

A research group [62] from Australia recently reported the morphology, thermal relaxation and mechanical properties of layered silicate nanocomposites of high-functionality epoxy resins. Three different types of resins were used:

bifunctional DGEBA, trifunctional triglycidyl *p*-amino phenol (TGAP), and tetrafunctional tetraglycidyldiamino diphenylmethane (TGDDM). All were cured with diethyltoluene diamine (DETDA). MMT modified with octadecylammonium cation was used for the preparation of nanocomposites. The nanocomposites were prepared using in situ intercalative polymerization method. In a typical synthesis, OMLS was first dispersed in the resin at 80 °C using a stirrer at 500 rpm. After mixing the resin–OMLS blend for 30 min the curing agent was added and the system kept under vacuum for another 60–90 min at around 70 °C. The blends were then cured for 2 h at 100 °C, 1 h at 130 °C, 12 h at 160 °C followed by a post-cure for 2 h at 200 °C.

The morphology of the cured samples was investigated using WAXD and different microscopy techniques. WAXD patterns of the MMT concentration series shows that the organoclay with an initial *d*-spacing of 2.3 nm is mainly exfoliated in the DGEBA-based system. On the other hand, high content (10 wt%) OMLS shows intercalated structure, while DGEBA-based systems, resins of higher functionality, show distinctive peaks even at low OMLS loading, indicating that these nanocomposites have a lower degree of exfoliated structure. In the case of most nanocomposite systems, the peak observed around 2.5 nm correlates to the (002) plane and therefore represents only half the distance of the *d*-spacing.

AFM phase contrast images of the DGEBA nanocomposite containing 5 wt% layered silicate did not show individual layers, unlike TEM. A striated structure, however, can be seen with increasing phase intervals at the top of the picture. So from the AFM images it is established that although silicate layers are not homogeneously distributed in the matrix, some stacked layers are present.

Very recently, Chen et al. [63] synthesized an epoxy-MMT nanocomposite using a surface initiated method in order to understand the

interlayer expansion mechanism and thermal–mechanical properties of these nanocomposites. MMT modified with bis-2-hydroxyethyl methyl tallow ammonium cation (C30B) was used as the OMLS for nanocomposite synthesis. 3,4-Epoxycyclohexylmethyl-3, 4-epoxycyclohexane carboxylate was used as the epoxy monomer, and hexahydro-4-methylphthalic anhydride (HHMPA), ethylene glycol (EG), and benzyldimethylamine (BDMA) were used as curing agent, initiator and catalyst, respectively, during synthesis. In a typical preparative method, the epoxy monomer HHMPA was mixed in a molar ratio of epoxide groups to HHMPA of 1–0.87. The resulting mixture was denoted as the *resin* by authors. The desired amount of EG, BDMA and C30B were added to the resin, and the materials were then blended using an orbital mixture, until the blend became bubble free and homogeneously mixed. The blended samples were then immediately cured, first isothermally for up to 8 h at temperatures ranging from 70 to 140 °C, followed by 8 h at 180 °C, and finally 12 h at 220 °C under vacuum.

The curing mechanism for an epoxy–anhydride system with an alcohol initiator was studied. Amine catalysts like BDMA were added to the mixture to accelerate the reaction by facilitating the ring opening of epoxy groups. Several published papers indicate that intragallery onium ions can catalyze the epoxy curing reaction and thus lead to favorable conditions for obtaining exfoliated nanocomposites. To fully understand crosslinking reactions in the presence of C30B were due to hydroxy initiation and not due to catalytic reactions. For this reason, the extent of reaction of a resin containing C30B was compared to the extent of reaction for a neat resin and resins containing either EG or BDMA. It is found that curing kinetics of the resin–C30B system more closely resembles the curing kinetics of the resin–EG system than that of the resin–BDMA system. This is a direct indication that the nanocomposites are predominantly cured via initiation by the surfactant hydroxy groups and not by catalytic means. Also the curing rate of the pristine resin is significantly lower than that of the other mixtures. This highlights an important prerequisite for interlayer expansion, which is that extra-gallery polymerization rates should be slower than intra-gallery polymerization rates.

X. Kornmann [64] used three different curing agents Jeffamine D-230 and two cycloaliphatic polyamines: 3,3′-dimethylmethylenedi (cyclohexylamine) (3DCM) and Amicure bisparaaminocyclohexylmethane (PACM) in combination with diglycidyl ether of bisphenol A (DGEBA) epoxide resin. The structure of the clay in the nanocomposites is characterized by X-ray diffraction (XRD) and transmission electron microscopy (TEM).

Yilmazer et al. [65] synthesized diglycidyl ether of bisphenol A type epoxy resin-polyether polyol-organically treated montmorillonite ternary nanocomposites. The effects of addition of polyether polyol as an impact modifier investigated by X-ray diffraction, and scanning electron microscopy (SEM) showed that organically treated montmorillonite is intercalated by epoxy, since the interlayer spacing expanded from 1.83 to 3.82 nm upon nanocomposite synthesis.

Yang et. al. [66] synthesized epoxy-montmorilonite nanocomposites using montmorillonite clays (CWC, AMS and Kunipia-F with CEC 145,125 and 125 meqiv/100g respectively) obtained from three different sources, with different surfactants (alkylamines $[CH_3(CH_2)_{n-1}NH_2]$ n=6,12,and18, aminocarboxylic acids $[H_2N(CH_2)_{n-1}COOH]$, n=6 and12 and diamines $[H_2N(CH_2)_nNH_2]$ with n=6 and 12) using different methods of intercalation methods i.e. Ion exchange method, an acid base method by aqueous medium and an acid base method by vapor.

X. Kornmann and his team in [67] synthesized high-performance epoxy-layered silicate nanocomposites based on tetraglycidyl 4,4'-diaminodiphenylmethane (TGDDM) resin and cured with 4,4'-diaminodiphenyl sulfone (DDS) using fluorohectorite modified with dihydroimadazolines and octadecylamine as surfactants. XRD studies show that there is an increase in basal spacing by 1.4 to 2.8nm with different surfactants. TEM micrographs conform the increase in basal spacing, with parallel silicate layers typical for thermoset-layered silicate nanocomposites synthesized by in-situ

polymerization. The scanning electron micrographs of the nanocomposites based on different surfactants shows bright spots corresponding to aggregates of layered silicates.

In another paper Kornmann [68] studied the influence of the silicate surface Modification on the properties. They used different amines i.e. monoamine, diamine, and triamine oligopropyleneoxides and octadecylamine, benzyl amine and adduct of octadecylamine and benzylamine as surfactants with flurohectirite as layered silicate. The protonation of exclusively one amino group in each surfactant was attempted by addition of suitable amount of hydrochloric acid to solution so that these unprotonated amino reactive groups could possibly react with epoxy network during nanocomposite synthesis.

Pinnavaia et al. in [69] synthesized the glassy epoxy-clay nanocomposites with diprotonated forms of polyoxypropylene diamines of the type α,ω- $[NH_3CHCH_3CH_2(OCH_2CHCH_3)_xNH_3]^{2+}$ with x=2.6, 5.6 and 33.1 intercalated into montmorillonite and fluorohectorite clays. Here the intercalated onium ions functioned concomitantly as a surface modifier, intragallary polymerization catalyst, and curing agent. Depending upon the chain length of the diamine, different orientations of the propylene oxide chains were adopted in the clay galleries, resulting in basal spacings from 14 Å (lateral monolayer, x=2.6) to 45 Å (folded structure, x=33.1), which is much higher than the basal spacing in pristine clays. It was found that the clay-diamine intercalates greatly reduced the plasticizing effect of the alkyl chains on the polymer matrix when compared with clay-monoamine intercalates with less time and low cost needed for nanocomposite fabrication.

Properties of Epoxy-Clay Nanocomposites

- **Tensile Properties**

The evolution of the tensile modulus for the epoxy matrix with three different types of layered silicates was studied [60]. A C18-MMT, a C18A-magadiite, and a magadiite modified with methyl-octadecylammonium cation (C18A1M-magadiite) were used for nanocomposite preparation. For thermoset

matrices, a significant enhancement in the tensile modulus is observed for an exfoliated structure when alkylammonium cations with different chain length modified MMTs were used for nanocomposite preparations, with the exception of the MMT modified with butylammonium, which only gives an intercalated structure with a low tensile modulus.

Pinnavaia and Lan [57] reported the tensile strengths and moduli of epoxy-clay Nanocomposites.. The relationship between the alkylammonium cation chain length of the organoclay and the mechanical properties of the composites is reported for loadings of 10 wt % $CH_3(CH_2)_{n.l}NH_3$+-montmorillonite. The presence of the organoclay substantially increases both the tensile strength and the modulus relative to the pristine polymer. The mechanical properties increase with increasing clay exfoliation in the order $CH_3(CH_2)_7$-montmorillonite.

It is noteworthy that the strain at break for all of our epoxy-clay composites is essentially the same as the pristine matrix, suggesting that the exfoliated clay particles do not disrupt matrix continuity. Reinforcement of the epoxy-clay nanocomposites also is dependent on clay loading. The tensile strength and modulus for the $CH_3(CH_2)_{17}$-NH_3+-montmorillonite system increases nearly linearly with clay loading. More than a 10-fold increase in strength and modulus is realized by the addition of only 15 wt % (7.5 vol %) of the exfoliated organoclay. The rubbery epoxy matrix used in this work exhibits 40-60% elongation at break. It was propaosed that in case of the rubbery epoxy matrix used in this work the clay platelets in the cured polymer are partially aligned in the direction of the matrix surface. When strain is applied in the direction parallel to the surface, the clay layers will be aligned further. This strain induced alignment of the layers will enhance the ability of the particles to function as the fibers in a fiber reinforced plastics. Propagation of fracture across the polymer matrix containing aligned silicate layers is energy consuming, and the tensile strength and modulus are reinforced

.

Pinnavaia in [58] reported the tensile strengths and moduli for the aminecured epoxy-clay nanocomposites for loadings in the range 1-2 wt %. For the pristine amine-cured epoxy matrix, the tensile strength is 90 MPa and the

tensile modulus is 1.1 GPa. On comparing the mechanical properties it was found that the exfoliated nanocomposites show improved performance, in the modulus but not in the tensile strength, relative to the pristine polymer.

Vineeta Nigam and D.K.Setua [59] reported that a rise in the clay concentration from 0 to 6% leads to 100% increase in the tensile modulus, 20% increase in ultimate tensile strength, and 80% decrease in elongation at break values.

The tensile strength in [65] decreases with increasing amount of montmorillonite at constant polyol content. This is attributed to higher stress concentration effect of clay agglomerates at high clay contents.

- **Flexural Properties**

O. Becker et al. [62] determine modulus of nanocomposites using three point bend test. For all resins i.e. DGEBA, TGAP and TGDDM a monotonic increase in modulus with increasing organoclay concentrations was observed.
X. Kornmann et al. [64] reported the flexural moduli of the epoxy systems cured with Jeffamine D-230 and DCM at zero clay content were, respectively 2.95 and 2.61 GPa. For both systems, the flexural modulus increases substantially with the true clay content, despite the small amounts of clay added. Indeed, for the nanocomposite cured with jeffamine D-230, the modulus is increased by 43% with only 4.2 vol% of clay. The synthesis of a exfoliated nanocomposite structure allows the clay layers to more effectively swell in the epoxy matrix leading to the better dispersions and larger stiffness improvement. The explanation for this strong reinforcement effect is the increase in effective volume fraction of reinforcement entities as the distance between the clay layers is increased. The relative increase in flexural modulus is larger for the nanocomposite cured with Jeffamine D-230 than for the one cured with 3DCM.

- **Impact Properties**

Isik et al [65] studied the impact strength of the impact modified epoxy/montmorillonite nanocomposites. It was found that the impact strength of materials with no clay increases with increasing polyol content. It is observed that the impact strength decreases with respect to the clay content. Especially at high clay contents, clay particles agglomerate and act as stress concentrators.

- **Dynamic mechanical analysis (DMA)**

The effect of molecular dispersion of the silicate layers on the viscoelastic properties of the cross-linked polymeric matrix was probed using DMA in [55]. The temperature dependencies of the tensile storage modulus, *E',* and tanδ of the OMTS/DGEBA/BDMA composite containing 4% silicate by volume and the DGEBA/BDMA epoxy without any silicate was studied. The shift and broadening of the tan δ peak to higher temperatures indicates an increase in nanocomposite Tg and broadening of the glass transition. The shift in Tg as measured by the tan δ peak maximum is on the order of only a few degrees (4 ^{0}C for the sample) and cannot account for the significant increase in plateau modulus. Chemical bonding at the interface of the silicate and epoxy matrix could lead to hindered relaxational mobility in the polymer segments near the interface, which leads to broadening and increase of Tg. Below Tg both samples exhibit high storage modulus, with a slight decrease in *E'* with increasing temperature. Notably, *E'* in the glassy region below Tg is approximately 58% higher in the nanocomposite compared to the pure epoxy **(**2.44 x 10^{10} compared to 1.55 x 10^{10} dyne/cm^2 at 40 ^{0}C). Even more striking is the large increase in *E* at the rubbery plateau of the nanocomposite. The nanocomposite exhibits a plateau modulus approximately 4.5 times higher than the unmodified epoxy (5.0 x 10^8 compared to 1.1 x 10^8 dyn/cm^2 at 150 ^{o}C). These changes were found to be considerable, particularly in view of the fact that the silicate content is only 4% by volume.

Kornmann [68] showed that the Tg decreases with organoclay content for composites synthesised with ME-JEF T403. This could be explained on the basis of the fact that for the stoichiometry to be maintained in all the mixtures , a

smaller amount of the curing agent (with the reactive amino groups present in the surface modifiers taken in to account) was added when diamine – or triamine- exchanged Somasif ME-100 was used . Since the organosilicate did not exfoliate in the epoxy , so not all amine functions could react with the network. The stochiometry was no longer respected , so the composite synthesised with the protonated triamine-exchaqnged organosilicate, ME-T403, presented a steady decrease in its Tg with the true silicate content.

P.S.He et al [70] said that ,for intercalated nanocomposites, the glass transition temperature of epoxy corresponds to the epoxy resin cured out of the gallery from the results of DMTA, which is affected by the curing temperature and time , and the α' peak of the loss tangent of the nanocomposite disappears with the addition of the montmorillonite . DMTA proves that the glass transition temperature of the exfoliated nanocomposites decreases with the increase of the montmorillonite content, the storage modulus in the rubbery region increases with the increase of the montmorillonite content, and the amplitude of the storage modulus of the intercalated nanocomposites in the rubbery region increases with increasing the 16-mont loading.

- **Differential scanning Calorimetry (DSC)**

Ole Becker (62) investigate the effect of on octadecyl ammoinium ion exchanged organoclay on the cure of various high-performance epoxy resins by DSC. DSC temperature scans of the resin mixed with 0-10% of the organoclay only (no hardner) showed a single sharp peaks . It was found that the modified clay influences the DGEBA self-polymerization. The addition of 2.5wt% clay decreases the reaction peak temperature by almost 150^0C. Any further addition of clay only decreases the reaction peak temperature only slightly. The mechanism proposed for this say that the alkylamminium ion generates protons through dissociation and these protons catalyze the ring- opening polymerisation.The resins of higher functionalities ,TGAP and TGDDM, show a much smaller monotonic decrease in the reaction peak temperature by only 3-6^0C with each additional 2.5% of organoclay. The reason for this weaker effect for high functionality resin could be explained with the fact that these resins are

harder to exfoliate. Therefore, less organoclay or alkylamminium ions were accessible to catalyze the homopolymerisation reactions.

In the DSC curves of epoxy/amine /organoclay blends , the appearance of more than one peaks for the curing reaction of DGEBA system was found to be related to the different curing reactions. The catalyzed reaction occur at a lower temperature , and increases with increasing organoclay content. The second , high-temperature peak is due to the curing reaction outside the organoclay galleries and refer to non-catalyzed resin/hardner system. The TGAp and TGDDM based resin/organoclay/hardner systems show a single broad reaction peak with shoulder towards higher temperature. For TGDDM systems the cure reaction peak decreases with increasing clay concentration from 214^0C for neat systems to 183^0C for the blend containing 10% organoclayand these exothermic peaks are due to resin hardner cure reaction because the self-polymerisation for this system occur at temperature above 300^0C.

Vineeta Nigam and D.K.Setua [59] found that the onset temperature of curing (T_{onset}) is in the range of 85+-5^0C for all compositions of DGEBA/organoclay/DDM nanocomposites. They also show that an increase in the organoclay content caused a shift in the exothermal peak temperature ($T_{midpoint}$) to lower values and the catalytic effect of the octadecylammonium ion on epoxy ring opening polymerization leads to a decrease in the ultimate heat of reaction (ΔH).They also studied the DSC kinetic studies on the extent of reaction versus time. It was found that the cure rate of the pristine resin was enhanced by the addition of organoclay and the rate is also progressively increased with increasing clay content. The extent of reaction was also found to increase with time and stabilized up to 3 h in all cases, which is equal to the standard cure time adopted in the preparation of composites. A secondary reaction due to the organic modification of the clay was also found in the DSC plots. A gradual decrease of *Tg* with increasing concentration of clay indicates that it is not an absorbed layer effect, which usually increases the *Tg.* Rather, the polymer chains are tied through the surface of the silicate by electrostatic interaction, thus reducing the surrounding entanglements. Another hypothesis concerning the decrease of *Tg* is that there occurs a modification of the epoxy network by its

homopolymerization within the clay galleries. Indeed, if homopolymerization of the epoxy is favored between the layers, this may cause a displacement of stoichiometry in the epoxy network so that the *Tg* is reduced. The excess of unreacted curing agent may also plasticize the epoxy network. Due to the complexity of several possible reactions, it is difficult to determine which of these factors govern the decrease of *Tg.*

Kornmann [64] studied the cure kinetics of three epoxy systems to clarify the effect of curing agent on the nanocomposite structure. They showed that the curing agent has a major effect on the synthesis of exfoliated –clay nanocomposites . The exfoliation of the organophilic clay in epoxy systems is controlled by a relative difference in the reaction rates between the extragallery and the extragallery polymerization. The curing temperature controls both the cure kinetics and the diffusion rate of curing agents between the clay layers. By changing the cure temperature, the relative extent of intragallery and extragallery polymerization. The flexibility (i.e. molecular mobility) and the reactivity of the curing agent are important parameters, which influences the balance between the extragallery and the intragallery reaction rates.

Chen et al [66] determined the T_g of epoxy-clay nanocomposites by DSC. It was found that the epoxy polymer with out the addition of organoclay shows the Tg at 108.40C. The addition of Na+-montmorilloonite during the polymerization of epoxy-polymer decreased the T_g to 92.50C. The epoxy resins polymerized in the presence of 5 and 20 phr of $[H_3N(CH_2)_{17}CH_3]^+$-montmorillonite show a higher T_g's at 117.4 and 146.1^{0}C.

Kornmann [67] studied the influence of the organosilicates on the homopolymerisation of TGDDM and on the polymerisation of the TGDDM/DDS systems using DSC. The homopolymerisations of TGDDM and TGDDM with 10 wt% of ME-100 show similar behaviour with an exothermal peak at 3160C. The difference in intensity of the exothermal peak is caused by the presence lower amount of the polymer in the filled epoxy system. This suggest that the ME-100 have no influence on the homopolymerisation of the TGDDM. While with

organosilicates the exothermal peak shifts to lower temperature which indicates the influence of the surface modification on the homopolymerisation of the TGDDM resin. Since the reaction mechanism is acid catalysed, octadecylammonium ions were found to be more acidic and hence best modifier as compared to the protonated dihydro-imidazolines. DSC curves indicates that the flurohectorite ME-100 has no apparent catalytic effect on the polymerisation of the TGDDM/DDS while the ME-W75 have only a small influence on the polymerisation of the epoxy system. In contrast, the exothermal peaks of epoxy mixed with ME-HEODI and ME-RDI present a large tail at low temperature. This is attributed to the catalytic effect of the –OH groups present in their structure, catalyzing the ring-opening polymerisation of epoxy via H-bonding and hydrogen transfer. They also said that the position of the –OH group also influence the interlayer spacing i.e. in RDI the –OH is in the middle of the chain promotes larger layer sepration than HEODI in which group is on a side. Similarly the presence of a shoulder around 180^0C in the DSC curves of the ME-ODA /TGDDM system suggests that a secondary reaction occurs which is caused by the acidic catalysis of octadecylammonium ions on the ring opening polymerization.

- **Thermogravimetric Analysis**

Pinnavaia [69], showed that the TGA provides an additional information on the properties of both the onium ion intercalated clays and the epoxy-clay nanocomposites made from these clays. Chen et al [66] did the TGA of pristine clay and organoclay. They show that the clay has an affinity for water which is conformed by TGA, and weight loss below 200^0C were attributed to the desorption of water, which includes interlayer and interparticle water. The TGA curves show that the organoclay was more hydrophilic than unmodified clay.

CHAPTER 2

EXPERIMENTAL

2.1 Materials

The preparation of Epoxy-Clay Nanocomposites requires following raw materials.

- **Diglycidyl Ether of Bis-phenol A (DGEBA)** - The Epoxy resin DGEBA with weight-averaged molecular weight of 850 used was obtained from Ciba-Geigy Co. (Mumbai, Maharashtra, India).

- **Inorganic Clays -** The inorganic clays used in this study were Montmorillonite and Vermiculite. An industrially purified montmorillonite, K-10 grade was obtained from Sigma-Aldrich Co. (USA) while Vermiculite was obtained from Minelco Specialties (U.K).

- **Diamino diphenyl methane (DDM) -** An aromatic diamine DDM used as curing agent was obtained from Ciba-Geigy Co. (Mumbai, Maharashtra, India).

- **Octadecylamine –** The organic modifier of the clays, octadecylamine was obtained from Sigma-Aldrich Co. (USA).

- **Mould-** A single plate open mould with dimensions 150x150x4 mm was used. It was made out of tool grade steel. All the moulding surfaces were well ground and polished.

- **Silicone Oil-** silicone oil used as mould release agent was QZ-13, obtained from Ciba-Geigy Co. (Mumbai, Maharashtra, India).

- **Acetone-** Industrial grade acetone was used as a mould-cleaning agent.

2.2 Nanocomposite Preparation

Preparation of inorganic composite

Inorganic clays (Montmorillonite and Vermiculite) were dried in an oven at a temperature of 75°C for 24 h. The epoxy resin was mixed with 3.0 % and 6.0 wt % of the inorganic clays with respect to 100% of the epoxy resin as given in Table 2.1 and swelled for 3 h at 75°C. A stoichiometric amount of curing agent (27 g) was then added and mixed well. The mixture was out gassed in a vacuum oven and poured into a steel mold preheated at 75^0C. It was then cured for 3 h at 75°C and post cured for 12 h at 110°C.

Preparation of organoclay

The method was similar to that used by Usuki et al (r). Fifteen grams of the clay was dispersed into 1200mL distilled water at a temperature of 80°C. Octadecylammonium chloride [$CH_3(CH_2)_{17}$ $NH_3^+Cl^-$] was prepared by mixing 5.66 g octadecylamine [$CH_3(CH_2)_{17}$ NH_2] with 2.1 mL HCl solution (10*N*) in 300 mL distilled water. It was poured into the hot clay–water mixture at a temperature of 80°C and stirred vigorously for 1 h. The mixture was then filtered and washed with water in EtOH (50/50 vol %) until no chloride was detected in the mother liquor. The octadecylamine-exchanged clay was then dried at a temperature of 75°C for 3–4 days in a vacuum oven. Thereafter, the organoclay was stored in a dessicator.

Preparation of organoclay composites

The epoxy resin was mixed with the organophilic clay, in varied proportions of 0, 1.5, 3.0, 4.5, and 6.0 wt % with respect to 100 wt % of the epoxy resin (as given in Table 2.1) and was swelled for 3 h at 75°C. A stoichiometric amount (27 g) of the curing agent was then added. The mixture was out gassed in a vacuum oven and poured into a steel mold preheated at 75°C. It was then cured for 3 h at 75°C and post cured for 12 h at 110°C.

Table 2.1 defines the designations of samples and their constituents for all the tests carried out in this report. $EMMT_x$ and $EVMT_x$ stands for Epoxy-Montmorillonite and Epoxy-Vermiculite Nanocomposites. ‘ x ’ in the suffix indicates % age of the respective clay in the nanocomposite.

Table 2.1 Composition of the Epoxy-clay Nanocomposites

Sl.No.	Sample Designation	Epoxy Resin (g)	MMT/VMT (g)	DDM (g)
1	$EMMT_0$ /$EVMT_0$	100	0 /0	27
2	$EIMMT_1$ /$EIVMT_1$	100	3.0 /3.0	27
3	$EIMMT_2$ /$EIVMT_2$	100	6.0 /6.0	27
4	$EOMMT_1$/$EOVMT_1$	100	1.5 /1.5	27
5	$EOMMT_2$/$EOVMT_2$	100	3.0 /3.0	27
6	$EOMMT_3$/$EOVMT_3$	100	4.5 /4.5	27
7	$EOMMT_4$/$EOVMT_4$	100	6.0 /6.0	27

2.3 Characterization Techniques

Wide Angle X- Ray Diffraction

X-ray scattering techniques are most commonly applied for structural studies. The type of information that is obtained by x-ray scattering experiments include phase identification and quantification, crystallinity, crystallite size, lattice constants molecular orientations and structure. WAXD is most commonly used to probe the nanocomposite structure and occasionally to study the kinetics of the polymer melt intercalation .By monitoring the position, shape, and intensity of the basal reflections from the distributed silicate layers, the nanocomposite structure (*intercalated* or *exfoliated*) may be identified. For example, in an *exfoliated* nanocomposite, the extensive layer separation associated with the delamination of the original silicate layers in the polymer matrix results in the eventual disappearance of any coherent X-ray diffraction from the distributed silicate layers. On the other hand, for *intercalated* nanocomposites, the finite layer expansion associated with the polymer intercalation results in the appearance of a new basal reflection corresponding to the larger gallery height.
Wide angle x-ray scattering equatorial scans of the composites as well as fillers were performed at room temperature (25 ± 2°C) by using a Rigaku Rotaflex

diffractometer [Cu/K-alpha 1 radiation, λ=1.5418 Å, 30 kV, 20 mA, step scan: 4-20^0 {2θ}]. The scanning speed and the step size were kept at 6°/min and 0.2°, respectively. The corrected intensity was smoothed and plotted versus 2θ.The position of the peak maximum and corresponding *d*-spacing were computed from the Bragg's diffraction equation:

$$n\lambda = 2d\sin\theta$$

Where *n* is the order of reflection, λ is the wavelength of radiation, and *d* is the interlamellar spacing. The basal spacing for a characteristic 2θ diffraction peak was obtained directly from available software. The plots of Intensity vs. 2θ are shown at page Nos 57 and 58.

Fourier Transform Infrared Spectroscopy (FTIR)

The absorption versus frequency characteristics of light transmitted through a specimen irradiated with a beam of infrared radiation provide a fingerprint of molecular structure. Thus, infrared spectroscopy permits the determination of components or groups of atoms, which absorb in the infrared at specific frequencies, permitting identification of the molecular structure.

The spectra were taken by making KBr pallets with samples on NICOLET MAGNA – 750 spectrophotometer. The plots of % Transmittance vs. wave number cm^{-1} were obtained as given on page Nos 60 and 61.

Tensile Strength and Modulus

Tensile test, in a broad sense, is a measurement of the ability of a material to withstand forces that tend to pull it apart and to determine to what extent the material stretches before breaking. Tensile modulus is an indication of the relative stiffness of a material. Tensile strength is the load, required to break or fall the sample or yield, divided by the cross sectional area at the center of the sample, in tensile mode. Tensile modulus is the ratio of tensile stress and tensile strain.

$$\text{Tensile Strength} = \frac{\text{Tensile load at yield/break}}{\text{Cross sectional area}}$$

$$\text{Tensile Modulus} = \frac{\text{Tensile stress}}{\text{Tensile Strain}}$$

Tensile strength, tensile modulus and elongation at break were evaluated on Universal Testing Machine (UTM) [LLOYOD INSTRUMENTS; Capacity 10 Tons]. The samples were tested as per ASTM D 638. The crosshead speed was kept 5 mm/minute. The machine had hydraulic clamping unit. It had electronic display. The results were obtained in the form of plots of Stress vs. Strain. The results are mentioned in Tables 3.3(i) and 3.3(ii) at page No. 62.

Flexural Strength and Modulus

Flexural strength is the ability of the material to withstand bending forces applied perpendicular to its longitudinal axis. The stresses induced by the flexural load are a combination of compressive and tensile stresses. Flexural stress and strain are given by the following formulas:

Flexural strength/ stress = $3PL/ 2bd^2$

Where,
P = Flexural load (Kg);
L = Span length (cm);
b = width (cm); and
d = Thickness (cm).

Flexural Modulus = $6 Dd/ L^2$

Where,
D = Deflection (cm);
d = thickness (cm); and
L = Span length (cm).

Flexural strength and modulus were measured on Universal Testing Machine (UTM) [LLOYOD Instruments; capacity 10 Tons]. The samples were tested as per ASTM D 790 by a 3 point bend test. The crosshead speed was kept 5 mm/ minute. The span length was 64 mm. The results were given in the form of plots of load vs. displacement. The results are mentioned in Tables 3.4(i) and 3.4(ii) at page No. 65.

Impact Strength

Impact resistance is the ability of a material to resist breaking under a shock loading or the ability to resist the fracture under stress applied at high speed. Impact energy is a measure of toughness. The higher the impact energy of a material, the higher the toughness and vie versa.

Impact strength was measured on Izod impact specimens as per ASTM D-256 on an impact-testing machine (International Instruments, Mumbai). The results are given in the Tables 3.5(I) and 3.5(ii) at page No.67.

Thermal Analysis

Thermal analysis encompasses a family of measurement techniques that record the response of a material to being heated or cooled. Both kinetic and thermodynamic events may be characterized. The dependent variable is usually temperature, but may also be time-for example, when kinetic processes are being measured. The different thermal analysis techniques include Differential Scanning Calorimetry (DSC), Thrmogravimetric Analysis (TGA), Dynamic Mechanical analysis (DMA) etc.

Differential Scanning Calorimetry (DSC)

DSC is probably the most widely utilized of the thermal analysis techniques for characterizing thermosetting materials. Measurements include the extent and rate of chemical conversions; T_g, including verification; characteristic cure parameters; enthalpy relaxation associated with physical aging; and special applications such as pressure DSC and photocalorimetry. Although gelation is not directly detectable by DSC, when DSC is combined with

complimentary techniques, such as dynamic mechanical analysis and /or gelation theory it can yield valuable information such as extent of cure at gel point (α_{gel}) and the isothermal time to reach α_{gel} as a measure of gelation.

A differential scanning calorimetry (DSC) experiments were performed in a DSC 2910 instrument (TA Instruments Inc., New Castle, DE, USA). The temperature range of the equipment was from -150^{0}C to 600^{0}C. The weight of the sample required to be within the range of 0.5mg to 100 mg. The heating rate was kept 10 ^{0} C/minute and temperature range was kept from ambient to 300 ^{0} C for the samples of all compositions. The results were obtained in the form of:

- Initiation temperature (T_{onset}) - onset point for curing.
- Peak temperature ($T_{midpoint}$).
- Glass transition temperature (T_g).
- Final temperature (T_{end}) – at which curing has completed.

The results are mentioned in Tables 3.6(i) and 3.6(ii) at pages No.69.

Thermogravimetric Analysis (TGA)

TGA is used primarily for determining thermal stability of polymers. The most widely used TGA method is based on continuous measurement of weight on a sensitive balance (called a thermobalance) as sample temperature is increased in air or in an inert atmosphere. This is referred to as nonisothermal TGA. Data are recorded as a thermogram of weight versus temperature. Weight loss may arise from evaporation of residual moisture or solvent, but at higher temperatures it results from polymer decomposition. Besides providing information on thermal stability, TGA may be used to characterise polymers through loss of known entity, such as HCl from poly (vinyl chloride). Thus weight loss can be correlated with percent vinyl chloride in a copolymer. TGA is also useful for determining volatilities of plasticizers and other additives. Thermal stability studies are the major application of TGA. A variation of the method is to record weight loss with time at a constant temperature, called isothermal TGA.

Modern TGA instruments allow thermograms to be recorded on microgram quantities of material. In this study, the TGA experiments were performed on TGA 2950 TA Instrument, USA with following characteristics:

Temperature Range	:	RT- 1000^0C
Weighing Capacity	:	1.0 gms
Heating Rate	:	0.1^0C – 100^0C/min
Atmosphere	:	Controlled Flow of Air/N_2
Flow Rate	:	100 cc/min
Balance Resolution	:	0.1 μgms

Test samples in the powder form were taken. The heating rate was kept 200/min and temperature range was kept from ambient to 900^0C, for the samples of all compositions. The TGA thermograms are shown at page nos 73 and 74.

Dynamic mechanical analysis (DMA)

Dynamic mechanical analyzer uses three different principles to study the viscoelastic response of a sample under oscillatory load. They are

- The sample may be driven in forced oscillation or allowed to resume its natural frequency.
- The stress may be applied in flexure, tension / compression, or torsion; and
- The load may be applied continuously and the modified oscillatory response of the sample measured.

In this study, forced oscillation with flexural stress in increasing mode was used. Dynamic mechanical analyzer used was DMA 2980 TA Instrument. USA with following characterstics:

Temperature Range	:	- 150 ^{0}C – 600 ^{0}C
Heating rate	:	0.1 ^{0}C – 50 ^{0}C/min
Modulus Range	:	10^3 Pa to 3 x 10^{12} Pa.

Atmosphere	:	Controlled flow of air.
Sample Size	:	50 x 10 x 4mm

The test samples were prepared using the electrically operated circular saw. The heating rate was kept 20^{o}/min and temperature range was kept from ambient to 250^{0}C, for the samples of all compositions. DMA test was carried out at a frequency of 5 Hz. The result are mentioned in Tables 3.8(i) and 3.8(ii) at page No. 75.

Scanning Electron Microscopy (SEM)

The scanning electron microscope (SEM) forms an image by scanning a probe across the specimen and in the SEM the probe is focused electron beam. The probe interacts with a thin surface layer of the specimen, a few micrometers thick at most. The detected signal commonly used to form the TV - type image is the number of low energy secondary electrons emitted from the sample surface. The advantages of the SEM are well known: images with a three-dimensional appearance, great depth of field, ease of operation and ease of specimen preparation. These advantages are translated into micrographs that are easier to understand .The surface of even large samples can be imaged directly in the SEM. Images can be formed by combinations of signals (secondary electrons, backscattered electrons and x-rays) and the electronic signals processed to form a variety of micrographs with exceptional detail. Micrographs showing surface topography and chemical contrast are readily obtained in a short time by SEM and they are often easy to interpret.

SEM studies were performed in a JEOL JSM 40 CF scanning electron microscope. Prior to the actual SEM observation, the samples were sputter-coated with gold without touching the surface. The morphology of the cross sectional surface of the frozen (liquid nitrogen) fractured surfaces of inorganic and organoclay composites, as observed by the SEM (Page Nos. 83-87) were also analyzed.

Chapter 3

RESULTS AND DISCUSSION

3.1 Wide Angle X- Ray Diffraction

The X-ray diffractrograms of pristine clays, organoclays and their respective nanocomposites are shown in Figures 3.1(i) and 3.1(ii) respectively while the values of 2θ and respective d-spacing for pristine clays, organoclays and their respective nanocomposites are summarized in Table 3.1.

Figure 3.1(i), representing the X-ray patterns of the IMMT, OMMT and their respective nanocomposites, shows that the interlayer spacing of the clay increases from 7.07Å (2θ = 12.50) for the crude clay (IMMT) to 14.72 Å (2θ = 5.99) for organophilic clay (OMMT). The two peaks in the OMMT diffraction pattern might results from the lateral monolayer and lateral bilayer structures respectively. The increase also indicates the intercalation of the long alkylammonium ions between the layers justifying the cation exchange process. The XRD patterns of the epoxy-OMMT nanocomposites did not show any significant peak especially due to low angle range selected. However, such findings can be correlated to formation of well-intercalated or exfoliated structures.

For VMT [Figure 3.1(ii)] the basal spacing of the clay increases from 12.55Å (2θ = 7.035) for IVMT to 17.50Å (2Å = 4.96) for OVMT, indicating the intercalation of alkylammonium ions with-in the clay galleries. The XRD pattern of epoxy-OVMT nanocomposites did not show any significant peak especially in the low angle range which indicate that well intercalated or exfoliated structures were formed.

For inorganic composites of IMMT and IVMT [Figure 3.1(i) (e) and Figure 3.1(ii) (e)] no change in the position of the peaks as compared to IMMT and IVMT clays respectively were observed. This is due to the fact that the epoxy

monomers could hardly overcome the electrostatic attraction between the negatively charged silicate layers for sufficient interlayer expansion required for the formation of nanocomposites.

Table 3.1 Summary of 2 θ and d-spacing values for IMMT, OMMT, IVMT, OVMT and their respective nanocomposites.

Sl. No.	Sample Designation	2-Theta (2θ)	d-Spacing (dÅ)
1	IMMT	12.50	7.07
2	OMMT	5.99	14.72
3	IVMT	7.035	12.55
4	OVMT	4.96	17.50
5	$EIMMT_1$	12.18	7.25
6	$EIVMT_1$	7.035	12.55

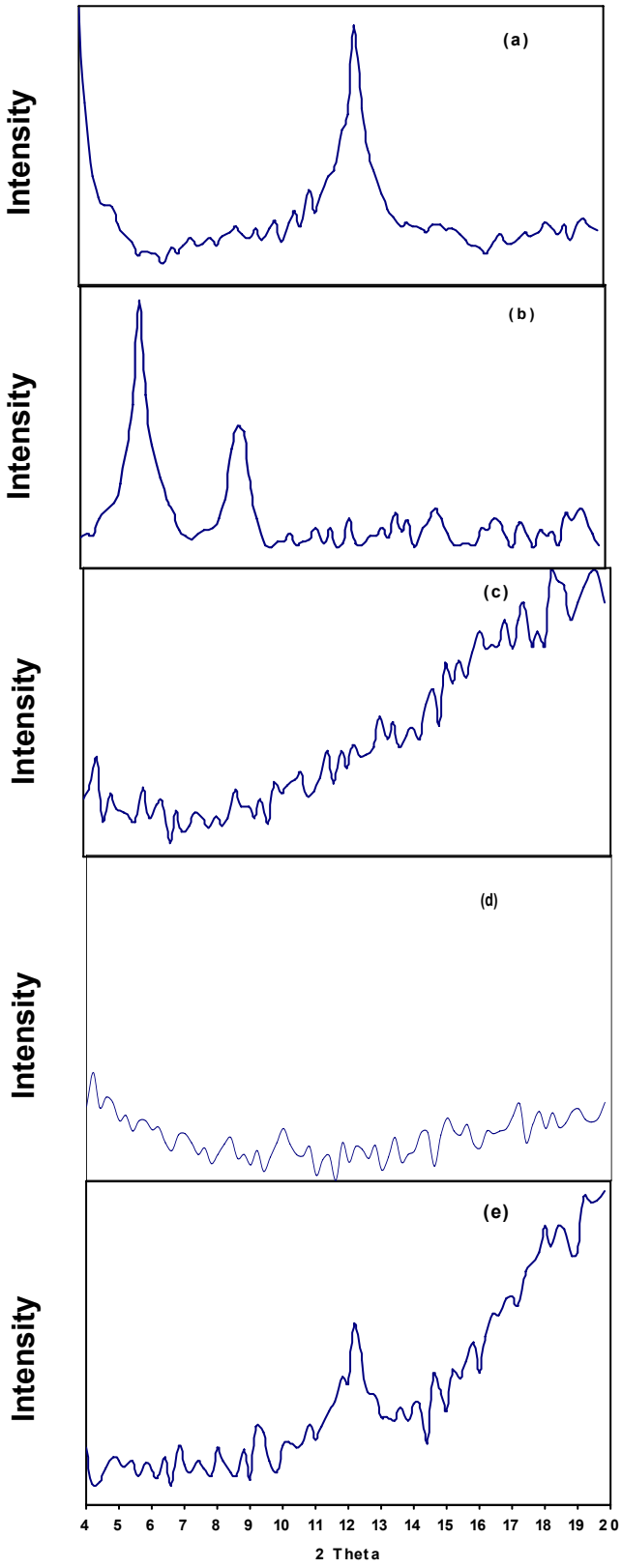

Figure 3.1(i) WAXS diffractograms of (a) IMMT (b) OMMT (c) Epoxy-OMMT(3%) Nanocomposite (d) Epoxy-OMMT(6%) Nanocomposite (e)Epoxy-IMMT(3%) Nanocomposite.

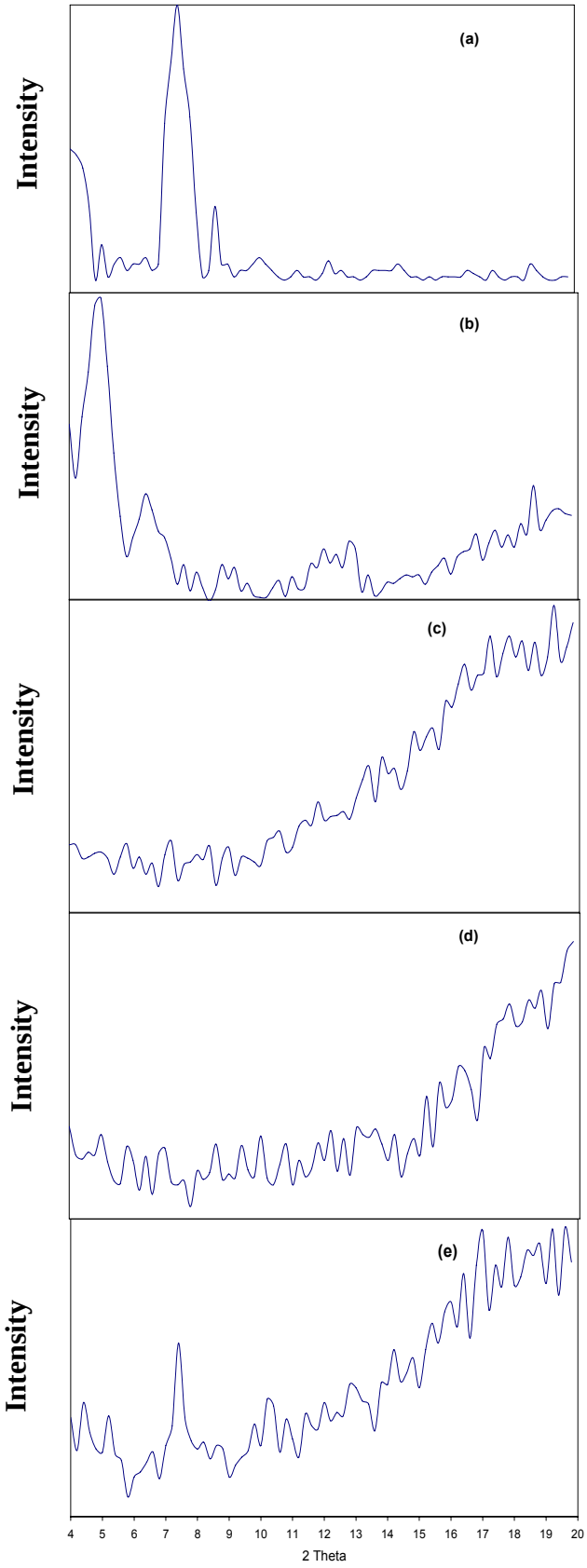

Figure 3.1(ii) WAXS diffractograms of (a) IVMT (b) OVMT (c) Epoxy-OVMT(3%) Nanocomposite (d) Epoxy-OVMT(6%) Nanocomposite (e)Epoxy-IVMT(3%) Nanocomposite

3.2 Fourier-Transform Infra-Red Spectroscopy (FTIR)

The FTIR studies of IMMT, OMMT, IVMT, OVMT and their respective nanocomposites was done and spectra's are in Figures 3.2 (i) and 3.2(ii) respectively.

For both IMMT and IVMT the prominent peaks due to SiO-H stretching and Si-O stretching appeared around 3420 cm^{-1} and 998 cm^{-1}[Figures 3.2(i) A and 3.2(ii) A respectively]. For OMMT and OVMT the presence of peaks in the range of 2600 –3000 cm^{-1} are due to N-H stretching of ammonium group under the C-H absorption along with the peaks of IMMT and IVMT conforming the modification of the inorganic fillers with long chain alkyl ammonium ions. [Figures 3.2(i) B and 3.2(ii) B respectively]. For neat Epoxy cured with DDM the peaks at 1100 cm^{-1} and 3400 cm^{-1} are due to ether group and O-H stretching respectively [Figures 3.2 B]. For the nanocomposites, peak for ether group at around 1100 cm-1 is observed along with the peaks of MMT and VMT while the peak for O-H stretching coincide with the broad SiO-H stretching at around 3400 cm^{-1} [Figures 3.2(i) D, E, F and 3.2(ii) D, E, F respectively].

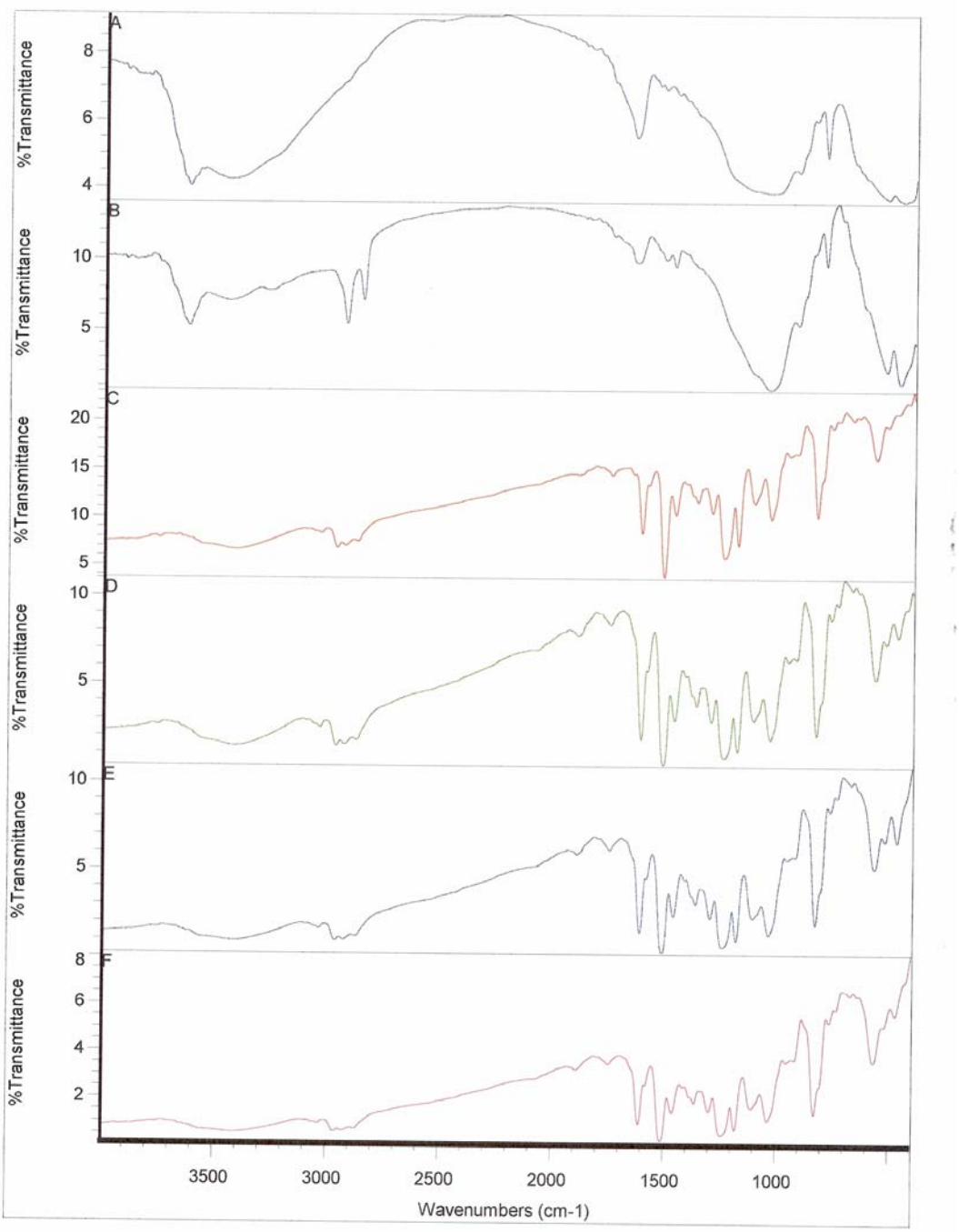

Figure 3.2(i) FTIR spectra's of (A) IMMT, (B) OMMT, (C) Neat Epoxy cured with DDM, (D) $EOMMT_2$, (E) $EOMMT_4$ and (F) $EIMMT_1$ respectively.

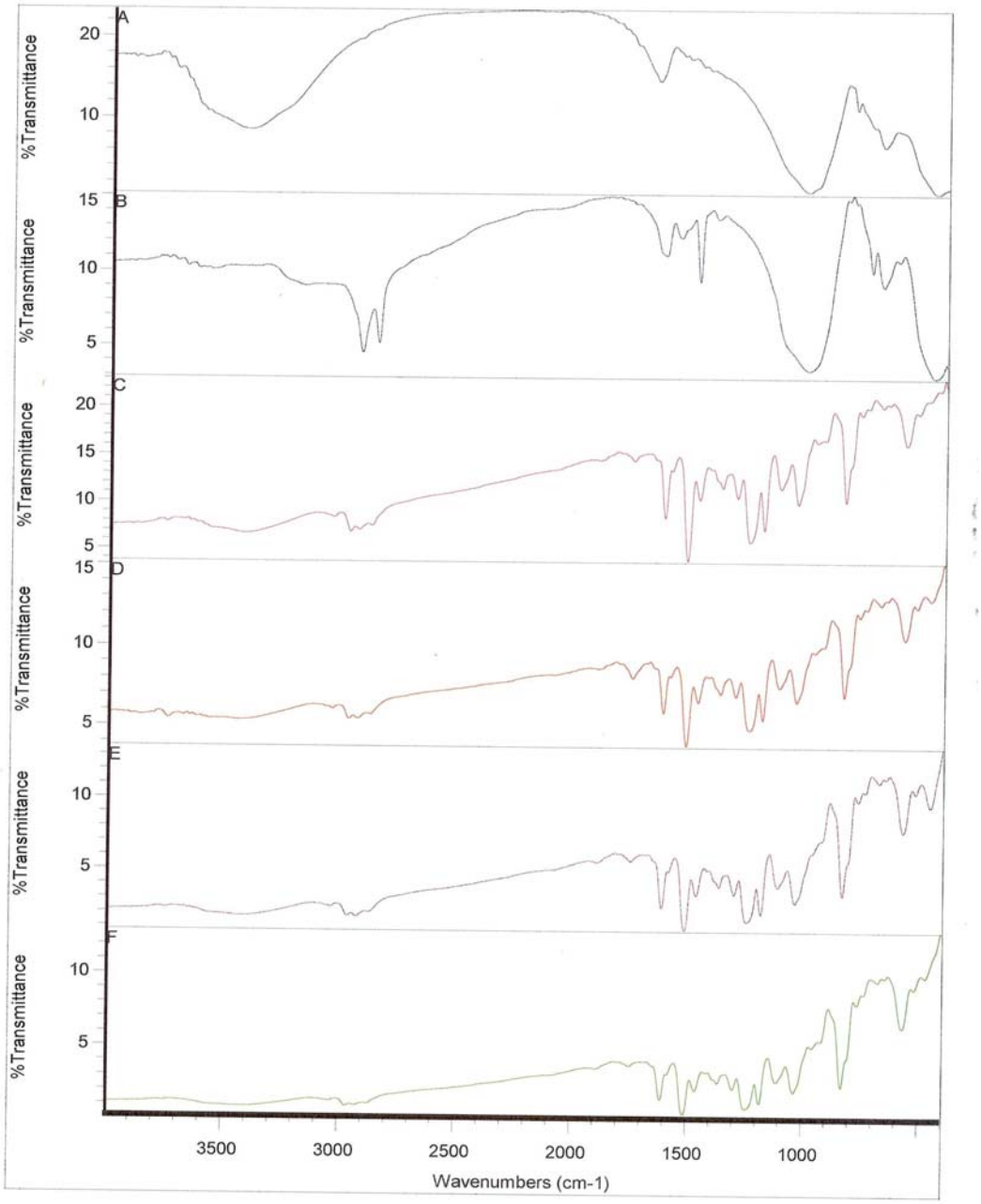

Figure 3.2(ii) FTIR spectra's of (A) IVMT, (B) OVMT, (C) Neat Epoxy cured with DDM, (D) $EOVMT_2$, (E) $EOVMT_4$ and (F) $EIVMT_1$ respectively.

3.3 Tensile Strength and Modulus

Tensile strength, modulus and elongation at break of DGEBA cured with DDM (with no clay) was found 38.74 MPa, 1.39GPA and 57% respectively. The tensile strength, tensile modulus and elongation at break of montmorillonite filled epoxy-clay nanocomposites and vermiculite filled epoxy-clay nanocomposites are given in Tables 3.3(i) and 3.3(ii) respectively.

Table 3.3(i) Tensile strength, tensile modulus and elongation at break of EMMT.

Sl.No.	Sample Designation	Tensile Strength (MPa)	Tensile Modulus (GPa)	Elongation At Break (%)
1	$EOMMT_1$	43.63	1.71	37
2	$EOMMT_2$	50.23	1.75	25
3	$EOMMT_3$	57.07	1.78	19
4	$EOMMT_4$	61.83	2.15	14
5	$EIMMT_1$	27.37	1.22	49
6	$EIMMT_2$	32.14	1.56	38

Table 3.3(ii) Tensile strength, tensile modulus and elongation at break of EVMT

Sl. No.	Sample Designation	Tensile Strength (MPa)	Tensile Modulus (GPa)	Elongation At Break (%)
1	$EOVMT_1$	46.23	1.40	43
2	$EOVMT_2$	49.22	1.43	30
3	$EOVMT_3$	53.10	1.50	19
4	$EOVMT_4$	59.99	1.62	16
5	$EIVMT_1$	32.19	1.40	46
6	$EIVMT_2$	34.63	1.41	40

It is found that a rise in OMMT concentration from 0 to 6% leads to 55% increase in the tensile modulus, 60% increase in ultimate tensile strength, and 75% decrease in elongation at break values while a rise in OVMT concentration from 0 to 6% leads to 17% increase in the tensile modulus, 59% increase in ultimate tensile strength, and 71% decrease in elongation at break values. This reinforcing effect of the organoclays could be due to better dispersion and compatibility of clay particles with polymer matrix. A comparison of inorganic and organoclay composites for tensile properties shows that the organoclay composite always shows better properties than the inorganic counterpart for both montmorillonite and vermiculite. It has also been observed that beyond a 6 wt % loading of the organoclay, the elongation at break value is lowered substantially so that a further increase of filler concentration was considered unnecessary.

The tensile strength ,modulus and elongation at break values for organo and inorganic composites were compared and comparison is mentioned at Figures 3.3(i) and 3.3(ii) for Epoxy-Montmorillonite and Epoxy-Vermiculite Nanocomposites respectively.

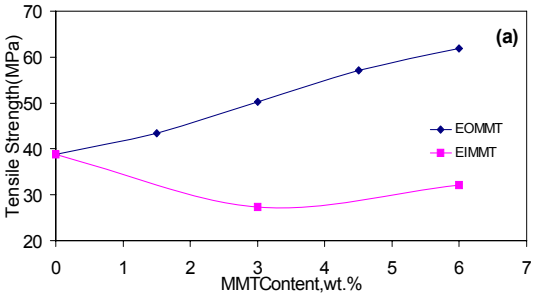

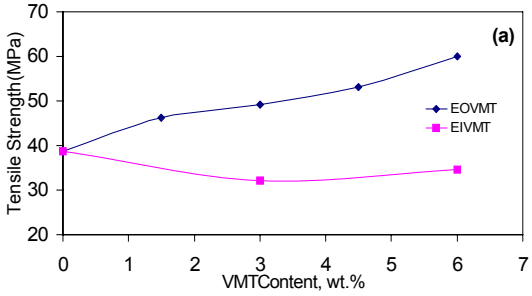

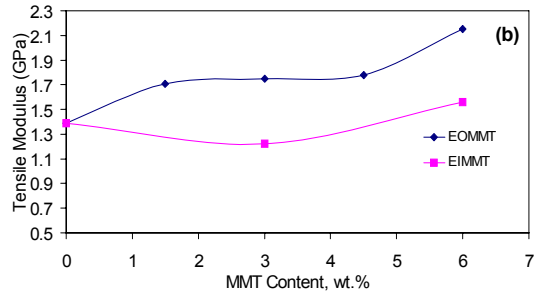

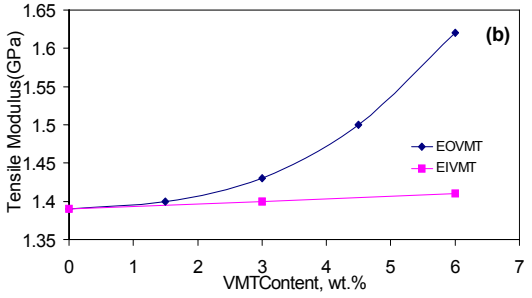

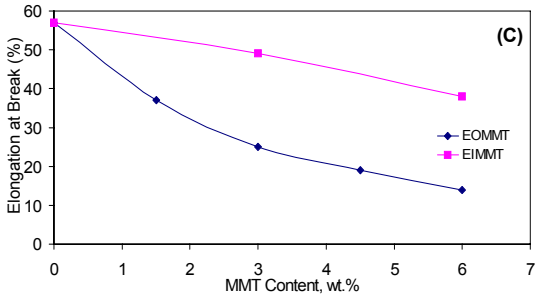

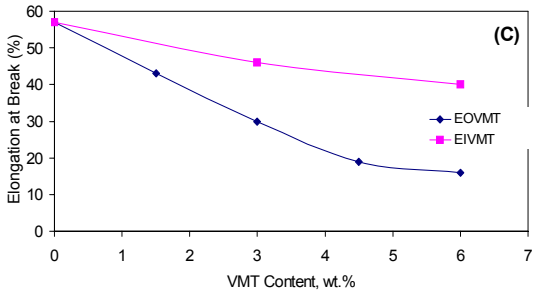

Figure3.3(i) **Figure3.3(ii)**

Figure 3.3 Tensile strength, modulus and elongation at break of EMMT and EVMT

3.4 Flexural Strength and Modulus

Flexural strength and modulus of DGEBA cured with DDM (with no clay) was found 57.38 MPa and 2.95 GPa respectively. The flexural strength and modulus of montmorillonite filled epoxy-clay nanocomposites and vermiculite filled epoxy-clay nanocomposites is given in Tables 3.4(i) and 3.4(ii) respectively.

Table 3.4(i) Flexural Strength and Flexural Modulus of EMMT

Sl.No.	Sample Designation	Flexural Strength (MPa)	Flexural Modulus (Gpa)
1	$EOMMT_1$	61.96	3.69
2	$EOMMT_2$	64.56	3.86
3	$EOMMT_3$	74.44	4.02
4	$EOMMT_4$	81.00	4.86
5	$EIMMT_1$	57.58	3.70
6	$EIMMT_2$	54.16	4.06

Table 3.4(ii) Flexural Strength and Flexural Modulus of EVMT

Sl.No.	Sample Designation	Flexural Strength (MPa)	Flexural Modulus (Gpa)
1	$EOVMT_1$	63.42	3.57
2	$EOVMT_2$	66.70	4.07
3	$EOVMT_3$	68.10	4.16
4	$EOVMT_4$	69.98	4.63
5	$EIVMT_1$	63.04	3.61
6	$EIVMT_2$	60.48	3.95

It is found that a rise in OMMT concentration from 0 to 6% leads to 65% increase in the flexural modulus and 41% increase in flexural strength while a rise in OVMT concentration from 0 to 6% leads to 58% increase in the flexural modulus and 22% increase in flexural strength despite of the small amounts of

the filler added. The reason behind this trend is that in exfoliated nanocomposites the clay layers swell more efficiently in the epoxy-matrix which leads to better dispersion and there would be larger stiffness improvement. Also with the increase in the distance between the layers due to exfoliation an increase in the effective volume fraction of the reinforcment entities causes better reinforcement. Flexural properties of organoclay nanocomposites are also better than the conventional IMMT and IVMT filled nanocomposites due to poor dispersion of inorganic fillers in the polymer matrix.

The Flexural strength and Flexural modulus for organo and inorganic composites were compared and comparison is mentioned at Figure 3.4(i) for Epoxy-montmorillonite and Figure 3.4(ii) for Epoxy-Vermiculite Nanocomposites respectively.

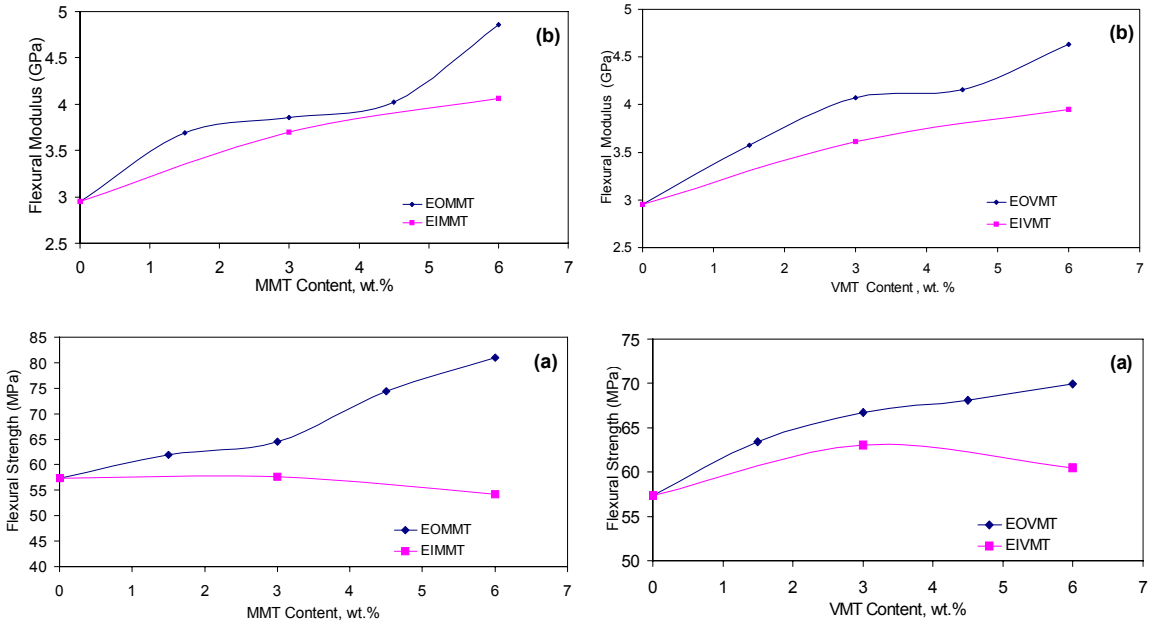

Figure 3.4(i) **Figure 3.4(ii)**

Figure 3.4 Flexural Strength and Flexural Modulus

3.5 Impact Strength

Impact strength of DGEBA cured with DDM (with no clay) was found 16.5 Kg.cm/cm. The flexural strength and modulus of montmorillonite filled epoxy-clay nanocomposites and vermiculite filled epoxy-clay nanocomposites is given in Tables 3.5(i) and 3.5(ii) respectively.

Table 3.5(i) Impact Strength of EMMT

Sl.No.	Sample Designation	Impact Strength (Kg.cm/cm)
1	$EOMMT_1$	21.28
2	$EOMMT_2$	26.17
3	$EOMMT_3$	21.81
4	$EOMMT_4$	19.28
5	$EIMMT_1$	13.07
6	$EIMMT_2$	8.75

Table 3.5 (ii) Impact Strength of EVMT

Sl.No.	Sample Designation	Impact Strength (Kg.cm/cm)
1	$EOVMT_1$	19.98
2	$EOVMT_2$	21.30
3	$EOVMT_3$	18.21
4	$EOVMT_4$	13.78
5	$EIVMT_1$	12.60
6	$EIVMT_2$	8.36

The impact strength of OMMT filled and OVMT first increases reaches to maximum for 3% clays and then again decreases. The increase in impact strength is 58% for OMMT filled nanocomposites and 29% for OVMT filled nanocomposites with 3% clay contents. This can be explain on the basis of the fact at high clay contents, clay particles agglomerate and act as stress concentrators decreasing the impact strength. For conventional composites a decreasing trend in impact strength is found with increased filler . The reason for

these trends could be that the organic modification of clay results in better dispersion of clay particles in polymer matrix and thus increase in impact strength was found for low clay content but in case of conventional composites the compatibility of inorganic clays is not good with organic polymer matrix so that the clay particles act as stress concentrators at all concentrations.

The Impact Strength for organo and inorganic composites were compared and comparison is mentioned at Figures 3.5(i) and 3.5(ii) for Epoxy-Montmorillonite and Epoxy-Vermiculite nanocomposites

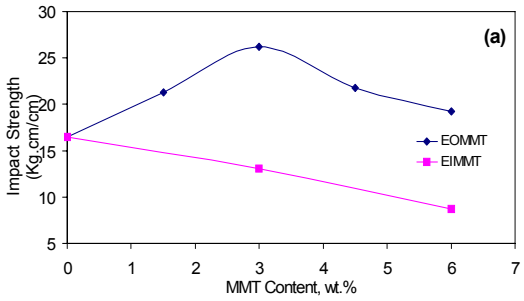

Figure3.5(i)

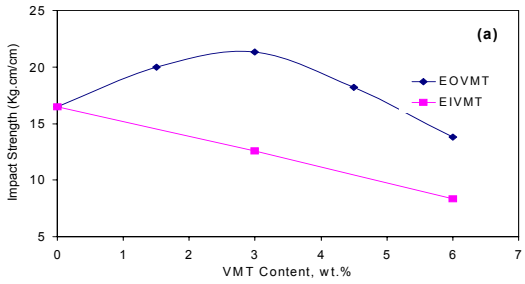

Figure3.5(ii)

Figure 3.5 Impact strength EMMT and EVMT**.**

3.6 Differential Scanning Calorimetry (DSC)

The curing of the epoxy and epoxy-clay nanocomposites was monitored through differential scanning calorimetry (DSC). For neat epoxy cured with DDM the the values for Tonset, Tmidpoint, Tend and Tg and ΔH are observed 95^0C, 164.1^0C, 263.5^0C, 76.3^0C and 363.8 J/g respectively.

The results of the DSC scans of montmorillonite filled Nanocomposite and and Vermiculite filled Nanocomposite are summarized in Tables 3.6(i) and 3.6(ii) respectively.

Table 3.6(i) Summary of the DSC results for EMMT

Sl. No.	Sample Designation	T_{onset} (^{0}C)	$T_{midpoint}$ (^{0}C)	T_{end} (^{0}C)	T_g (^{0}C)	Heat of Reaction (ΔH) J/g
1.	$EOMMT_1$	93	163.31	261.5	161.31	362.0
2.	$EOMMT_2$	89	161.78	256.8	159.78	353.8
3.	$EOMMT_3$	86	152.32	253.7	150.32	352.4
4.	$EOMMT_4$	83	148.39	249.9	146.39	311.8
4.	$EIMMT_1$	87	160.99	255.6	158.99	354.2
5.	$EIMMT_2$	89	160.89	259.9	157.89	371.0

Table 3.6(ii) Summary of the DSC results for EVMT

Sl. No.	Sample Designation	T_{onset} (^{0}C)	$T_{midpoint}$ (^{0}C)	T_{end} (^{0}C)	T_g (^{0}C)	Heat of Reaction (ΔH) J/g
1.	$EOMMT_1$	94.5	161.62	258.6	149.62	773.4
2.	$EOMMT_2$	90.4	161.58	256.2	149.58	771.5
3.	$EOMMT_3$	87.6	161.52	253.4	149.52	733.5
4.	$EOMMT_4$	83.9	160.11	251.7	148.11	725.9
5.	$EIMMT_1$	88.4	161.76	251.6	149.76	351.0
6.	$EIMMT_2$	91.2	155.25	246.5	152.25	359.2

It is found that the onset temperature of curing (T_{onset}) is in the range of 85+-8^{0}C while with an increase in the organoclay content causes a shift in the exothermal peak temperature ($T_{midpoint}$) to lower values and the catalytic effect of the octadecylammonium ion on epoxy ring opening polymerization leads to a decrease in the ultimate heat of reaction (ΔH) for all compositions of DGEBA/organoclay/DDM nanocomposites. A gradual decrease of Tg with increasing concentration of clay indicates that it is not an absorbed layer effect, which usually increases the Tg. Rather, the polymer chains are tied through the surface of the silicate by electrostatic interaction, thus reducing the surrounding entanglements or this decrease of Tg with increase in organoclay concentration could be due to the fact that there occurs a modification of the epoxy network by its homopolymerization within the clay galleries. Indeed, if homopolymerization of the epoxy is favored between the layers, this may cause a displacement of stoichiometry in the epoxy network so that the Tg is reduced. The excess of unreacted curing agent may also plasticize the epoxy network. Due to the complexity of several possible reactions, it is difficult to determine which of these factors govern the decrease of Tg.

Figures 3.6(I) and 3.6(ii) show the DSC scans of EMMT and EVMT respectively.

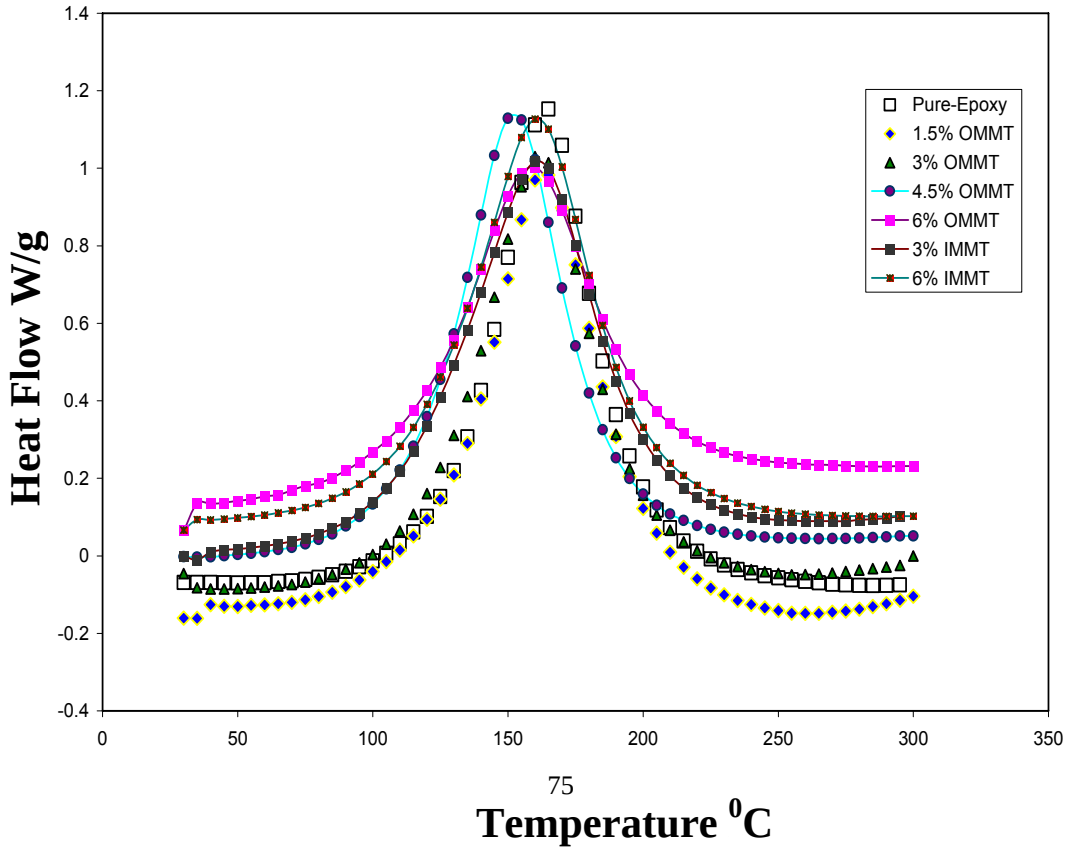

Figure 3.6(i) DSC Curves of EMMT

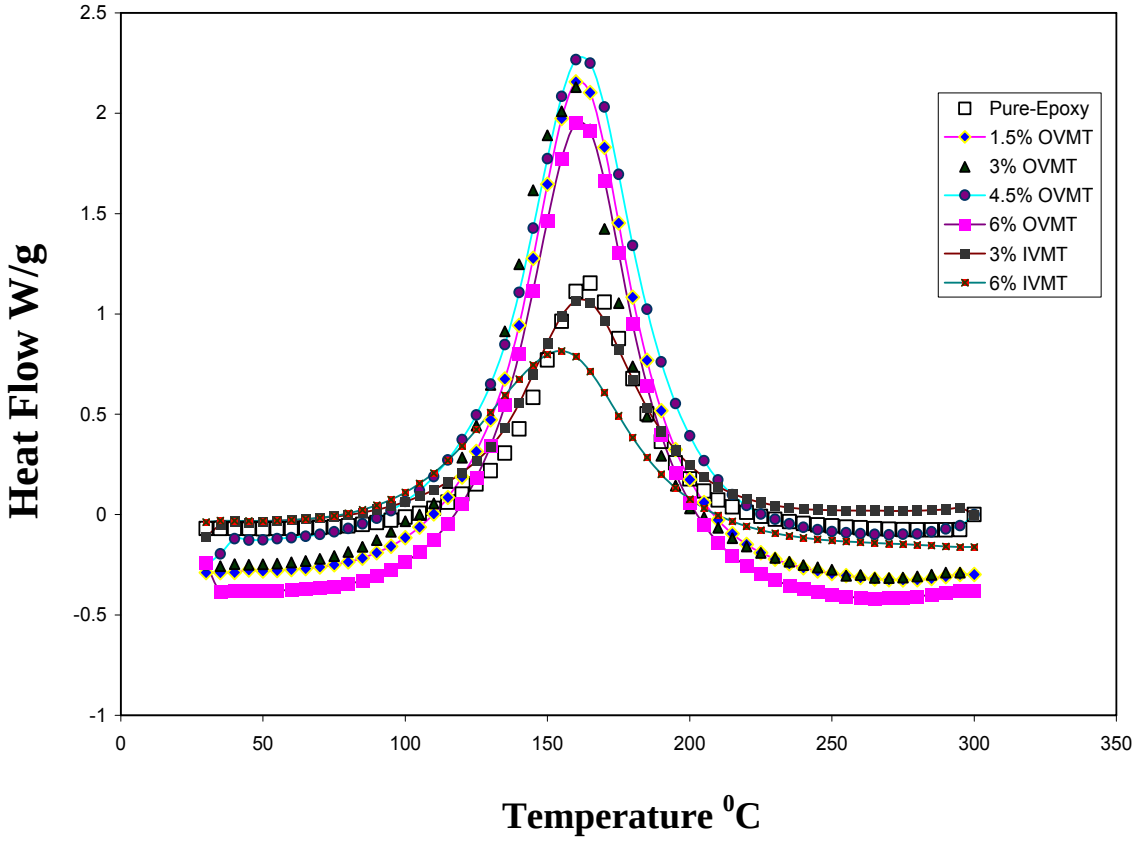

Figure 3.6(ii) DSC Curves of EVMT.

3.7 Thermogravimetric Analysis (TGA)

Thermal stability of the fillers as well as nanocomposites was studied using thermogravimetric analysis (TGA). The TGA thermograms of IMMT, OMMT and IVMT, OVMT are shown in Figures 3.7(i) and 3.7(ii) respectively.

The TGA thermograms of IMMT and IVMT [Figures 3.7(i) and 3.7(ii)] conform that they have an affinity for water and weight losses are attributed to the desorption of water, which includes interlayer, interparticle and constitution water. The weight loss by OMMT and OVMT is due to the decomposition of the ammonium ions confirming the modification of inorganic fillers.

For both OMMT filled and OVMT filled nanocomposite the thermal stability decreases with increase in the filler content as evident from the temperatures corresponding to different weight losses. This could be due to the fact that with the increase in OMMT and OVMT the organic content increases which has low thermal stability while with IMMT and IVMT filled nanocomposite the thermal stability increases (increase is more pronounced with 6% IMMT and 6% IVMT as compared to 3% IMMT and 3% IVMT). This could be due to increase in concentration of thermally stable inorganic fillers.

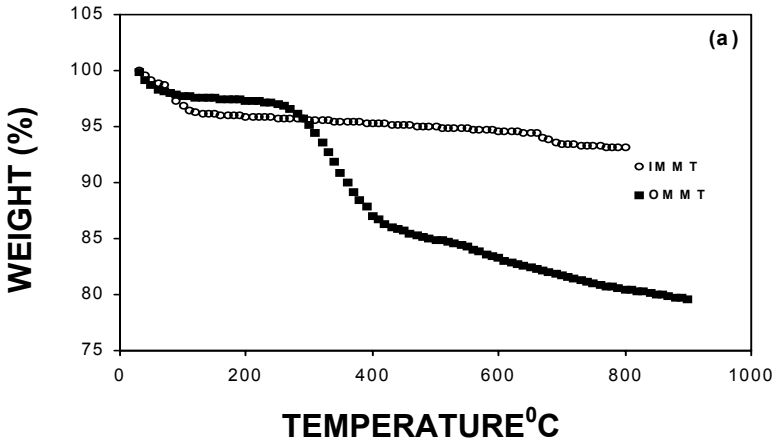

Figure 3.7(i) TGA Thermograms of IMMT and OMMT

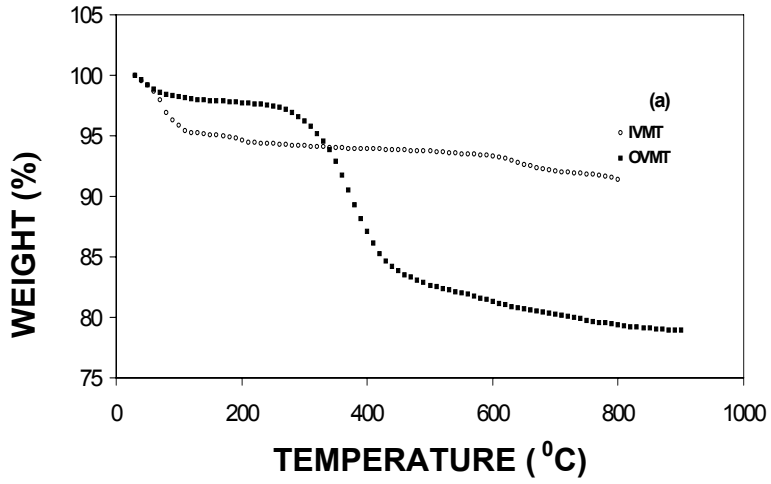

Figure 3.7(ii) TGA Thermograms of IVMT and OVMT

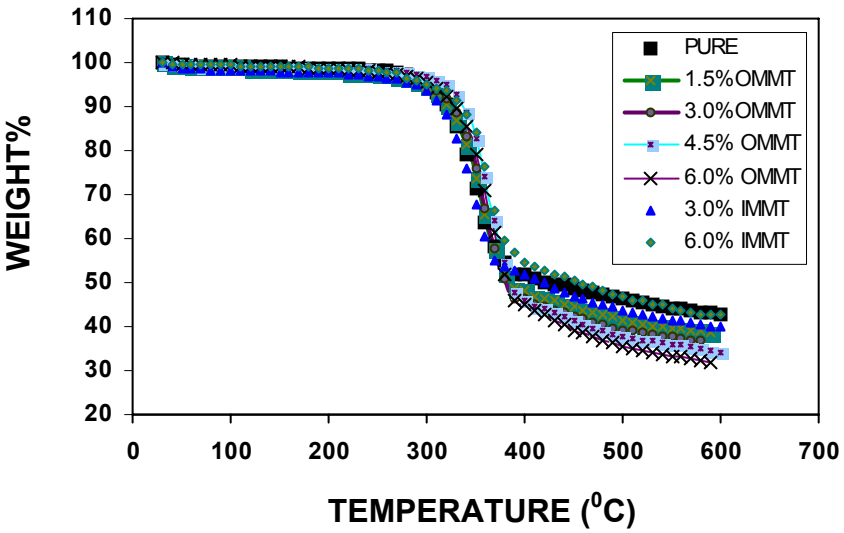

Figure 3.7(iii) TGA Thermograms of EMMT

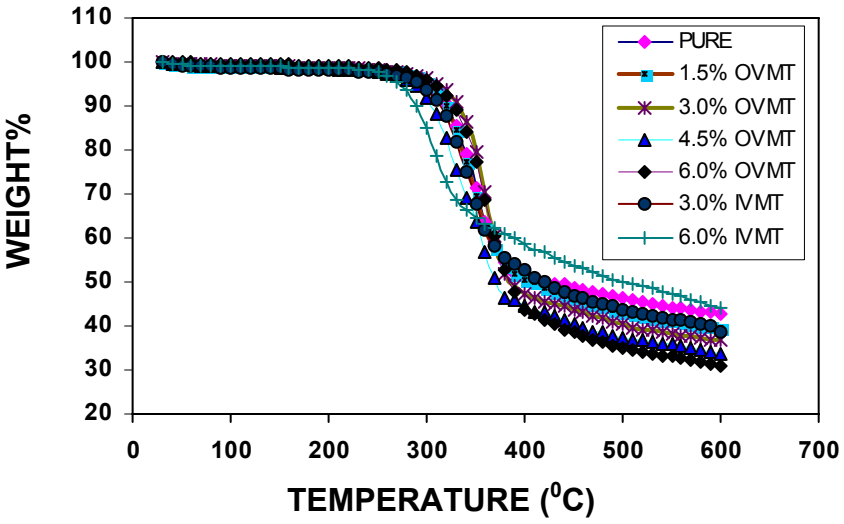

Figure 3.7(iv) TGA Thermograms of EVMT

3.8 Dynamic Mechanical Analysis(DMA)

For pure-epoxy cured with DDM the value of Tanδ was observed 0.6727 (at 5Hz) and glass transition temperature (Tg) was observed 181.76 ^{0}C (at 5Hz).

The DMA results of Montmorillonite filled Nanocomposite and Vermiculite filled Nanocomposite are summarized in Tables 3.8(i) and 3.8(ii) respectively.

Table3.8(i) Summary of DMA results of EMMT (At 5Hz)

Sl. No.	Sample Designation	Tan δ	Glass Transition Temperature T_g (^{0}C)
1	$EOMMT_1$	0.7074	179.46
2	$EOMMT_2$	0.9552	175.00
3	$EOMMT_3$	0.7626	172.23
4	$EOMMT_4$	0.6778	169.43
5	$EIMMT_1$	0.6705	167.40
6	$EIMMT_2$	0.7444	173.35

Table3.8(ii): Summary of DMA results of EVMT (At 5Hz)

Sl. No.	Sample Designation	Tan δ	Glass Transition Temperature T_g (^{0}C)
1	$EOVMT_1$	0.7395	171.08
2	$EOVMT_2$	0.8404	169.40
3	$EOVMT_3$	0.7626	167.30
4	$EOVMT_4$	0.6777	164.53
5	$EIVMT_1$	0.6185	185.00
6	$EIVMT_2$	0.7390	180.00

DMA studies shows that the glass transition temperature of both montmorillonite filled nanocomposites and vermiculite filled nanocomposite decreases with the increase of the OMMT and OVMT content which is identical to the DSC results. The intensity of tanδ peaks or damping factor for both OMMT

filled and OVMT filled nanocomposites first increases up to 3% filler content and then decreases. The storage modulus in the rubbery region for both montmorillonite filled nanocomposites and vermiculite filled nanocomposites increases with the increase of the OMMT and OVMT contents.

Figures 3.8(i), 3.8(ii), 3.8(iii), 3.8(iv), 3.8(v) and 3.8(vi) shows the Tan Delta, Storage Modulus and Loss Modulus of montmorillonite filled nanocomposites and vermiculite filled nanocomposites respectively.

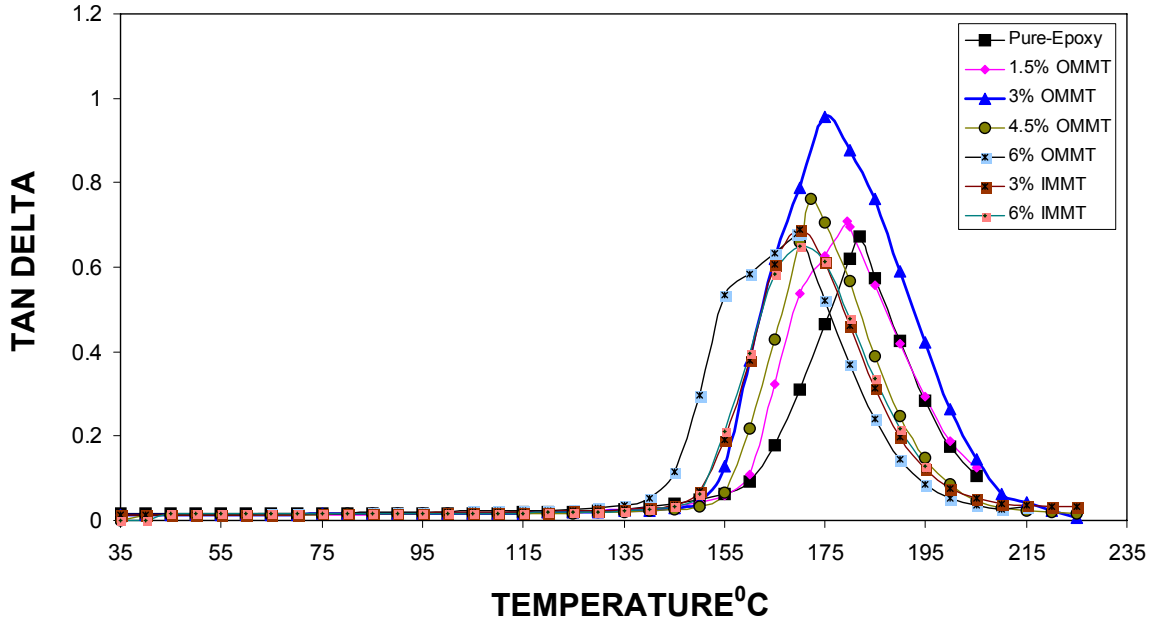

Figure 3.8(i) Loss tangent of EMMT

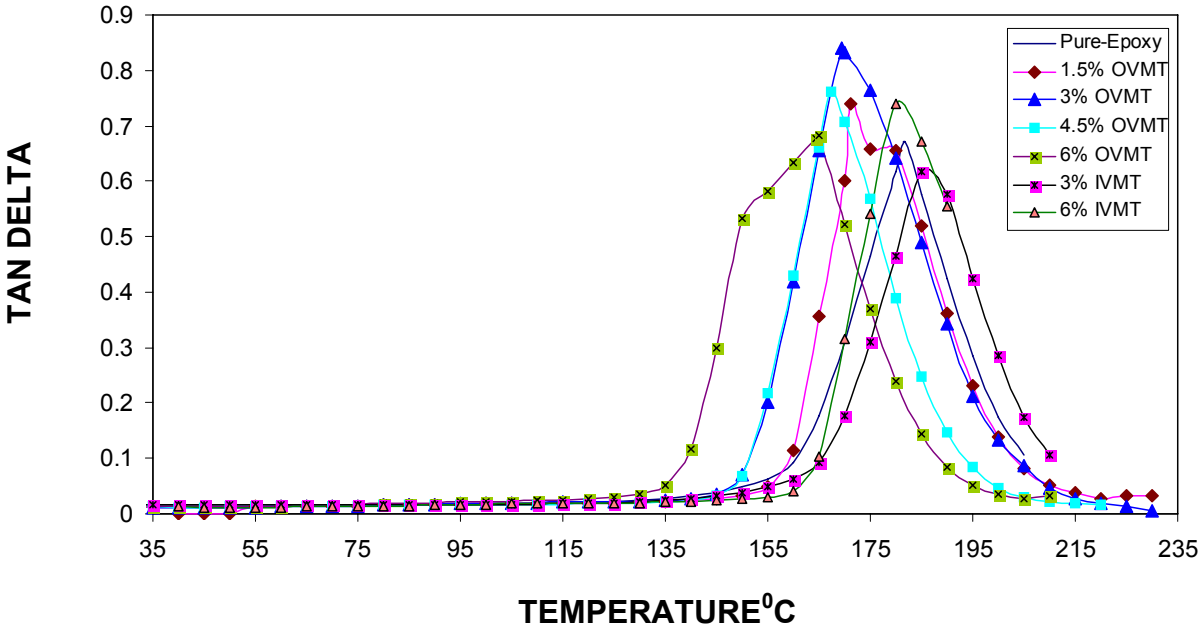

Figure 3.8(ii) Loss tangent of EVMT

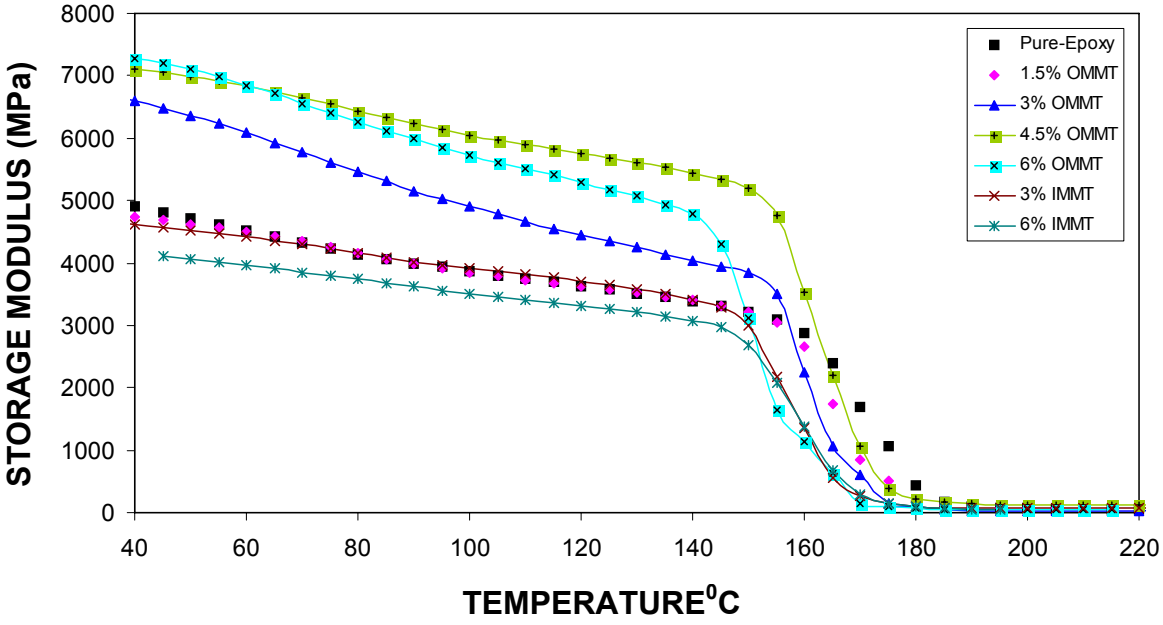

Figure 3.8(iii) Storage Modulus of EMMT

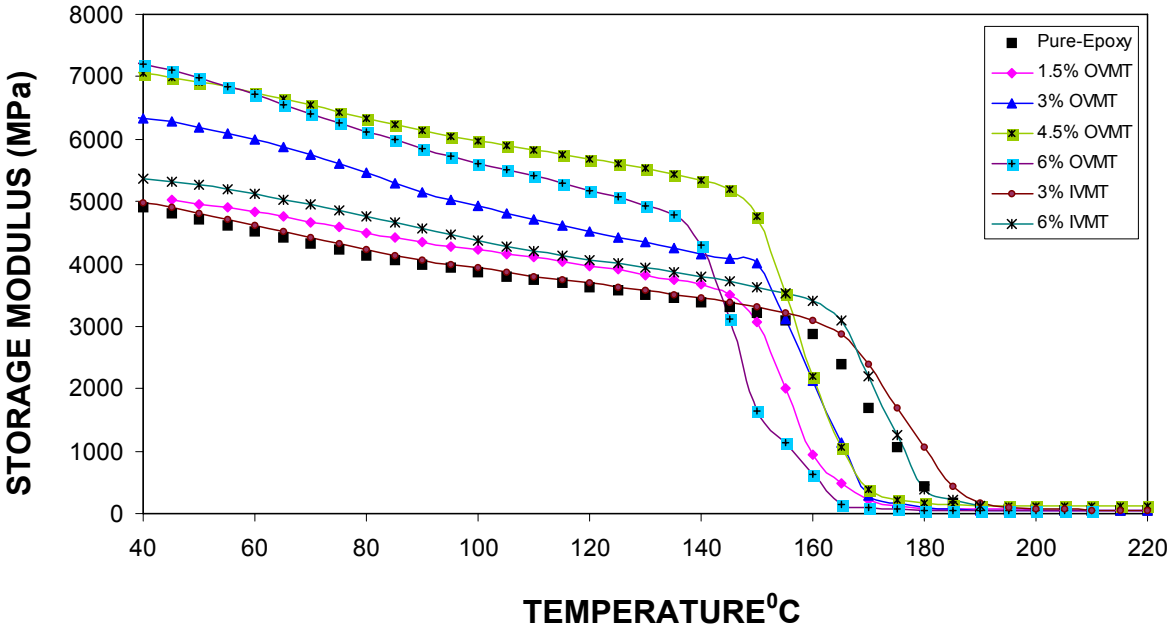

Figure 3.8(iv) Storage Modulus of EVMT

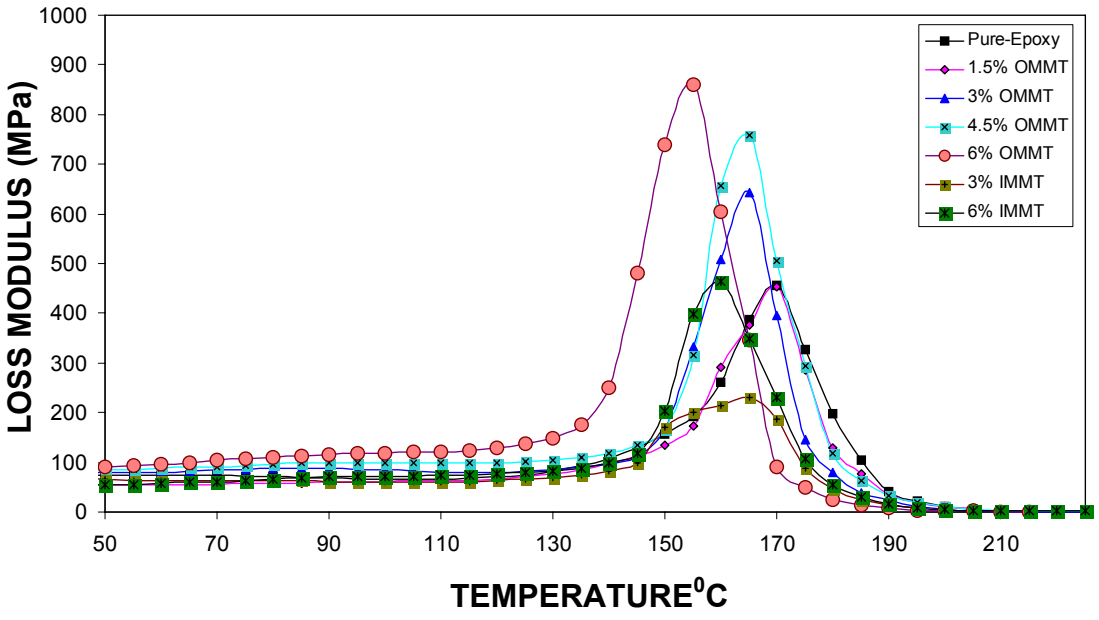

Figure 3.8(v) Loss Modulus of EMMT

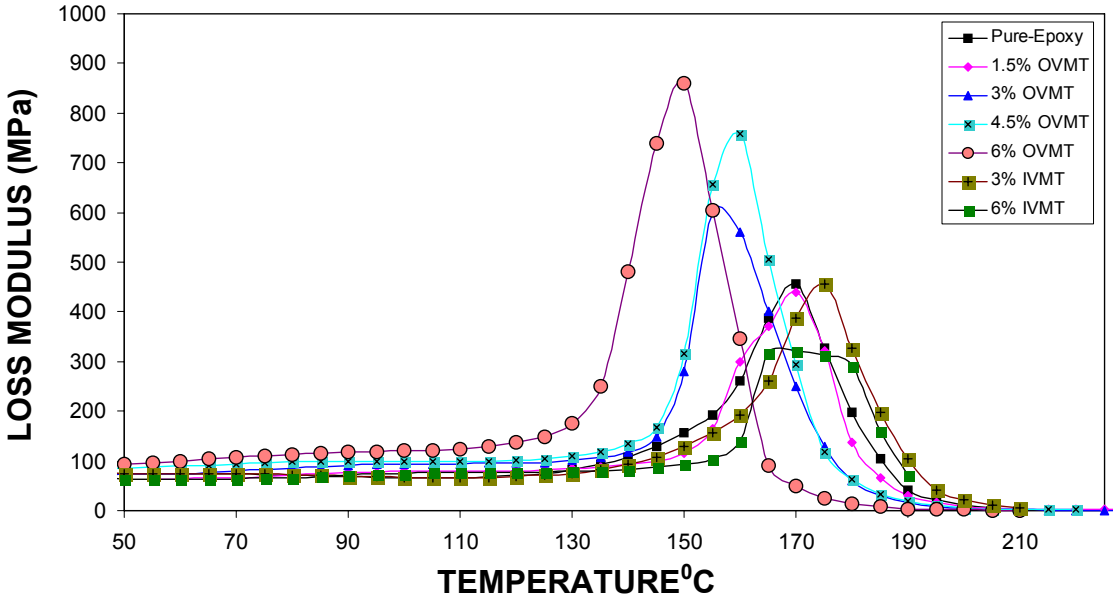

Figure 3.8(vi) Loss Modulus of EVMT

3.9 SCANNING ELECTRON MICROSCOPY (SEM)

Of late, the SEM has emerged as an important tool for investigation of the failure mechanism of polymer nanocomposites. During evolution of mechanical properties of the nanocomposites, various methods of testing are adopted . These include tear, flexing, impact set, heat build-up and all these necessitate to subject the test specimens under various modes of testing in a variety of testing equipment's. Moreover in all such cases, a fracture surface is always being obtained which when studied under SEM offers valuable information on homogeneity of filler, nature and type of failure, aspect ratio and reinforcement characteristics of fillers, degree of distribution and dispersion of dispersed phase into continuous matrix as well as formation of any vacuoles, phase coalescence or interpenetrating network formation etc. With the above objective in mind, a detailed study has been conducted for investigation of Epoxy-clay Nanocomposites with the help of SEM.

SEM studies on impact failure of Epoxy-clay nanocomposites was done. SEM fractrograph of impact failed cross-sectional surface of neat epoxy resin is shown in figure 3.9(i). The parabolic type of the shear yielding coupled with formation of shear lips at turning points are observed. These are the characteristics of typical brittle failure.

The impact strength of brittle plastics could be significantly enhanced by incorporating a rubbery phase in the form of small well-dispersed particle. Provided that adhesion between the dispersed phase and the matrix resin is proper so that the dispersed particles can act as stress raisers or generate an energy absorbing capability of the composite through a change in the mechanical deformation process either through promotion of extensive shear yielding or craze formation or through deviation or deflection of tear paths from proceeding straight. A combination of all above or sum of two or more process could also be evident depending on the system of study or concentration of filler agglomerates. As for example, in the case of high-impact polystyrene(HIPS), interfacial adhesion is promoted by graft polymerization of butadiene with the polystyrene matrix. In case of compatabilised thermoplastic elastomeric

vulcanizates (TPVs), chemical modification of dispersed phase or matrix followed by dynamic vulcanization of network generate chemical interaction between matrix and dispersed globules and thereby enhances the impact strength of the blends. Properties of miscible polymer blends may be intermediate between those of the individual components (i.e. additive behavior). In other cases, the property may exhibit either +ve or –ve deviation from additivity, as illustrated in Figure. For example, both modulus, impact and tensile strengths of compatible blends exhibit a small maximum at some intermediate blend composition and then would normally go through diminishing values.

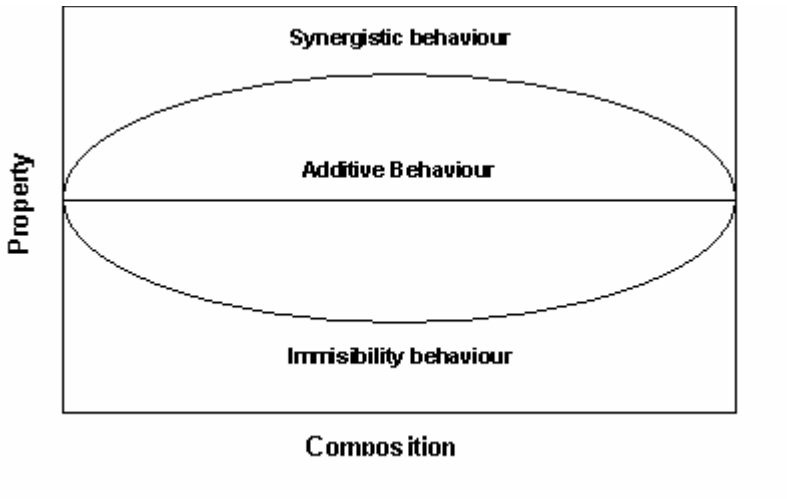

Figure 3.9

The immisibility behavior or fall in property beyond a certain filler concentration is attributed to a loss in free volume corresponding to a negative volume change of mixing ($-\Delta Vm$) due to unfavorable adhesion between the phase components.

Figure 3.9(ii) shows impact failed surface topography of epoxy resin containing 3-wt.% unmodified montmorillonite. The features observed in Figure3.9 (i) are still present with occasional resistance to fracture line growth at few points by filler particles. However, there is very little interaction between filler with the matrix and also seen at higher magnification [Figure3.9 (iii)] is extensive filler conglomeration signifying improper adhesion. Impact strength, therefore,

impairing due to addition of montmorillonite at 3wt% loading. Increasing filler concentration without any surface modification of filler further deteriorates impact strength. As evident in figures 3.9(iv) and (v) we see extensive brittle failure of the matrix with diminishing shear yielding as well as formation of grooves due to ejection of filler clusters on the fracture surface.

Sharp contrast is observed when the same filler is organo-modified. Better hydrophobic-hydrophobic interactions developed enhances adhesion between filler and the matrix. Figure 3.9(vi) is the impact failed surface of epoxy nanocomposites with 1.5 wt% of organo-modified montmorillonite, show rounded tear paths both formed around the filler boundary as well as terminating on the surface itself with little growth are observed. At higher magnifications, the filler-matrix adhesion is more predominant. The impact strength is therefore, seen to be more than pristine resin [Figure 3.9(vii)]. Maximum impact strength is however obtained at 3wt% filler concentration. In this case, as given in Figure 3.9(Viii) we see extensive crazing with interconnecting filler particles. The dispersion of filler is perfectly homogeneous and also become spheroidal as a result of the deformation process. Also seen, the crazes are oriented perpendicular to the impact loading on the test specimen. At a higher magnification as in Figure 3.9(ix), the craze proliferation and bifurcation observed signify a means of adequate energy dissipation or toughening of the otherwise brittle epoxy resin.

Further increase of filler concentration beyond 3wt% loading could not generate a concomitant increase in the impact strength. As shown in the Figure 3.9(x), we see the fracture topography gets modified with similar features in case of Figure 3.9(vi) with 1.5wt% filler. Figure 3.9(xi) also shows filler agglomeration and improper distribution in the composite. The relative surface area available to generate adequate filler matrix adhesion is reduced with relative increase in extent of filler agglomeration and so also the value of impact strength. We therefore see in Figures 3.9(xii) and (xiii), the impact strength is progressively reduced with increasing concentration of filler exceeding 3wt% loading. Addition of inorganic vermiculite as such in to epoxy resin does not

merit any improvement of impact property, as shown in Figures 3.9(xiv) to (xvi). Figure 3.9(xiv) also shows formation of deep grooves and detachment of filler agglomerates from matrix surface. Figure 3.9(xvii) is SEM photomicrograph of impact failed cross-section of 1.5 wt% organo-modified vermiculite containing composite. Although deflection of fracture fronts across the boundary of filler is evident, but the average size of an agglomerate is much bigger than organo-montmorillonite as shown in Figure 3.9(viii). Combed shaped branching on main fracture fronts, however are observed [Figure 3.9(xviii)], resulting in a marginal increase in impact strength compared to pristine resin [Figures 3.9(i) and 3.5(ii)].

A substantial change in the nature of fracture surface is, however, observed with increasing filler content upto 3wt%. Figure 3.9(xix), as expected, shows enhanced toughening and features similar to mechanism discussed above. However, compared to the case of organo-montmorillonite with similar 3wt% loading, the filler size in case of vermiculite is more [Figure 3.9(xx)]. Therefore, vermiculite was found to be less reinforcing in nature compared to montmorillonite even after organic modification of the filler. As seen in the case of montmorillonite, further increase of filler loading beyond optimum value of 3 wt%, the morphology gets converted to the case of inappropriate filler concentration e.g. with 1.5 wt%. The same feature is also observed for vermiculite, as shown in Figures 3.9 (xxi) and (xxii). These features closely resembles our observations of reduction of impact strength of organo-vermiculite containing composites containing filler upto 4.5 wt% [Figures 3.9(xxi) and (xxii)] or upto 6.0 wt% [Figures 3.9(xxiii) and (xxiv)].

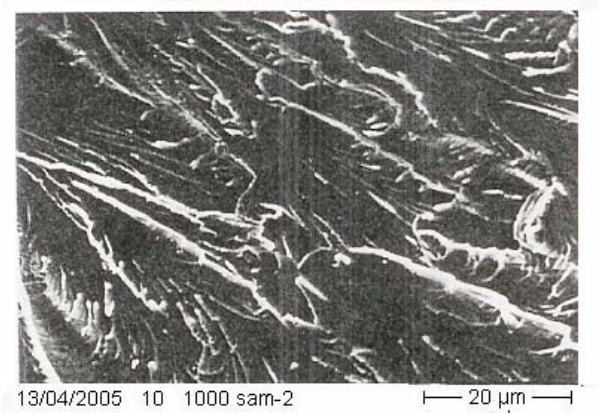

Figure 3.9(i)
Impact Fractrographs of
Neat-Epoxy

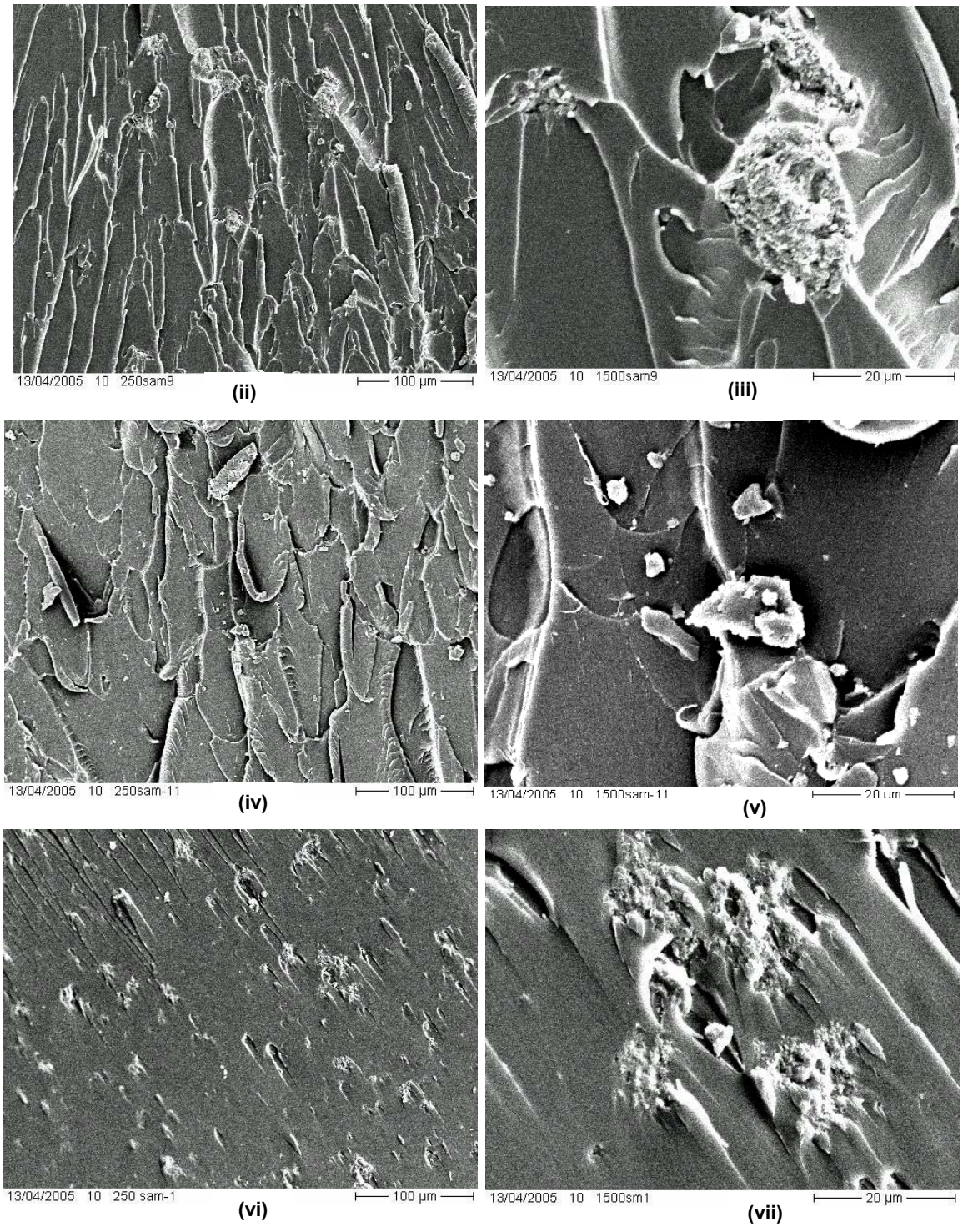

Figure 3.9 (ii), (iii), (iv), (v), (vi) and **(vii)** are Impact Fractrographs of $EIMMT_1$, $EIMMT_1$, $EIMMT_2$, $EIMMT_2$, $EOMMT_1$ and $EOMMT_1$ respectively.

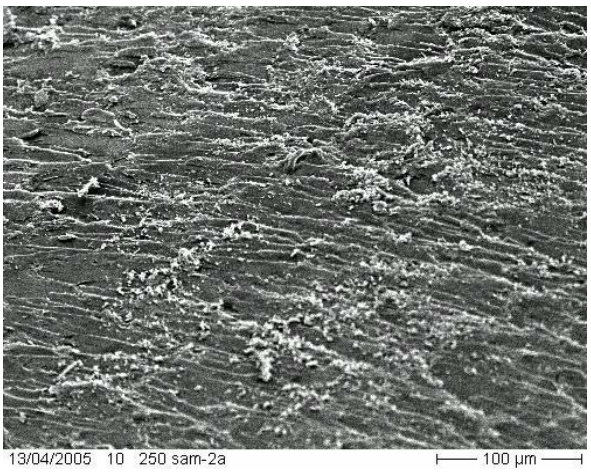

(viii)

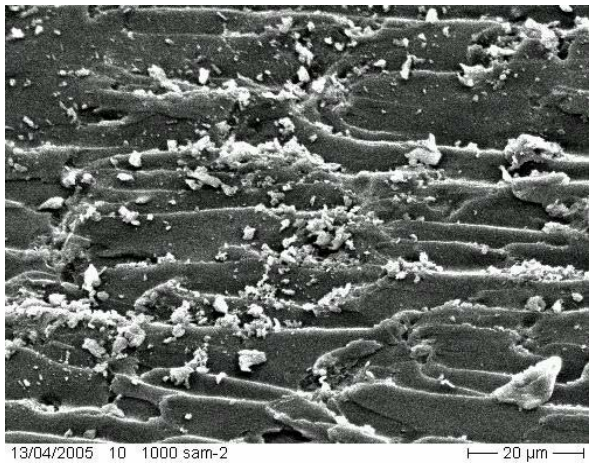

(ix)

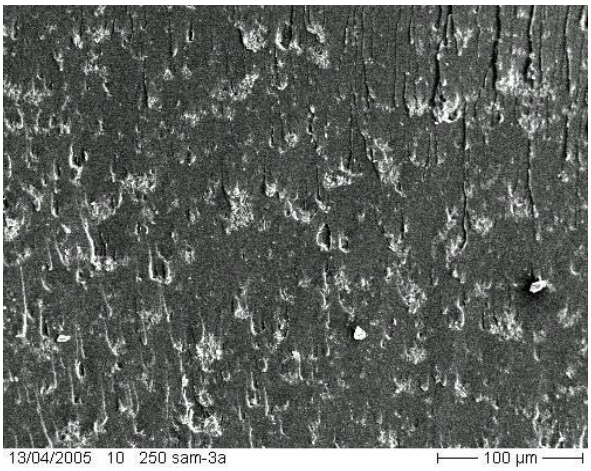

(x)

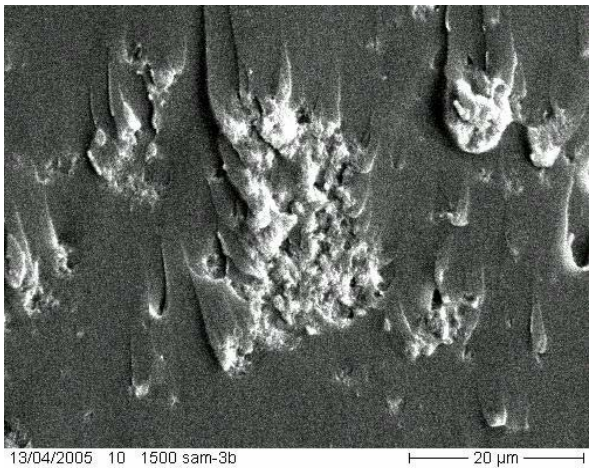

(xi)

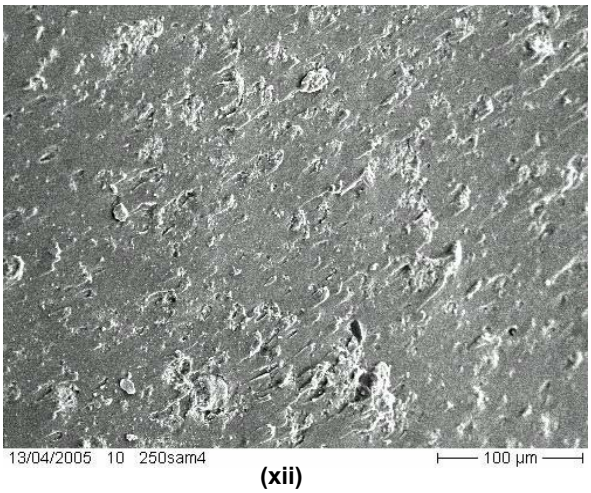

(xii)

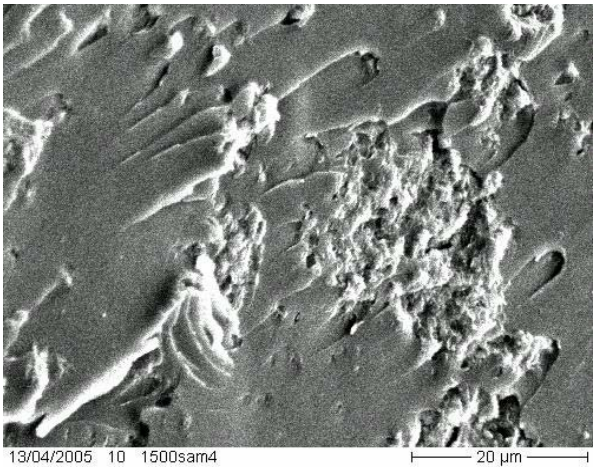

(xiii)

Figure 3.9 (viii), (ix), (x), (xi), (xii) and **(xiii)** are Impact Fractrographs of EOMMT2, EOMMT2, EOMMT3, EOMMT3 and EOMMT4, EOMMT4 respectively.

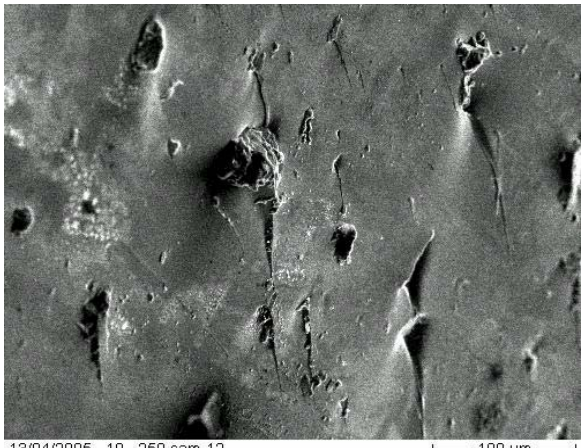

(xiv)

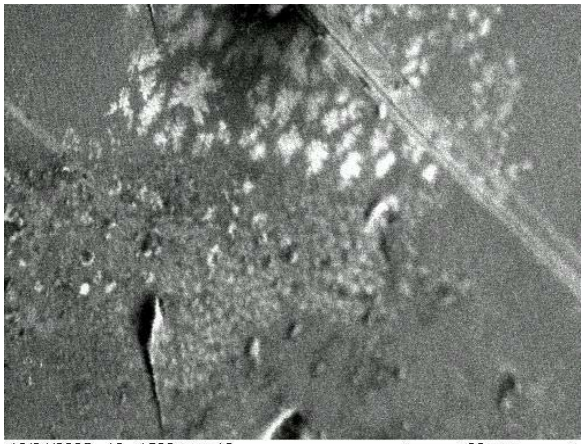

(xv)

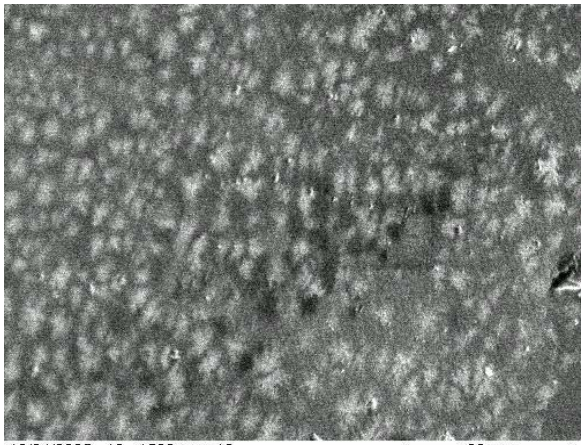

(xvi)

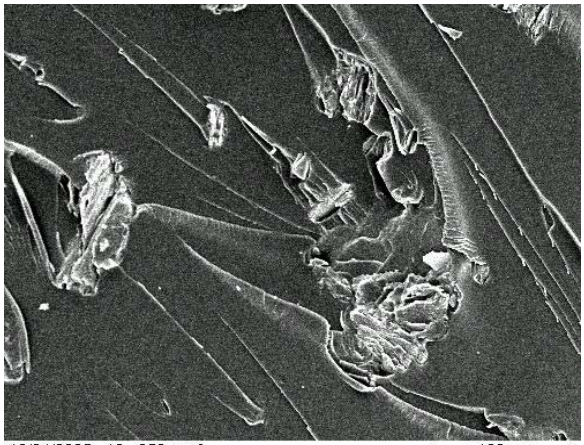

(xvii)

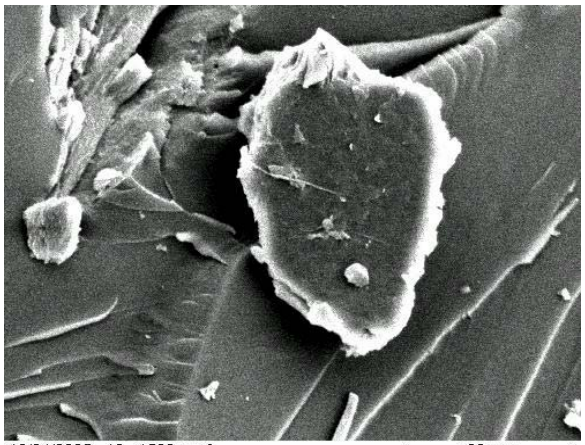

(xviii)

(xix)

Figure 3.9 (xiv), (xv), (xvi), (xvii), (xviii) and **(xix)** are Impact Fractrographs of EIVMT1, EIVMT1, EIVMT2, EOVMT1, EOVMT1 and EOVMT2 respectively.

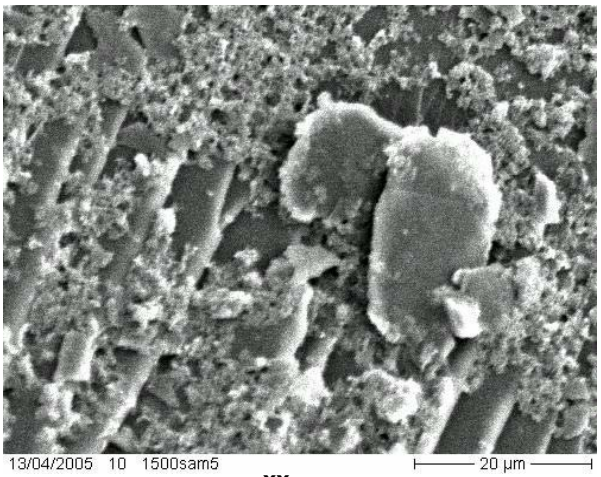

xx

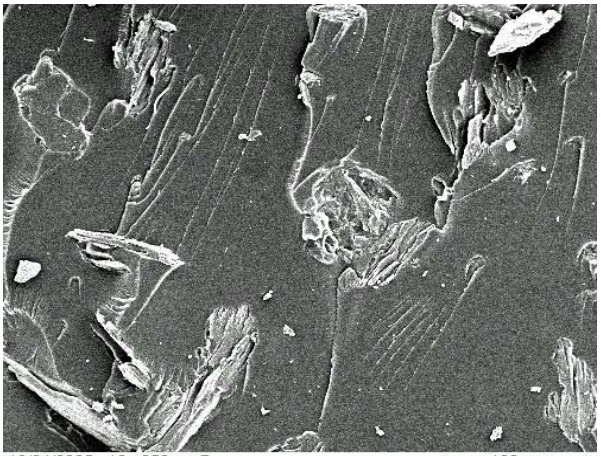

xxi

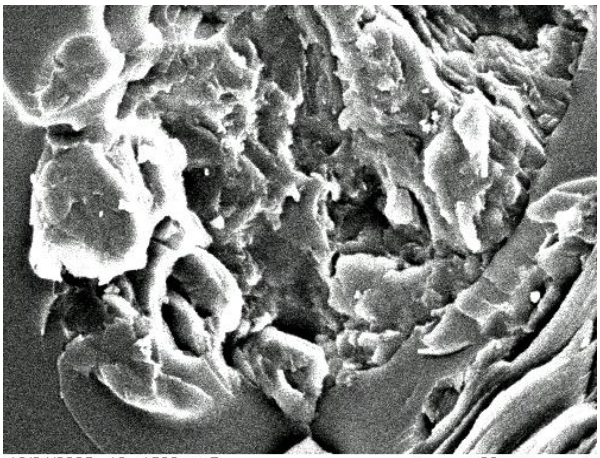

xxii

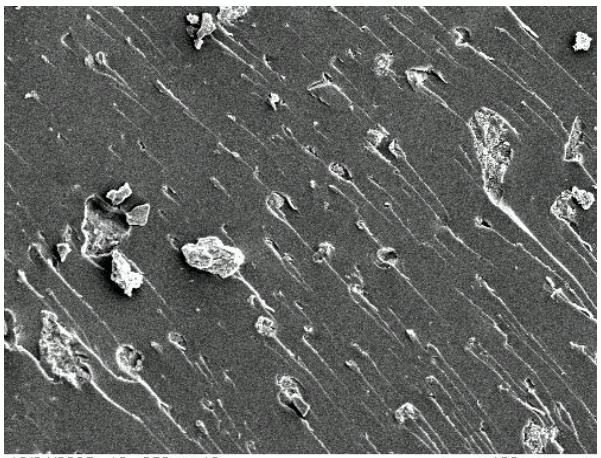

xxiii

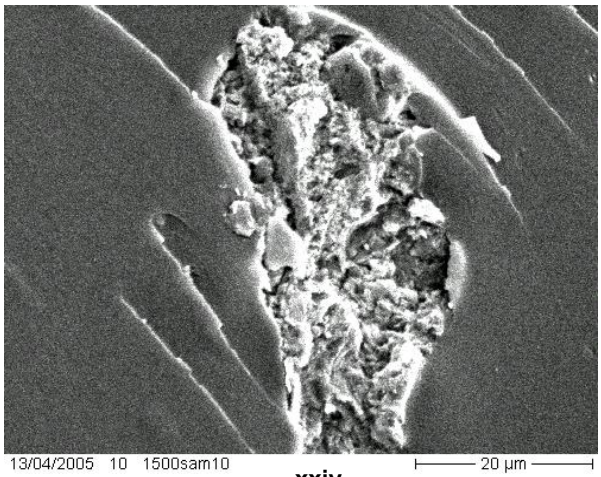

xxiv

Figure 3.9 (xx), (xxi), (xxii), (xxiii) and **(xiv)** are Impact Fractrographs of EOVMT2, EOVMT3, EOVMT3, EOVMT4 and EOVMT4 respectively.

Chapter 4

Summary and Conclusion

1) Octadecylammonium ion exchanged for Na-ion of pristine clays resulted in exfoliation for staggered clay galleries, which is an essential prerequisite for formation of a nanocomposite.

2) A substantial improvement in mechanical properties of the epoxy –organoclay nanocomposites suggests an overwhelming increase of the effective volume fraction of the clay into polymer network. Mechanical properties of the nanocomposite attain maximum value at 6 wt %loading of the duly exfoliated organoclay. Beyond that level, the fall in mechanical properties is due to improper filler dispersion as well as the filler exceeding nanosize due to agglomeration.

3) Thermal stability of the organocomposite is less than inorganic composite. This is probably due to the presence of organic species (e.g., octadecylammonium ions), which is less thermally stable than inorganic species.

4) WAXS analysis gives insight into the mechanism of exfoliation and relative efficacy of the organic and inorganic clays.

5) SEM shows that nanocomposite has better matrix filler interaction than inorganic composite. The studies also demonstrate a finer dispersion of the clay particles in nanocomposite as compared to the conventional composite.

Chapter 5

Scope Of Future Work

During this studies it was found that an increase in the organoclay content causes an increase in impact strength and loss tangent (damping factor) with maximum at 3% loading. In future, studies can be carried out on the development of laminates at this optimum value of organoclays using Epoxy resin with different fabrics like Kevlar, Glass fabric. Also rubber toughening of these nanocomposites may result in the good structural materials which can be used in variety of applications in aerospace industry and in tanks along with industrial sectors for structural and automotive applications.

References

[1]. J.E. Mark, Ceramic reinforced polymers and polymer-modified ceramics. *Polym. Eng. Sci.* 36 (1996), pp. 2905–2920.

[2]. E. Reynaud, C. Gauthier and J. Perez, Nanophases in polymers. *Rev. Metall./Cah. Inf. Tech.* 96 (1999), pp. 169–176.

[3]. T. von Werne and T.E. Patten, Preparation of structurally well defined polymer–nanoparticle hybrids with controlled/living radical polymerization. *J. Am. Chem. Soc.* 121 (1999), pp. 7409–7410.

[4]. N. Herron and D.L. Thorn, Nanoparticles. Uses and relationships to molecular clusters. *Adv. Mater.* 10 (1998), pp. 1173–1184.

[5]. P. Calvert, Potential applications of nanotubes, in: T.W. Ebbesen (Ed.), Carbon Nanotubes, CRC Press, Boca Raton, FL, 1997, pp. 277–292.

[6]. V. Favier, G.R. Canova, S.C. Shrivastava and J.Y. Cavaille, Mechanical percolation in cellulose whiskers nanocomposites. *Polym. Eng. Sci.* 37 (1997), pp. 1732–1739.

[7]. L. Chazeau, J.Y. Cavaille, G. Canova, R. Dendievel and B. Boutherin, Viscoelastic properties of plasticized PVC reinforced with cellulose whiskers. *J. Appl. Polym. Sci.* 71 (1999), pp. 1797–1808.

[8]. A. Okada, M. Kawasumi, A. Usuki, Y. Kojima, T. Kurauchi and O. Kamigaito, Synthesis and properties of nylon-6/clay hybrids. In: D.W. Schaefer and J.E. Mark, Editors, *Polymer based molecular compositesMRS Symposium Proceedings, Pittsburgh, vol. 171* (1990), pp. 45–50.

[9] R.A. Vaia, H. Ishii and E.P. Giannelis, Synthesis and properties of two-dimensional nanostructures by direct intercalation of polymer melts in layered silicates. *Chem Mater* 5 (1993), pp. 1694–1696.

[10] G.Lagaly, Smectite “Clays as Ionic Macromolecules in Development in ionic Polymers-2”, Elsevier Applied Science publishers (1986), 77-115.

[11] E.P. Giannelis, R. Krishnamoorti and E. Manias, “Polymer-Silicate Nanocomposites Model System for Confined Polymers and Polymer Brushes”, Adv. Polym. Sc. 138, 107-116, (1999).

[12] M.Alexandre and P.Dubois, “Polymer-Layered Silicate Nanocomposites: Preparation, Properties and Uses of New Class of Materials”, Mater. Sc. And Engg. 28, 1-50, (2000).

[13] A. Blumstein, Polymerization of adsorbed monolayers: II. Thermal degradation of the inserted polymers. *J Polym Sci A* 3 (1965), pp. 2665–2673.

[14] Krishnamoorti, R.A. Vaia and E.P. Giannelis, Structure and dynamics of polymer-layered silicate nanocomposites. *Chem Mater* 8 (1996), pp. 1728–1734.

[15] R.A. Vaia, R.K. Teukolsky and E.P. Giannelis, Interlayer structure and molecular environment of alkylammonium layered silicates. *Chem Mater* 6 (1994), pp. 1017–1022.

[16] O.C. Wilson, Jr., T. Olorunyolemi, A. Jaworski, L. Borum, D. Young, A. Siriwat, E. Dickens, C. Oriakhi and M. Lerner, Surface and interfacial properties of polymer-intercalated layered double hydroxide nanocomposites. *Appl. Clay Sci.* 15 (1999), pp. 265–279.

[17] C.O. Oriakhi, I.V. Farr and M.M. Lerner, Thermal characterization of poly(styrene sulfonate)/layered double hydroxide nanocomposites. *Clays and Clay Minerals* 45 (1997), pp. 194–202.

[18] R.A. Vaia and E.P. Giannelis, Lattice of polymer melt intercalation in organically-modified layered silicates. *Macromolecules* 30 (1997), pp. 7990–7999.

[19] M. Xu, Y.S. Choi, Y.K.Kim, K.H. Wang and I. J. Chung, “Synthesis and Characterization of Exfoliated Poly(styrene-co-methyl Methacrylate)/clay Nanocomposites via Emulsion Polymerization with AMPS”, 44, 6387-6395, (2003).

[20] J. Wu and M.M. Lerner, Structural, thermal, and electrical characterization of layered nanocomposites derived from sodium-montmorillonite and polyethers. *Chem Mater* 5 (1993), pp. 835–838

[21] D.J. Harris, T.J. Bonagamba and K. Schmidt-Rhor, Conformation of poly(ethylene oxide) intercalated in clay and MoS_2 studied by two dimensional double-quantum NMR. *Macromolecules* 32 (1999), pp. 6718–6724.

[22] H.J. Choi, S.G. Kim, Y.H. Hyun and M.S. Jhon, Preparation and rheological characteristics of solvent-cast poly(ethylene oxide)/montmorillonite nanocomposites. *Macromol Rapid Commun* 22 (2001), pp. 320–325.

[23] H.G. Jeon, H.T.Jung, S.W.Lee and S.D.Hudson, “Morphology of Polymer Silicate Nanocomposites: High Density Polyethylene and a Nitrile”, Polymer. 41, 107-113, (1998).

[24] K. Yano, A. Usuki, A. Okada, T. Kurauchi and O. Kamigaito, Synthesis and properties of polyimide–clay hybrid. *J. Polym. Sci.: Part A: Polym. Chem.* **31** (1993), pp. 2493–2498.

[25] J.Xu, Y.Z.Meng, R.K.Y. Li, Y.Xu, A.V.Rajulu; Preparation and Properties of Poly(vinylalcohol)- Vermiculite nanocomposites; Journal of Polymer Science: Part B: Polymer Physics, Vol.41, 749-755, 2003.

[26] P. Reichert, J. Kressler, R. Thomann, R. Mülhaupt and G. Stöppelmann, Nanocomposites based on a synthetic layer silicate and polyamide-12. *Acta Polym.* 49 (1998), pp. 116–123.

[27] A. Akelah and A. Moet, “Polymer-Clay Nanocomposites: Free Radical Grafting of Polystyrene on to Organophilic Montmorillonite Interlayers”, J. Mater. Sc. 31, 3589-3596, (1996).

[28] J. Tudor, L. Willington, D. O’Hare, B. Royan, Intercalation of catalytically active metal complexes in phyllosilicates and their application as propene polymerization catalysts, Chem. Commun. (1996) 2031–2032.

[29] Y.C. Ke, C.F. Long and Z.N. Qi, Crystallization, properties, and crystal and nanoscale morphology of PET–clay nanocomposites. *J. Appl. Polym. Sci.* 71 (1999), pp. 1139–1146.

[30] Q.Wu, Z.Xue, Z.Qi and F.Wang, “Synthesis and Characterization of Pan/clay Nanocomposite with Extended Chain Conformation of Polyaniline, Polymer 41, 2029-2032, (2000).

[31]. B.Lepoittevin, M.Devalckenaere, N.Pantoustier, M.Alexandre, D.Kubies, C.Calberg, R.Jerome and P.Dubois, “Poly(Є-caprolactone)/Clay Nanocomposites Prepared by Melt Intercalation: Mechanical, Thermal and Rheological Properties”, Polymer 43, 4023-4023, (2002).

[32] T.Agag and T.Takeichi, “Polybenzoxazine-Montmorillonite Hybrid Nanocomposites: Synthesis and Characterization”, Polymer 41, 7083-7090, (2000)

[33] T.Takeichi, R. Zeidam and T.Agag, “Polybenzoxazine/Clay Hybrid Nanocomposites: Influence of Preparation Method on the Curing Behavior and Properties of Polybenzoxazines, Polymer 43, 45-53, (2002).

[34] J.W.Cho and D.R.Paul, “Nylon-6 Nanocomposites by Melt Intercalation, Polymer 42**,** 1083-1094, (2001).

[35] K.H.Wang, M.H.Choi, C.M.Koo, Y.S.Coi and I.J.Chung, “Synthesis and Characterization of Maleated Polyethylene/clay Nanocomposites”, Polymer 41, 9891-9826, (2001)

[36] S.W.Kim, W.H.Jo, M.S.Lee, M.B.Ko and J.Y.Jho, “Preparation of Clay Dispersed Poly(styrene-co-acrylonitrile) Nanocomposites using Poly(Є-caprolactone)as a Compatibilizer”, Polymer 42**,** 9837-9842, (2001).

[37] B. Liao, M.Song, H. Liang and Y. Pang, “Polymer-Layered Silicate Nanocomposites 1. A Study of Poly(ethylene oxide)/Na^+-Montmorillonite Nanocomposites as Polyelectrolytes and Polyethylene-block-Poly(ethylene glycol) copolymer/Na^+-Montmorillonite Nanocomposites as Fillers for Reinforcement of Polyethylene”, Polymer 42,1007-10011,(2001).

[38] S.C. Tjong, Y.Z. Meng; Preparation and Characterization of Melt Compounded Polyethylene/Vermiculite nanocomposites. Journal of Polymer Science: Part B: Polymer Physics, Vol.41, 1476-1484, 2003.

[39] J.Xu, Y.Z.Meng, R.K.Y. Li, Y.Xu, A.V.Rajulu; Preparation and Properties of Poly(vinylalcohol)- Vermiculite nanocomposites; Journal of Polymer Science: Part B: Polymer Physics, Vol.41, 749-755, 2003.

[40] S.C.Tjong, Y.Z.Meng; Impact Modified Polypropylene/Vermiculite Nanocomposites; Journal of Polymer Science: Part B: Polymer Physics, Vol.41, 2332-2341, 2003.

[41] S.C. Tjong, Y.Z.Meng, and A.S. Hay; Novel Preparation and Properties of Polyprolylene –Vermiculite nanocomposites; Chem. Mater ; Vol 14, 44-51, 2002.

[42] K.A. Carrado and L.Q. Xu, “In-situ synthesis of Polymer-Clay Nanocomposites from Silicate Gels, Chem. Mater. 10, 1440-1445, (1998).

[43] C.R.Tseng, J.Y.Wu, H.Y.Lee and F.C.Chang, “Preparation and Characterization Behaviour of Syndiotactic Polystyrene-Clay Nanocomposites, Polymer 42,10063-10070, (2001).

[44] Y.Kojima et al., “One-pot Synthesis of Nylon-6 Hybrid”, J. Polym. Sci. Part.A:Polym. Chem. 31, 1755-1761, (1993).

[45] N. Hasegawa, M. Kawasumi, M. Kato, A. Usuki and A. Okada, Preparation and mechanical properties of polypropylene–clay hybrids using a maleic anhydride-modified polypropylene oligomer. *J. Appl. Polym. Sci* 67 (1998), pp. 87–92.

[46] D.C. Lee and L.W. Jang, Preparation and characterization of PMMA–clay hybrid composite by emulsion polymerization. *J. Appl. Polym. Sci.* 61 (1996), pp. 1117–1122

[47] M.W. Noh and D.C. Lee, Synthesis and characterization of PS–clay nanocomposite by emulsion polymerization. *Polym. Bull.* 42 (1999), pp. 619–626.

[48] S. Sinha Ray, K. Yamada, M. Okamoto and K. Ueda, New polylactide/layered silicate nanocomposites. 2. Concurrent improvements of material properties, biodegradability and melt rheology. *Polymer* 44 (2003), pp. 857–866.

[49] A. Okada and A. Usuki, The chemistry of polymer–clay hybrids. *Mater. Sci. Eng.* C3 (1995), pp. 109–115.

[50] R.Magarphan, W.Lilayuthalert, A.Sirivat and J.W.Schwank, “ Preparation, Structure, Properties and Thermal Behavior of Rigid rod Polyimide/montmorillonite Nanocomposites”, Comp.Sc.and Tech**.** 61, 1253-1264, (2001).

[51] J.W. Gilman, Flammability and thermal stability studies of polymer layered-silicate (clay) nanocomposites. *Appl. Clay Sci.* 15 (1999), pp. 31–49.

[52]. F. Dietsche and R. Mülhaupt, Thermal properties and flammability of acrylic nanocomposites based upon organophilic layered silicates. *Polym. Bull.* 43 (1999), pp. 395–402.

[53] J.W. Gilman, T. Kashiwagi, S. Lomakin, E.P. Giannelis, E. Manias, J.D. Lichtenhan, P. Jones, Nanocomposites: radiative gasification and vinyl polymer flammability, in: Proceedings of the 6th European Meeting on Fire Retardancy of Polymeric Materials (FRPM’97), University of Lille, France, 24–26 September 1997, pp. 203–221.

[54] J.W. Gilman, T. Kashiwagi, J.E.T. Brown and S. Lomakin, Flammability studies of polymer layered silicate nanocomposites. *SAMPE J.* 43 (1998), pp. 1053–1066.

[55] P.B. Messersmith and E.P. Giannelis, Synthesis and characterization of layered silicate-epoxy nanocomposites. *Chem Mater* 6 (1994), pp. 1719–1725.

[56] M.S. Wang and T.J. Pinnavaia, Clay–polymer nanocomposites formed from acidic derivatives of montmorillonite and an epoxy resin. *Chem Mater* 6 (1994), pp. 468–474.

[57] T. Lan and T.J. Pinnavaia, Clay-reinforced epoxy nanocomposites. *Chem Mater* 6 (1994), pp. 2216–2219.

[58] T. Lan, P.D. Kaviratna and T.J. Pinnavaia, Mechanism of clay tactoid exfoliation in epoxy-clay nanocomposites. *Chem Mater* 7 (1995), pp. 2144–2150.

[59] Vineeta Nigam, D.K.Setua, G.N.Mathur, Kamal K. Kar, Epoxy-Montmorillonite Clay nanocomposites: Synthesis and Characterisation. J Appl Poly Sci, Vol. 93, 2201-2210 (2004).

[60] Z. Wang, T. Lan and T.J. Pinnavaia, Hybrid organic–inorganic nanocomposites formed from an epoxy polymer and a layered silicic acid (Magadiite). *Chem Mater* 8 (1996), pp. 2200–2204.

[61] X. Kornmann, H. Lindberg, L.A Bergland; Synthesis of epoxy-clay nanocomposites. Influence of the nature of clay on structure. Polymer, Vol 42, 1303-1310, 2001.

[62] O. Becker, R. Varley and G. Simon, Morphology, thermal relaxations and mechanical properties of layered silicate nanocomposites based upon high-functionality epoxy resins. *Polymer* 43 (2002), pp. 4365–4373.

[63] J.S. Chen, M.D. Poliks, C.K. Ober, Y. Zhang, U. Wiesner and E.P. Giannelis, Study of the interlayer expansion mechanism and thermal–mechanical properties of surface-initiated epoxy nanocomposites. *Polymer* 43 (2002), pp. 4895–4904.

[64] X. Kornmann, H. Lindberg, L.A Bergland; Synthesis of epoxy-clay nanocomposites. Influence of the nature of the curing agent on structure. Polymer, Vol 42, 4493-4499, 2001.

[65] IsilIsik, Ulku Yilmazer and Goknur Bayram;Impact modified epoxy/montmorillonite nanocomposites: synthesis and characterization, Polymer ,Vol. 44, 6371-6377,2003.

[66] K.H.Chen and S.M.Yang; Synthesis of Epoxy-Montmorillonite Nanocomposite ; Journal of Applied Polymer Science, Vol. 86,414-421,2002.

[67] X. Kornmann, R. Thomann, R. Mulhaupt J. Finter and L.A Bergland; High Performance Epoxy-Layered Silicate Nanocomposites; Polymer Engineering and Science, Vol. 42,No 9, 1815-1826, 2002.

[68] X. Kornmann, R. Thomann, R. Mulhaupt J. Finter and L.A Bergland ; Synthesis of Amine-Cured ,Epoxy-Layered Silicate Nanocomposites: The Influence of the Silicate Surface Modification on the properties; Journal of Applied Polymer Science, Vol.86, 2643-2652, 2002.

[69] Costas S. Triantafillidis, Peter C. Le Baron, and Thomas J. Pinnavaia; Thermoset Epoxy-Clay Nanocomposites: The Dual Role of α,ω-Diamines as Clay Surface Modifiers and Polymer Curing Agents; Journal of Solid State Chemistry, Vol167, 354-362, 2002.

[70] Wei-Bing Xu, Su-Ping Bao,and Ping-Sheng He; Journal of Applied Polymer Science; Vol. 84, 842-849, 2002.